Power-to-methanol process: a review of electrolysis, methanol catalysts, kinetics, reactor designs and modelling, process integration, optimisation, and techno-economics

> (i) Author and affiliation details can be edited in the panel that appears to the right when you click on the author list.

Siphesihle Mbatha[a,b,*], Raymond C. Everson,(iD 0000-0003-4894-963X)[b,*], Nicholas M. Musyoka,(iD 0000-0001-9830-9265)(L-7798-2015)[a], Henrietta W. Langmi ,(iD 0000-0002-3299-0059)[c], Andrea Lanzini[d] and Wim Brilman[e]

[a]HySA Infrastructure Centre of Competence, Centre for Nanostructures and Advanced Materials (CeNAM), Chemicals Cluster, Council for Scientific and Industrial Research (CSIR), Pretoria, 0001, South Africa, smbatha@csir.co.za

[b]Centre of Excellence in Carbon-based Fuels, School of Chemical and Minerals Engineering, Faculty of Engineering, North-West University, Private Bag X6001, Potchefstroom, 2531, South Africa, Ray.Everson@nwu.ac.za

[c]Department of Chemistry, University of Pretoria, Private Bag X20, Hatfield, 0028, South Africa

[d]Department of Energy (DENERG), Politecnico di Torino, Corso Duca Degli Abruzzi, 24, Turin, 10129, Italy

[e]Sustainable Process Technology, Faculty of Science and Technology, University of Twente, PO Box 217, 7500 AE Enschede, The Netherlands

Funding Information

Table of Contents Entry

This review evaluated power-to-methanol and its key technologies with detailed analysis from a process system engineering perspective. It offers a holistic view and highlights key gaps and opportunities for improvements.

Abstract

In this paper, the power-to-methanol chain is reviewed from a process system engineering perspective with detailed assessments of major technologies. The evaluation encompasses electrolysis technologies and catalyst developments, kinetics, reactor technology options for methanol synthesis, as well as their design principles, modelling techniques, and research and optimisation gaps. The review extends to discuss process synthesis considering water-based and co-electrolysis-based power-to-methanol routes with reference to process integration, optimisation, modelling techniques, industrial applications and the associated techno-economics. Key gaps and opportunities for improvements are identified. The novelty of the paper lies in the holistic evaluation of technology design, performance and modelling. Foremost among the findings, advanced and detailed models of the electrolysis units, methanol reaction kinetics (*e.g.* considering identifiability and sensitivity) and methanol reactor with improved predictive capabilities under varying conditions are required. Additionally, the overall design, flexibility and reliability requirements concerning variable power-to-methanol deserve further detailed investigation. On the other hand, studies on the model-based process synthesis of power-to-methanol are limited, especially those considering dynamic modelling, multi-objective, process configuration and scheduling optimisations, and techno-economic and environmental analyses under uncertainty conditions. The few model-based studies available are mostly based on deterministic approaches and sequential pinch-analysis. Furthermore, limited studies evaluate power-to-methanol in the context of CO_2/energy/H_2 utilisation industrial hubs and repurposing/retrofitting of existing infrastructures (with part of the capital cost already offset) taking advantages of synergies and application-specific analysis of methanol, which may give additional attractive business cases. Lastly, incentives and dynamics in renewable electricity, electrolysis, CO_2 utilisation and the methanol market hold a strong position to make power-to-methanol feasible and must be investigated further to support policy decisions.
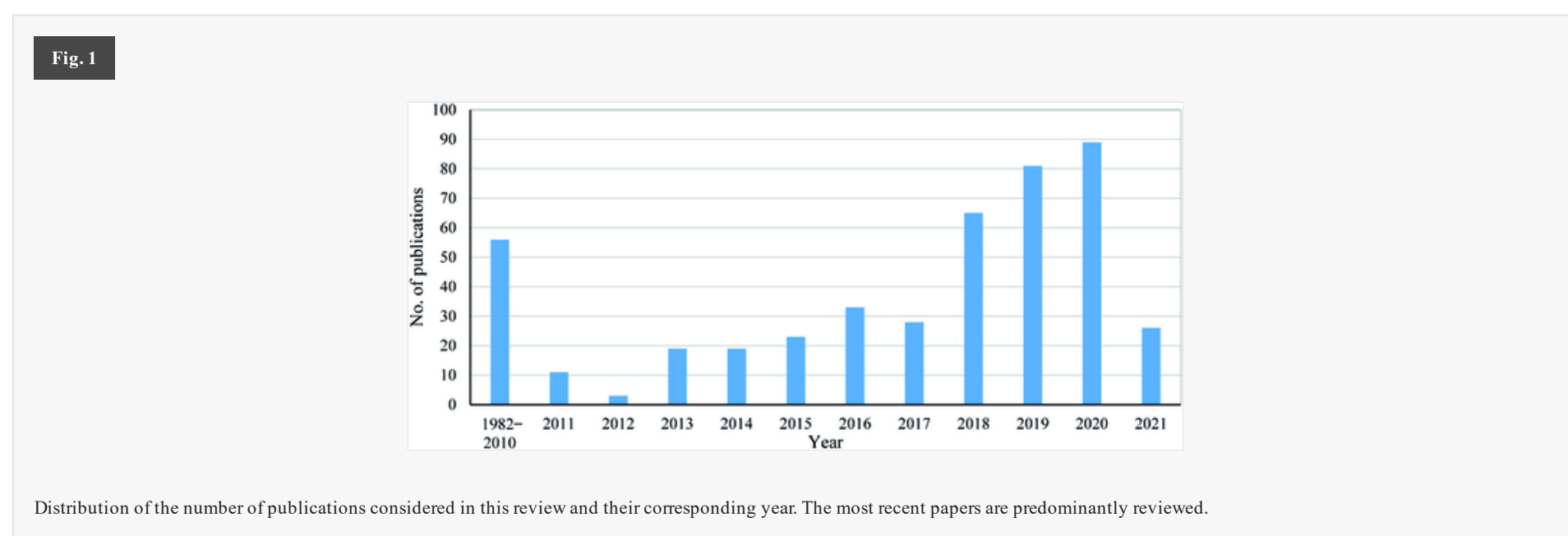
1. Introduction

Worldwide, there exists an urgent need to reduce the dependence on fossil fuel resources as a result of the environmental issues related to its processing, *i.e.* substantial CO_2 and SO_x emissions, particulate emissions and water pollution. Greener and renewable alternatives have been sought and proposed as solutions to mitigate the dependency on fossil fuels as resources of energy and chemical/fuel products. In the pool of renewable alternatives, solar and wind energy generators are more advanced and have great potential to widely penetrate the market in the near to longer term.[1–3] Their scalability and significant CO_2 reduction potential stands out.[4] However, three challenges arise with the adoption of solar and wind, *i.e.* (i) bridging the gap between energy supply and demand posed by resource intermittencies; (ii) coupling CO_2 recycling with solar and wind energy; and (iii) achieving an effective reduction of CO_2 across all energy-utilising and chemical-dependent sectors using solar and wind.

These challenges are interlinked with opportunities presented by carbon capture and utilisation (CCU) technologies, as well as the agenda for the future sustainable supply of energy and chemicals. The pivotal solution to mitigate these challenges is energy storage, and the term corresponding to this capability has been coined as 'sector coupling'.[5]

Chemical energy storage has great potential due to the higher energy density, as well as the dual benefit for effective CO_2 reduction across multiple fossil fuel-dependent sectors. This sustainably bridges the gap between energy supply and demand over extended periods and provides a method of producing carbon-based fuels using non-fossil carbon sources (waste CO_2). Chemical energy storage is achievable by storing power (*e.g.* excess power from variable sources) in the form of energy-dense liquids that are easy to handle (compared to gaseous alternatives, *i.e.* power-to-gas), hence the term power-to-liquids. In this case, power-to-methanol is considered as one of the attractive options.[6] Methanol is versatile as a chemical, energy carrier and intermediate feedstock for other value-added fuels and chemicals (*e.g.* dimethyl-ether).[6] Methanol has favourable attributes such as its ease of handling, existing industrial infrastructure, lower pollutant emissions upon combustion, higher stoichiometric CO_2 utilisation rate compared to methane, and the emergence of technologies such as methanol fuel cells that increase its potential utilisation.[7,8] The adoption of a green methanol economy can assist in bypassing numerous challenges associated with green hydrogen economy (*e.g.* its handling and storage, transportation difficulties and low volumetric density).[9] However, the full potential of methanol has not yet been leveraged, at least industrially. A huge cross-sectoral market can be created through a methanol economy at reasonable cost.[6]

Several review papers in the context of renewable power-to-methanol (PtMeOH) are available in literature.[10–12] This process is sometimes referred to in literature as 'green methanol production'. In this review paper, we offer the most critical and relevant research improvements and gaps in the topic of renewable PtMeOH chain from a process system engineering perspective. The paper considers the process performance, relevant technologies (electrolysers, CO_2 capture, catalysts and reactors), their design principles, modelling and overall process integration and optimisation, and methods and the techno-economics. The paper compares the performance of two prominent power-to-methanol routes *i.e.* co-electrolysis and pure steam electrolysis (with subsequent direct CO_2 hydrogenation to methanol). The review extensively captures the highlighted subcomponents and it is distinct from other recently published review papers in that it provides a thorough and holistic analysis of technology design, performance and modelling, encompassing aspects such as kinetics, electrolysis and reactor design principles and modelling (steady state and dynamic), process integration and optimisation and the associated gaps, all which, according to the authors' knowledge, have not been recently reviewed, particularly in the context of renewable power-to-methanol. Critical research directions in the area of PtMeOH for CO_2 utilisation and the storage of renewable energy are discussed. Fig. 1 shows the distribution of the number of relevant papers considered in this study per year.

Fig. 1

Distribution of the number of publications considered in this review and their corresponding year. The most recent papers are predominantly reviewed.

The review is structured as follows: Section 2 gives a broad overview of the PtMeOH process performance and the associated technologies. Section 3 presents the state-of-the-art of electrolysis technologies, design practices, and modelling and optimisation gaps. Section 4 briefly evaluates the CO_2 sources, the associated capture technologies, synergistic aspects with renewable powered-electrolysis, and highlights the flexibility requirements in the capture technology. Section 5 discusses catalysts and reactors for methanol synthesis, and extends to kinetics, reactor design and modelling techniques and opportunities for further optimisation. Section 6 presents the state-of-the-art of process synthesis in PtMeOH with reference to process integration, optimisation, modelling techniques and the associated techno-economics, environmental and incentives analysis. Section 7 concludes the review paper and highlights opportunities for innovation in the PtMeOH technology chain.

2. Power-to-methanol: overview

The storage of renewable power in methanol – produced *via* hydrogen (or syngas) from electrolysis and waste CO_2 as inputs – has been studied (Table 1) and its process performance recently demonstrated.[13] The Carbon Recycling Institute (CRI)'s George Olah plant, Mitsui Chemicals in Japan and Mitsubishi Hitachi Power Systems Europe GmbH (MHPSE) have demonstrated PtMeOH process.[11,14–17] This section gives a broad overview of the PtMeOH process performance, associated technologies and their limitations; and henceforth lays a foundation for subsequent sections. The production of green methanol from solar and wind consists of four main steps: a source of renewable energy, the production of H_2 (electrolysis) or syngas (co-electrolysis), a CO_2 source, methanol synthesis and purification. Fig. 2 shows technologies associated with each step and typical applications of methanol. For the synthesis reaction(s), a sustainable source of the CO_2 as a feed is required. The sources of CO_2 and associated capture technologies are vast; and as a result they are only briefly evaluated in this review paper.[3,12] Electricity and heat production processes are the biggest global CO_2 emitters (42%).[12] Detailed analysis of energy (electricity and heat) sources is beyond the scope of this review. However, variable solar photovoltaic (PV) and wind were demonstrated to be the attractive sources of power for the PtMeOH process, more especially from an environmental perspective.[3,18]

Table 1

Highlights of studies that investigated power-to-methanol processes

Reaction	Rxn conditions	Scale	Power source	Electrolyser(s)	Reactor(s)	Electrolyser efficiency	Reactor conversion efficiency	Energy efficiency	Recycle ratio	Highlights	Ref.
Direct CO_2 to methanol *vs.* two step CO_2 to	$P = 16$ bar	Commercial	Grid	—	Lurgi fixed bed reactor	—	Direct: 21%	Direct[d]: 82%	—	- Operation costs of electrolyser	44
	$T = 250$ °C						Indirect[c]:	Indirect[d]:		- An indirect process has the water gas shift step with a CO_2	

Process	Conditions	Scale	Energy source	Electrolyser	Reactor				Purity	Notes	Ref.
methanol (indirect)	$T = 800$ °C, RWGS						50%	80%		conversion efficiency of 60%, below the high temperature SOEC electrolyser efficiency. It is important to note that the two-step process is not the same as co-electrolysis. On the other hand, the direct CO_2 to methanol energy efficiency is a high estimate	
CO_2 hydrogenation	$P = 78$ bar, $T = 260$ °C	Commercial	Grid	PEM/HT-SOEC	Plug flow reactor	—	46%	PEM/MeOH: 45.3%, SOEC/MeOH: 54.8%	—	- High capital expenditure and short lifetime of SOEC - High operational expenditure of PEM/MeOH - Low methanol selling price	25
Co-electrolysis syngas; Hydrogenation (CE); CO_2 hydrogenation (SE)	$P = 50$–100 bar, $T = 260$ °C	Variable	Grid	HT SOEC	Fixed bed	—	—	SE: 75%, CE: 79%	—	- Levelised production cost of methanol is dominated by electricity - Capital expenditure is dominated by the electrolyser stack cost	24
Co-electrolysis syngas; Hydrogenation; CO_2 hydrogenation (SE)	$P = 67.4$ bar, $T = 265$ °C	Commercial	—	SOEC – for CE, alkaline – for SE	Fixed bed		—	CE: 41%, SE: 22%	99 mol%	- High electricity requirements by electrolysis unit	4
CO_2 hydrogenation	$P = 78$ bar, $T = 210$ °C	Commercial	Coal grid	—	Fixed bed	—	22%	—	—	- High heat exchanger operating expenditure - High capital expenditure of the compression system	26
Syngas hydrogenation	$P = 65$ bar	Variable	Grid, thermal plant, wind	Alkaline electrolyser	Plug flow reactor	30–42%	30.5–35.3%	70%	99 mol%	- High electricity cost - High capital expenditure of the electrolyser - High methanol production cost - Low and thermodynamically limited electrolysis efficiency	27
CO_2 hydrogenation	$P = 80$ bar, $T = 260$ °C	Lab scale	Solar, wind	Proton-conducting SOEC	One pot with SOEC	—	—	—	—	- High cost of investments - High operating expenditure of the electrolyser - High logistics cost for storage and delivery of H_2	9
CO_2 hydrogenation	—	Grid scale	Solar PV and wind	PEM	—	65%	—	—	78.4%[e]	- High reactor and battery system cost and capacity - Selling some of the electricity stored in the battery to customers for demand increases profitability	28
CO_2 hydrogenation	—	Commercial	Geothermal energy	Alkaline electrolysis	—	—	—	65%	—	- Incentives/policy and political support can increase competitiveness	14 and 15
CO_2 hydrogenation	$P = 80$ bar, $T = 240$ °C	—	Hydro, PV, grid wind	Pressurised alkaline electrolyser	—	—	—	—	—	- High costs of electricity, low methanol selling prices - Availability of the electricity from solar and wind plays a big part in the plant production capacity	29
Two step CO_2 to methanol	$P = 50$ bar	Commercial	Solar	PEM	Cascade adiabatic	—	40%	30–40%	—	- High cost of renewable H_2 production - Incentives enhance competitiveness *e.g.* electricity/CO_2 policies	2
Co-electrolysis syngas	$P = 50$ bar, $T = 250$ °C	Small scale	Solar, wind	HT SOEC	Condensation FB	—	99.5%	40.1[f], 53.0%[g]	—	—	32
CO_2	$P = 65$ bar	Commercial	Solar, wind,	HT Re-	Adiabatic	82.99%[a],	27%	27%[a], 33%[b]	—	—	30

hydrogenation			hydro	SOEC		95.04%[b]	

Fig. 2

Power-to-methanol process steps and associated technologies.

2.1 Process performance assessment

Methanol can either be produced from syngas or the direct hydrogenation of CO_2. As a result, the PtMeOH process can be divided into two main process routes: (i) H_2O/CO_2 co-electrolysis derived syngas to methanol (coSyn-MeOH); and (ii) steam electrolysis derived hydrogen to methanol (*via* the direct CO_2 hydrogenation route: dCO_2-MeOH). The other route is the two-step process in which H_2 production *via* steam electrolysis is coupled with reverse water gas shift reaction (RWGS) to produce syngas followed by methanol synthesis.

Conventional methanol production processes were designed primarily based on economics, thermodynamics, reactions and separations efficiencies. However, with the involvement of fluctuating renewable energy supply, stabilisation of the energy input(s) and synthesis reactor feed composition becomes one of the key tasks within the process. To stabilise the input power, correct rectification (*e.g.* transistor-based rectifiers), a battery system or additional stable renewable source such as biomass can be used,[19–21] whereas to stabilise the feed composition, hydrogen storage tanks (or in case of syngas – a conditioning reactor) are used if justifiable by efficiency and economics. System partitioning and part load operation are also possible.[19,20,22]

To evaluate the process performance, energy efficiency and economics are the most commonly used criteria in literature.[2,23,24] Analyses of studies in Table 1 show that recent interest is directed to dCO_2-MeOH,[9,14,15,25–30] but few consider the coSyn-MeOH route.[4,31,32] This is justifiable since the dCO_2-MeOH process, when optimised, will allow large utilisation of CO_2, and it is characterised by less by-product formation and low hot spot formation within the reactor; thus slightly simplifying the process compared to that based on syngas-to-methanol.[33–35] However, the dCO_2-MeOH process has its downsides such as the higher hydrogen requirements ($CO_2 : H_2 = 1 : 3$ or $1 : 2.5–5$ can be optimum[36–38]); thus increasing the size of the electrolysis unit and the energy requirements. Conventional grid, solar PV and wind are mostly considered as energy sources.[2,3,28,29] Studies by Andika *et al.*[28] and Bos *et al.*[39] pointed to the potential revenue addition achieved by adding the PtMeOH process and its pivotal role in the energy storage system for an isolated 100% renewable (respectively, solar and wind) energy system. Some studies also evaluate potential use of hydroelectric power and geothermal as energy sources in the PtMeOH chain.[14,15,29] Due to their unique characteristics, each of renewable energy sources has a different influence on the number of operating hours of the plant, production capacity, energy efficiency and the selling price of methanol in different geographic regions.[2,27,29]

The energy efficiency of the PtMeOH process depends mainly on the operating point of the integrated electrolyser, the exergy destruction due to chemical reaction(s) and associated cooling requirements, system-level heat integration potential, waste heat recovery from external processes, the intensity of the renewable solar source and/or the CO_2 capture method (*e.g.* sorbent working capacity).[2,24,31,32,39,40] From rigorous analysis of the data in Table 1, the overall energy efficiency of the PtMeOH process is in the range of 39 to 80%.[24,39,41]

The overall process energy efficiency strongly depends on the technologies used in the process chain,[23] most importantly the electrolyser. Low temperature electrolysis, *i.e.* alkaline water electrolysis (AWE)[4,27,29] and polymer electrolyte membrane (PEM) electrolysis[2,25,28] are the most investigated technologies in the power-to-methanol process chain. Recent efforts are directed towards high temperature solid oxide electrolyser (SOEC)[9,24,25] and reversible solid oxide cells (ReSOC).[30,42] The overall energy efficiency is higher for co-electrolysis-based syngas-to-methanol processes (40–80%) than direct CO_2 hydrogenation (39–75%).[4,24,36,43]

The upper energy efficiency ranges represent SOEC-based processes, while the middle to lower ranges pertain to PEM- and AWE-based processes (both PEM and AWE are applied only in the direct CO_2 hydrogenation route).[4,24,36,43]

On the other hand, reactor conversion efficiencies are higher for the syngas-to-methanol reaction than direct CO_2 conversion to methanol,[44] thus larger reactors are required for CO_2 hydrogenation in the case of fixed bed reactors to enhance conversion. However, this strongly depends on the type of reactor used and the pressure and temperature conditions. Léonard *et al.*[32] and Bos and Brilman[45] demonstrated that using a reactor with a condensation step to separate water and methanol from the CO_2/H_2 reaction system can increase conversion efficiency to 99.5%, which is near full conversion at 250 °C and 50 bar.

Other authors such as Kiss *et al.*[46] and Khunathorncharoenwong *et al.*[47] proposed the use of a stripping unit and an alcohol (in their case ethanol)-assisted reaction, respectively, to enhance the CO_2 conversion efficiency. The alcohol-assisted process increased the single pass conversion efficiency and reduced hydrogen compression (by 25%) since a fraction of H_2 was generated *in situ* from ethanol dehydration, for example. However, it rendered the methanol separation step complex and energy intensive (up to 88–96% of the total duties) due to the formation of methanol by-products (azeotropes).

2.2 Current process limitations

The analysis of PtMeOH process studies and technologies paves the way to understanding the critical bottlenecks within the process and ultimately the areas for process improvement. The key bottlenecks highlighted in most studies are associated with the cost of electricity, the electrolyser system, methanol synthesis reactor conversion and energy consumption by auxiliaries.[9] In addition to these, are the associated energy efficiency, selling price of methanol, CO_2 capture and purification costs, and the number and cost of heat exchangers and compression units. Although diverse scenarios are observed in different geographic locations and for various renewable energies, in general, the PtMeOH process is currently not economically feasible in most regions except for countries with cheap/free renewable energy and carbon tax higher than 100 € per ton of CO_2 (e.g. Sweden with carbon tax of 110 € per ton CO_2).[4,9,14,25,26,28,29,48–50] Elaborate techno-economic, environmental and incentives analyses of the encompassing PtMeOH processes are deferred to Section 5.4 of this review.

In addition to the above-mentioned challenges, other limitations exist that are worth highlighting before assessing power-to-methanol technologies. Some are well known and mostly related to electrolysis and methanol synthesis. These limitations are divided into elementary and complex constraints, as presented in Table 2. Elementary limitations refer to fundamental challenges such as those associated with catalytic materials, among others. Complex limitations comprise constraints that cannot be a product of a single step/unit or phenomenon, but as a result of the interplay of multiple steps or factors. Attempts to solve these limitations, summarised in Table 2, will be discussed in the subsequent sections, per technology and process layout or design.

Table 2

Major elementary and complex limitations of the power-to-methanol process

Elementary limitations	Complex limitations
Exothermicity of the methanol reaction	Low single-pass conversion and therefore notable CO_2 purge rate/emission
Thermodynamic equilibrium limitations	Energetic consumption/low energy efficiency
Kinetics/unconcluded reaction mechanism	Equipment flexibility requirements, e.g. short start-up, part-load, etc.
High CO_2 activation energy	Poor catalyst selectivity and limited catalyst adaptation to dynamic operations
Mass transfer limitations	Catalyst deactivation
Water formation	Availability of cheap electricity and favourable policy incentives
Reverse water gas shift reaction	Electrolyser stack degradation
	High cost of attractive electrolysers
	Availability of CO_2 sources and cost-effective capture method (a function of CO_2 source purity and compositions)
	Hydrogen and methanol market price

3. Electrolysis technologies

Hydrogen and/or syngas are vital components for the methanol process chain with significant impact on the economics. Thus, it is fitting to analyse the state of the art of renewable hydrogen production technologies from the perspective of their potential as candidates for integration with variable solar and wind energy sources.[51,52] These technologies are based on the perennial method termed 'water electrolysis'. Several good review articles on electrolysis technologies are available in literature such as Olivier et al.,[53] Ursua et al.,[54] Jensen et al.,[55] Stolten and Krieg,[56] Zeng and Zhang,[57] Carmo et al.,[58] Hansen,[59] Ebbesen et al.[60] and Laguna-Bercero[61] and more recently Roode-Gutzmer et al.,[12] Brauns and Turek,[52] Venkataraman et al.,[62] Küngas,[63] Kumar and Himabindu,[64] Falcão and Pinto,[65] Andika et al.[66] and Wirkert et al.[67] This section extends to discuss key design practices, modelling and optimisation gaps pertaining the electrolysis technologies, particularly based on solid oxide cells. Recent reviews that focus on the design and modelling of alkaline water-based electrolysers (AWE)[52,53] and polymer exchange membrane (PEM)[53,65,67] electrolysers are available in the literature; thus this section comprehensively assess AWE, PEM and solid oxide electrolyser design, modelling and optimisation.

3.1 State-of-the-art and research and development activities

Electrolysis of water may occur at low (20–80 °C) or high temperatures (500–950 °C).[64] Low-temperature electrolysis technologies are typically alkaline-based electrolysis and PEM electrolysis, which are both available commercially.[52,64,68] The less mature technologies are high-temperature solid oxide electrolyser cells (HT-SOEC) and the so-called reversible solid oxide cell with the capability to switch between electrolysis and fuel cell mode when needed.[51,62,67,69]

In modern electrolysis technologies, the co-electrolysis of CO_2 and H_2O are possible at the high temperature range (typically in the range of 800–850 °C) currently permitted by solid oxide cells.[63,66,70] However, reaction mechanisms are complex and not fully understood.[70] In addition, an undesirable solid carbon formation reaction via Boudouard reaction may occur during co-electrolysis depending on the applied conditions.[70] This exothermic reaction is important for consideration during design and typically an O/C ratio greater than 1.5 must be maintained to suppress it. The electrolysis process is an endothermic and non-spontaneous chemical reaction.[53] Technologies such as SOEC can also operate at peculiar conditions of thermoneutral voltage in which overpotential irreversibility (that becomes heat) balances the endothermic electrolysis enthalpy of reaction.[54] Increasing the temperature decreases electrical energy, but increases the thermal energy. Table 3 gives a performance comparison of the electrolyser technologies, and a summary of their research and development status.

Table 3

Comparison of AWE, PEM and SOEC electrolyser technologies[48,52,63–65,69,76,81–83]

Parameters	Electrolyser technology		
	AWE	**PEM**	**SOEC**
H_2 production rate (Nm^3 h^{-1})	5–1400	1–400	>40

Nominal power (MW)	0.03–6	0.01–6	>0.1
Typical operating pressure (bar)	3–30	4–30	>30
Cell temperature (°C)	60–90	20–80	750–950
Current density (A cm^{-2})	0.25–0.45	1.0–2.0	0.3–1.0
Specific energy consumption (kW h Nm^{-3} H_2)	3.8–6	4–6.5	≤3.7
Nominal stack efficiency based on LHV of H_2 (%)	60–80	60–90	79–100[a]
Nominal system efficiency (%)[b]	51–70	46–80	76–96
Load flexibility (%)	10–100	0–160	−100 to 100
Cold start-up time	1–2 hours	5–10 minutes	Hours
Warm start-up time	1–5 minutes	<10 seconds	15 minutes
Ramp-up rate (% per second)	6.7	40.6	0.1
Ramp-down rate (% per second)	10	40.6	3
Cell area (m^2)	<3.6	<0.13	<0.06
System degradation (%/1000 hours)	0.13	0.25	0.4–6
Stack lifetime (hours)	55 000–120 000	10 000–100 000	<40 000
State-of-the-art electrode materials	Nickel-based materials	Cathode: platinum (or Pt alloy) Anode: iridium	Cathode: nickel-yttria stabilised zirconia (Ni-YSZ for O^2-based $SOEC^-$) and nickel-yttrium-doped barium cerate zirconate (Ni-BCZY for H^+-based SOEC) Anode: perovskites such as lanthanum–strontium–manganite (LSM), $La_{1-x}Sr_xCo_{1-y}Fe_yO3-\delta$ (LSCF)[c]
State-of-the-art electrolyte materials	Alkaline electrolyte: KOH or NaOH with asbestos diaphragm as a cell separator	Perfluoro-sulfonic acid/Nafion polymer electrolyte membrane.	Yttria-stabilised zirconia (YSZ for O^2-based SOEC), $BaCeO_3$ (for H^+-based SOEC)
Promising electrode materials	Alloyed nickel electrode and Nafion polymer	Base metal catalysts and composite membranes	Mixing oxides of different amounts with commercial electrodes to improve stability, ceria-based electrolytes
Promising electrolyte materials	—	—	$La_{1-x}Sr_xGa_{1-y}Mg_yO_{2.85}$ (LSGM)
Current R&D focus	Zero gap electrolysis design, better electrode design, increasing the current density and operating temperature, reduction of over-potential and ohmic losses of the half reactions, development of new diaphragm and electrode materials.	Membranes with high tolerance to impurity, balance between cost and mass manufacturing, finding cheaper electrocatalyst materials, high pressure (~100 bar) electrolyser stacks, durability of membranes. Improving the efficiency.	Demonstration and systematic evaluation, long-term tests to improve stability/durability Thermal cycling, improving sealing technology, lowering the electrolyte conductivity temperature to ~450–700 °C via reducing electrode polarisation resistance, reducing the cold start-up time, scale up, improving the chemical stability of the electrolyte and its specific area resistance, and understanding the co-electrolysis reaction mechanism

Table Footnotes

[a] At the thermoneutral voltage (~1.28 V at 600–900 °C or 1.48 at 25 °C).

[b] Including the auxiliary and heat supply.

[c] Electrode used by Sunfire technology.

3.1.1 Alkaline water electrolysers

Alkaline water-based electrolysers (AWE) are based on an electrolyte (typically KOH/NaOH) that provides hydroxyl (OH^-) anion transfer between the two electrodes of the electrolyser. The main advantages of alkaline electrolysis technologies are their low annual maintenance cost, and long operation lifetime/durability (30 years) and reliability under fixed (continuous) operation conditions.[52] Although AWE has long been commercialised and is cheaper than other electrolysis technologies, it is still expensive relative to the fossil fuel-based hydrogen production technologies and less efficient (due to high parasitic current losses). On the other hand, it is currently not considered a good candidate for integration with intermittent energy sources due to its low part-load range (10–25% of the nominal load) as gas contamination (H_2 in O_2) increases with the decrease in power availability, long cold start (>30 minutes) and warm start times.[20,52,71] A significant decrease in the faradaic efficiency is present below a current density of 50–100 mA cm^{-2} for the AWE.[52,72] Research and development on AWE technology is currently focused on making the technology more efficient and cost effective, by modifying it to operate at higher temperatures, current density (>500 mA cm^{-2}) and pressures, and highly dynamic conditions.[52,68]

3.1.2 Polymer-exchange membrane electrolysers

Polymer-exchange membrane (PEM) electrolysers contain a proton (H^+)-conductive membrane within its membrane electrode assembly to allow proton transfer, but inhibit gas diffusion between the two electrode sides of the electrolyser.[64] Some features of PEM are now reported.[73–75] This is a mature technology at the 1–5 MW scale. It offers the following: high purity gas delivery (99.999%), high compactness, commercial operation at up to 3.0 A cm^{-2}, demonstration of performance on laboratory scale at 10 A cm^{-2}, high energy efficiency (70–80% higher heating value at 1 A cm^{-2}), depending on the operating current density and temperature, and durability of continuous operation (>60 000 h). Systems with increased capacities are becoming commercially available (systems of up to 7–10 MW are now available on the market and development of up to 100 MW is underway). Further features include excellent flexibility and reactivity at system level for operation with transient power sources, and operation under pressure (200 bar demonstrated, 350 bar prototypes).

PEM electrolysers are well adapted to operate under intermittent renewable supply with an extended load flexibility (0–160%) range and fast cold start time (<10 minutes). This technology is relatively expensive, primarily due to its use of precious metals (*e.g.* Pt, Ru and Ir) as electro-catalysts. Research and development (R&D) activities on these electrolysers are focused on the development of cheaper catalyst materials or reducing the content of the precious materials, particularly iridium (from ~0.5 g-Ir kW^{-1} to 0.01 g-Ir kW^{-1}) and platinum (<0.01 g-Pt kW^{-1}), cheaper current collector and separator plate coating materials, and more durable membranes that are capable of operating at higher current densities (>3 A cm^{-2}).[64,73,74] Besides, increasing the operating pressure could lower downstream H_2 compression costs.[47] However, a 10% decrease in the faradaic efficiency of the PEM cell with an increase in pressure (20 to 130 bar) was reported by Grigoriev *et al.*[75]

3.1.3 High-temperature solid oxide electrolyser and reversible solid oxide cells

Increasing the operating temperature of the SOEC electrolyser improves chemical kinetics, the oxygen (O^{2-}) ion or proton (H^+) conduction of the ceramic electrolyte, and the thermodynamics and efficiency.[67,68,74] Thus, the SOEC operating temperature is within the range of 750–950 °C and is therefore referred to as high-temperature solid oxide electrolyser (HT-SOEC). The HT-SOEC technology can also be designed to operate in reverse (fuel cell) mode (*i.e.* ReSOC).[62] HT-SOEC is a promising breakthrough technology and, as a result, like PEM electrolysis and AWE, it also benefits from decreasing capital costs.[12,76] However, it is still currently expensive (with a projected cost >2800 € per kW) than PEM electrolysis and AWE, and potentially less flexible (in terms of start-up and load) than PEM electrolysis.[12,76] The key advantages of HT-SOEC include the ability to perform co-electrolysis reaction (*i.e.* syngas is produced and water is consumed within the electrolyser), which eliminates the need for the water-gas-shift-reactors with associated challenge of water formation. Unlike HT-SOEC, in the case where syngas is produced using the reverse water–gas-shift-reactor, water needs to be subsequently separated before the reactants are fed to the methanol synthesis reactor. Other advantages of HT-SOEC include the use of non-noble electro-catalysts materials, less electricity input requirements, high faradaic efficiency (100%) and energy efficiency (79–96%) compared to AWE and PEM electrolysers.[11,64,66–68,76–80] The SOEC produces 30% more products at the same electric input (*e.g.* ≤3.7 kW h $Nm_{H_2}^{-3}$) compared to PEM and AWE technologies.[76]

The HT-SOECs are currently in the development stage and entry level of the commercial market, with Sunfire and several other companies and research institutions pursuing work on the development of SOEC technologies.[76] The ReSOC is still at a very early stage of development (Technology Readiness Level (TRL) 3–4).[62,81,82,84] However, due to its flexible dual capability and scalability, the ReSOC is attractive for distributed microgrid application in the context of power to methanol to power and for standalone systems with co-generation (methanol and electricity as end products guided by demand and pricing structures).[62,84,85] The ReSOC has been demonstrated by Sunfire considering H_2 as the energy carrier instead of methanol.[62,76,86] The ReSOC can maintain high efficiency even at a part-load of 15% of the rated capacity.[85]

From a material perspective, high-temperature sealing materials for high-pressure operation, improving the durability and medium temperature (500–750 °C) conductivity of the electrolyte and electrodes material, novel fabrication methods, advanced models and analysis of degradation mechanisms, and the understanding of co-electrolysis reaction mechanisms are key areas of R&D.[67,69,70,87] For its integration with variable renewable energy sources, SOEC and ReSOC technologies will benefit greatly from shorter cold start-up times, more durable ceramics, which are more resistant to pressure fluctuations, gas cross-over and thermal stresses, and mass production and automation to reduce cost.[51,67,85]

In addition, advancing SOEC and ReSOC technology towards a sector-coupling solution is still required. Section 3.2 evaluates the equipment design, modelling and optimisation activities and gaps for the SOEC technology, with a few highlights of ReSOC.

3.2 Equipment design and modelling

The work on AWE, PEM, SOEC design evaluated herein is focused on three key design principles: reducing capital and operating costs, increasing stack lifetime/durability, and increasing the efficiency and flexibility of the technologies. Furthermore, progress and gaps in model developments for each technology are assessed.

3.2.1 Design and modelling of the AWE

3.2.1.1 Reducing the capital and operating costs

Cell design configuration in the AWE technology can be categorized into two prominent types being (i) the monopolar and the (ii) bipolar cell design. Monopolar configurations are primarily based on parallel cell configuration while the most used bipolar configurations are based on series/accumulation connections, electrically and

geometrically.[88,89] Bipolar configurations are more compact than monopolar, thus giving shorter paths for electrical current and thereby reducing losses such as ohmic losses.[89] However, bipolar cell configurations are characterised by parasitic currents and high manufacturing costs.[89] Nonetheless, owing to the use of non-noble metals, the capital cost of AWE is relatively cheaper ($800–$1500 kW^{-1}). Although the capital cost of the AWE system can still be reduced further to <$500 kW^{-1} by novel cell designs to achieve higher current density/minimum area resistance, optimised manufacturing techniques and making the technology more compact, production cost (>$4 per kg per H$_2$) dominates the total cost of the AWE system.[90] From an operation perspective, to maintain system integrity, it is crucial to balance the pressure between the hydrogen and oxygen side.[91] The energy to drive the reaction at cell level dominates the overall electrical energy demand of the AWE system.[90] One key strategy, currently under investigation, to reduce the hydrogen production costs concerning the use of AWE is to modify the electrolysis operating conditions. State of the art AWE are operated at low temperatures (see Table 3). The heat capacity of the KOH solution, which is a function of KOH concentration and temperature, has a strong effect on the energy consumption and the production cost.[90] Holm et al.[90] assessed the economic feasibility of high temperature and high pressure (200 bar) liquid-phase operation of the AWE. The authors further deduced that the energy consumption of the AWE decreases from 74.1 kW per h per kg per H$_2$ at 25 °C to a minimum of 55.4 kW per h per kg per H$_2$ at 287 °C (above this temperature, the energy consumption increases). However, the authors assumed a constant resistivity at temperature above 286 °C and hence the validity and effect of this assumption must be explored further with experiments. On the other hand, the change in vapor pressure with temperature result into a higher cost of recycling heat from the output stream of the AWE system and hence higher production cost.[90] The authors deduced that an optimal range corresponding to higher temperature liquid-phase operation is 270–310 °C, which emanates from consideration of trade-offs between the cell efficiency improvement and the potential of increasing energy/production cost as a consequence of increasing temperature.[90] However, subject to feasible pressure operation window, the optimal temperature range can still be pushed higher or lower. High pressure operation is also known to be associated with increase in capital cost and raises safety concerns in the AWE system due to an increased potential of gas cross-over and hence dangerous mixing of H$_2$ and O$_2$. To make high pressure operation feasible considering safety, highly stable separators with low ionic resistivity are required. The energy consumption can also be reduced by about 22% if excellent AWE electrocatalysts, able to achieve good activation energy and charge transfer close to a unity are developed.

3.2.1.2 Increasing the lifetime and durability

Although, the AWE technology is characterised by long term stability and low degradation, the presence of KOH creates a detrimental corrosive environment to the AWE materials. The current state-of-the-art zirconium dioxide- and polysulfonate-based separator materials can degrade and dissolve under alkaline solution. Currently, the duration of the catalyst used in the AWE technology is about 40 000 h. Increasing the duration of the catalyst reduces the replacement cost. Targets are looking at improving the duration of the catalyst by e.g. doubling it to 80 000 h and to current density of 2000 mA cm^{-2}.[90] AWE technology with nickel-based electrodes and Zirfon-based separator have also been tested for dynamic (intermittent) operation conditions for a total duration of about 13000 h and showed no severe degradation in the cell and its components. However, more testing under dynamic conditions are required to ascertain the absence of severe degradation using nickel hydrides and hydrogen embrittlement as indicators. On the other hand, research focusing on increasing the temperature of the AWE have pointed a potential increase in degradation of the brittle ceramics and/or nickel-based cell for temperatures exceeding 200 °C. Nonetheless, materials such as palladium are also promising candidates. However, more research is needed in this direction concerning stress tests and degradation and associated cost trade-offs at varying conditions e.g. input current density and temperature.

3.2.1.3 Increasing efficiency and flexibility

AWE is characterised by low efficiency and low flexibility. The presence of hydrogen bubbles and their flow over the AWE electrodes has been discussed as a key factor affecting the efficiency and choice of design parameters of the AWE.[91] From a first principles perspective, this is so because the hydrogen bubbles tend to influence the energy and mass transfer in the gas electrodes, and as the coverage of the electrode by hydrogen bubbles increase, the electrolysis efficiency decreases.[91] Hydrogen molecules can be transferred to the liquid electrolyte and the mechanism is generally referred to as the ionic transfer mechanism which can occur via migration, convection and diffusion.[91] Design configurations such as the zero-gap combined with modern Zirfon diaphragms are aimed at increasing the efficiency of the AWE by reducing the area resistance. However, they still have their own challenges, such as high ohmic resistance, uneven current distribution, and lack of experimental data and detailed understanding.[92] On the other hand, high temperature liquid-phase operation can enhance the efficiency of the AWE, but this design strategy tends to affect the feasible operation pressure window of the system due to difficulties in managing the equilibrium pressure of water at higher temperatures and hence increases the cost, as previously dicussed.[90] Direct high pressure operation of the AWE has also been discussed as a potential design strategy for enhancing the energy efficiency of the AWE system, however this strategy will require modifications in cell design taking into considerations safety aspects. The other strategy for improving the energy efficiency concerns the improvement in the catalyst used in the AWE system. On the other hand, although alkaline electrolysis are simple to scale and have been used commercially for more than 10 years, they exhibit low flexibility in terms of part-load operation as highlighted in Section 3.1.1 above. Due to low flexibility (low partial load range) and challenges with handling intermittent supply, good rectification and buffer storage of dynamic electricity input is required. With the addition of rectifiers and buffer storage such as batteries, the energy efficiency penalties were observed, even though the hydrogen production increase with, for example, efficient rectifiers under dynamic operating conditions.[93] Additionally, the latter technologies increase the system costs. Thus improving the capability of flexible operation of AWE will play a pivotal role. Currently, ionic conduction and gas impurities (typical to form at part-load) limits the fast response and part-load operation (10 to 15%) of the AWE. Alternatively, a small electrolyser size will give higher operation hours.[94] Ultimately, novel cell design (e.g. self-repairing electrodes) and operation strategies (e.g. variation of operating pressure, temperature with load) will make AWE more flexible.

3.2.1.4 Modeling of the AWE

Models are critical tools for cell and system designs, and for predicting beyond what is experimentally feasible.[95] Modeling of the AWE has been done extensively in literature and some of the developed models, their multi-physics (i.e. thermal behavior, cell voltage, gas purities, current, gas evolution and resistivity) and diagnostics analysis have been validated experimentally under steady-state and unsteady conditions.[88,96–100] However, this is still an open research field. Table 4 summarizes the models concerning the AWE. AWE models have also been validated under dynamic conditions and shown to have a reasonable error of about 3%.[101] A recent study by Avci et al.[91] assessed the two-phase flow and hydrogen gas flow dynamics within the alkaline-water-based electrolysis technology using a physical model. The authors studied the effect of void fraction, bubble diameter and the velocity of the bubble. Due to existence of multi-phase flow, the model can be complex and thus often requires assumptions, such as homogeneous equilibrium flow, for simplification. Limited studies are focused on computational fluid dynamics (CFD) modelling of the AWE to describe its multi-physics (e.g. gas and liquid transport, the electrical current conservation, the flow velocity profile, gas hold-up, etc.).[95,97,102] Using CFD, a good approximation of performance can be made by considering just 2D models.[95] Opportunities for improving AWE models exists, such as extending the validity range of the empirical models with further experimentations. It is evident from the analysis of Table 4 that more work can be done to simplify and improve accuracy of the models e.g. in voltage, activation overpotentials, mass and heat transfers and product gas purity predictions taking into account various interplaying factors, and incorporating geometries of the cells and experimental derived charge transfer coefficient.[95,104] Limited models are developed considering multi-scales e.g. atomic to electrode to cell-levels and degradation. In June 2020, VoltaChem and TNO[105] announced their ambition to develop an advanced degradation model for the AWE technology. The majority

of the models are aimed at estimating the size, electricity utilization rate, cost and efficiency of the technology with the aim to assess its role in the overall system concerned. [89,94,106] Thus more research work is needed to enhance the AWE models.

Table 4

Alkaline water-based electrolysis (AWE) technology models

Applications	Model type	Typical assumptions	Advantages	Disadvantages/limitations	Exemplary ref.	Possible improvements
Stack to system level	Lumped parameters	- Lumped thermal capacitance and use of faradays law for output-consumption terms	- Simple and accurate voltage, capacitances and resistance evaluations can be performed as a function of operating conditions	- Limited by assumption of homogeneous stack distribution of temperature, concentration and pressure, neglect of some physical domains	[101], [107] and [108]	- Consider elaborating losses and control aspects
		- Typically formulated as equivalent circuit model typically based on electrochemical impedance spectroscopy (EIS)				- Consider auxiliaries
		- Homogeneous temperature, concentration and pressure distribution (no gradients)				- Increase validation range *e.g.* under unsteady conditions
		- Applies Ohm's and Kirchhoff's laws				
	Distributed dynamics	- Empirical model of the velocity of gas bubbles and bubble coverage factor	- Evaluates the dynamics and safety related matters	- Exclude geometric aspects and elaborate thermal models to reduce complexity	[89], [93], [94], [99], [106] and [109–111]	- Consider concentration gradients, dissolved concentration profile, multizonal formulation
		- Area averaged void fraction and lumped thermal capacitance dynamic model	- Assist control of the system	- Gas-crossover is a critical phenomenon in AWE technology		- Consider dynamic models of the auxiliary equipment, prognostics and diagnostics
		- Homogeneous equilibrium flow	- Can predict voltage and product gas quality fluctuations (correlated to mass transfer)	- Less developed and less experimentally validated		- Consider losses *e.g.* thermal, current and elaborate mass transfer by incorporation of gas crossover models as a function of operating conditions
		- No relative velocity				
		- 1D-3D flow regime				
		- Laminar electrolyte flowrate				
		- Film model for mass transfer		- Hydrogen is typically considered as the ideal gas		- Elaborate (real-time) control models
		- Negligible gas density				
		- Negligible gas cross-over and bubble accumulations				
	Input–output	- Reactions associated with overpotential proceed *via* Tafel kinetics	- Can predict voltage and product gas quality (related to mass transfer)	- Mostly empirical and developed under steady state conditions	[89], [104] and [112]	- Consider improving validity range gas evolution efficiency and product gas quality models with more experimentation under industrially relevant conditions (>25% KOH and T > 70 °C)
		- Empirical *e.g.* resistivity, gas evolution efficiency and product gas purity	- Simple to use and adapt	- Oversaturation factor typically applied to account for predicted impurity concentration deviation from experiments		- Consider concentration gradients and dissolved concentration profile
		- Linear resistivity at higher temperatures and negligible concentration overpotential	- Based on extensive steady state experimentation and continuously adjusted	- Exclude geometric aspect		- Consider developing these models for diagnosis, prognostic and control
		- Homogeneous and 1D distribution of the current	- Easily to couple to auxiliaries *via* efficiency link and inputs	- Charge transfer coefficient has been proven by some authors to vary with temperature		- More experimental validation of the charge transfer coefficient over pilot or semi-commercial stack
		- Ideal gas thermodynamics law and uniform distribution of pressure		- Pressure, temperature and concentration distributions may be non-homogenous		- Better model for activation overpotentials
		- 0D model of the product gas quality				

		Assumptions	Advantages	Limitations	Refs	Recommendations
		- Gas bubbles are completely removed (perfect separation) - Film model for mass transfer - 100% faradaic efficiency, no mass transfer in the gas separators and pipes - No recombination reactions and monodispersed bubble distribution - Constant charge transfer coefficient: 0.5 - All cells behaves the same as one representative cell				
Stack level	Lumped parameters	- Lumped thermal capacitance - Typically formulated as equivalent circuit model typically based on electrochemical impedance spectroscopy (EIS) - Homogeneous temperature, concentration and pressure distribution (no gradients) - Applies Ohm's and Kirchhoff's laws	- Simple and accurate voltage, capacitances and resistance evaluation can be a function of operating conditions	- Limited by assumption of homogeneous stack distribution temperature, concentration and pressure, neglect of some physical domains	88, 107 and 108	- Consider elaborating losses and control aspects - Increase validation range *e.g.* under unsteady conditions
	Distributed dynamics	- All cells behaves the same as one representative cell - Empirical model of the velocity of gas bubbles and bubble coverage factor - Area averaged void fraction - Homogeneous equilibrium flow - No relative velocity and 1D-3D flow regime - Laminar electrolyte flowrate and film model for mass transfer - Negligible gas density and gas cross-over and bubble accumulations	- Provides more details about the feasible operating window - Takes into account the geometry and interconnection of the stack. Features PID control	- Can be complex - Less developed in literature - Gas-crossover is a critical phenomenon in AWE technology - Hydrogen is typically considered as the ideal gas	89, 93 and 94	- Consider improvements of the stack thermal model considering different interfaces - Consider losses *e.g.* thermal, current and elaborate mass transfer by incorporation of gas crossover models as a function of operating conditions - Consider incorporating degradation model
	Input–output	- Reactions associated with overpotential proceed *via* Tafel kinetics - Empirical *e.g.* resistivity, gas evolution efficiency and product gas purity - Linear resistivity at higher temperatures and negligible concentration overpotential - Homogeneous and 1D distribution of the current - Ideal gas	- Can predict voltage and product gas quality (related to mass transfer) - Simple to use and adapt - Based on extensive steady state experimentation and continuously adjusted	- Pressure, temperature and concentration distributions may be non-homogenous - Charge transfer coefficient has been proven by some authors to vary with temperature - Hydrogen is typically considered as the ideal gas - Gas-crossover is a critical phenomenon in AWE technology	98, 104 and 113	- Consider improving validity range gas evolution efficiency and product gas quality models with more experimentation under industrially relevant conditions (>25% KOH and $T > 70\ °C$) and activation overpotentials model. Consider concentration gradients and dissolved concentration profile - Consider developing these models for diagnosis, prognostic and control. More experimental validation of the charge transfer coefficient over pilot or semi-commercial stack

		thermodynamics law and uniform distribution of pressure				
		- 0D model of the product gas quality and monodispersed bubble distribution				
		- Gas bubbles are completely removed (perfect separation) and no mass transfer in the gas separators and pipes				
		- Film model for mass transfer				
		- 100% faradaic efficiency and constant charge transfer coefficient: 0.5				
		- No recombination reactions and all cells behaves the same				
Cell level	Lumped parameters	- Lumped thermal capacitance	- Accurate voltage, capacitances and resistance evaluations can be performed as a function of operating conditions	- Limited by assumption of homogeneous stack distribution temperature, concentration and pressure, neglect of some physical domains	101, 107 and 108	- Improve accuracy (reduce error to <3%)
		- Equivalent circuit model and typically based on electrochemical impedance spectroscopy (EIS)	- Easy to use and models features losses and can be used for topology designs (rectifiers-AWE)			- Increase validation range *e.g.* under unsteady conditions
		- Homogenous temperature distribution				
		- Applies Ohm's and Kirchhoff's laws				
	Distributed dynamics	- Empirical model of the velocity of gas bubbles and bubble coverage factor	- Flow phases and mass transfer can be analyzed	- Multi-phase flow can make the model complex and often require simplifications	89, 91, 95–97, 100, 102 and 103	- Improve understanding of hydrogen bubbles flow mechanism and coverage model with experimentation using accurate sensors
		- Area averaged void fraction	- Considers the interface between the gas–liquid boundaries (by averaging *e.g.* void fraction)	- In two-phase flow, relative velocity exists		- Understanding of annular flow regime
		- Homogeneous equilibrium flow	- Considers the balance of forces acting on the gas bubbles *e.g.* adhesion and cohesion or buoyancy and drag forces	- Less developed		- Experimentation under supercritical phases are required
		- No relative velocity	- Considers flow-field/regime/geometry and electrode–electrolyte interfaces	- Hydrogen is typically considered as the ideal gas		- Evaluate effect of high pressure *e.g.* on heat capacity and KOH dissolution
		- 1D–3D flow regime	- Limits and optimum conditions can be assessed	- Lack of elaborate physical model for bubble void fraction and bubble coverage		- Consider accurate estimation of overpotential and thermal behavior
		- Laminar electrolyte flowrate	- Distribution of thermal, concentration balance and pressure can be analysed	- Fick's law cannot be used if the gas molecular weight varies significantly		- Consider addition of electrolyte flowrate and product gas quality models as a function of conditions
		- Film model for mass transfer	- Considers intrinsic properties of the cells			- Consider electrolyte cycling strategies
		- Negligible gas density	- Some model considers losses and diagnosis and dynamics of the gas bubbles			- Consider multiple boundary layers and other geometries *e.g.* 3D zero-gap
		- Negligible and bubble accumulations	- Some models considers gas-crossover			- Integrate cell degradation models
		- Darcy law used for gas crossover driven by differential pressure and Fick's law for crossover driven by flux density				- Consider losses and detailed mass transfer by incorporating elaborate gas crossover models as a function of operating conditions
						- Consider negative lift coefficient and other bubble

Scale	Type	Assumptions	Pros	Cons	Ref.	Recommendations
						balancing forces e.g. wall and repulsion
	Input–output	- Reactions associated with overpotential proceed via Tafel kinetics	- Considers thermodynamics and kinetics	- Empirical and thus limited by the model validity range		- Generate more the data for higher temperature (286 °C) and direct high pressure operations e.g. for expansion of validity range of the empirical resistivity and gas purity
		- Empirical e.g. resistivity, gas evolution efficiency and gas purity	- Critical for assessment of input–output relationships and trade-offs analysis	- Homogenous temperature distribution		- Consider accurate estimation of overpotential e.g. concentration overpotential and concentration gradients in the electrode boundary layer
		- Linear resistivity at higher temperatures and negligible concentration overpotential	- Assist in predicting the cell-efficiency as a function of operating conditions including electrolyte concentration	- Charge transfer coefficient has been proven by some authors to vary with temperature		
		- Homogeneous and 1D distribution of the current	- Consider important factors such as electrode/diaphragm distance		90, 104 and 114	- Consider other factors such as bubbling rate and hydrogen as a real gas
		- Ideal gas thermodynamics law and uniform distribution of pressure and temperature		- Gas-crossover is a critical phenomenon in AWE technology		
		- Laminar electrolyte flowrate and negligible phase transition within the separators	- Simple to use and adapt			
		- Constant charge transfer coefficient				
	Degradation	—	- Relevant for stack managements and estimation of replacement costs	- Less developed for the AWE	—	- Consider generating more data and developing model correlation under intermittent conditions
			- Improves the diagnosis and control models	- A universal model is lacking and must be developed		- Develop model to be usable at stack level
Multiscale from microscale (e.g. atomic) to mesoscale (electrode)		- Based on density function theory (DFT), molecular dynamics and kinetic Monte Carlo (kMC) modelling	- Useful for design of electrocatalysts and electrolyte	- Complex and requires in-depth understanding	115–117	- More advanced operando experimental data are required to improve/ascertain predictions and simplifications
			- Models are typically experimentally validated where possible	- Costly		- Consider coupling these models to mesoscale and elaborating the catalysts active sites
			- Best captures the complex dynamics e.g. molecular dynamics	- Molecular dynamics is not suitable for simulation of larger time scale		- Consider data-driven artificial tools to predict missing level data, and manufacturing aspects
			- Provides valuable information related to mechanisms and interfaces			

3.2.2 Design and modelling of the PEM

3.2.2.1 Reducing the capital and operating costs

The design of the PEM features bipolar plate configurations. Unlike AWE, operation of PEM under balanced and unbalanced pressure conditions is possible. PEM is characterised by potential of compact stack design. Even so, PEM has higher system cost. About 50% or more of the PEM system cost corresponds to balance of plant (BOP) equipment. This is so since PEM requires serious control and management. While approximately 15–26% and 14% are contributed by the membrane electrode assembly cost for the total cost capital of the stack and system, respectively.[118] Increasing the power or size of the system and optimising manufacturing methods (ease of scaling up the production rate, particularly the electrodes) can reduce the cost of the PEM technology. On the other hand, a large current density may also be critical to reduce the cost associated with BOP. Once the technology is at the level of economy of scale, the high cost will shift to membrane electrode assembly. For the latter, reducing the noble metals especially Ir catalyst loading in the PEM will reduce the capital cost significantly.[119] The price of Ir has increased to more than double in the last decade.[118,119] Kibsgaard & Chorkendorff[119] recently evaluated the limiting factors and potentials for scale up of the PEM technology catalysts. Ir is a serious limiting factor in scaling up (thus taking advantage of economies of scale to reduce capital) of the PEM technology since Ir is normally produced at <10 tonnes per year and hence it would require roughly 40 years of Ir production to achieve $1TW_{H_2}$ production industry using PEM technology.[118,119] Furthermore, the Ir-based oxygen-evolution reaction side tends to have strong effect on efficiency (hence production costs) due to its higher overpotential. On the other hand, platinum (Pt)-based cathode is used in the PEM, even though Pt is a noble metal with numerous competitive uses and hence its use in PEM has to be reduced; it can be easily scaled to $1TW_{H_2}$ production levels. On the other hand, the none-noble catalysts such as phosphides-based catalysts are promising candidates to replace Pt, but they require higher loading to be able to achieve an equivalent performance as Pt-based cathodes, and this may be less economically attractive in the long run.[119] How the none-noble catalysts influences the compactness of the technology remains an open research question. In the short term, to accelerate the widespread adoption of PEM, reduction of Ir by novel and easy-to-scale electrode manufacturing techniques will play a bigger role in reducing the capital cost. Ultimately, the improvements in designing highly active and stable none-noble catalysts for PEM will have a stronger effect on reducing its capital and production costs. Relatively, the capital cost reduction will play a big role in the adoption of PEM electrolyser in

particular if it can be achieved while keeping almost the equivalent performance as the current state of the art technologies.[118] Nonetheless, other strategies are devoted to reducing the production costs of the technology and encompasses modifying its operating conditions such as increasing the temperature and pressure (*i.e.* the so called-high temperature (HT-PEM) and high pressure PEM (HP-PEM)). Additionally, the costs of hydrogen production using PEM like other electrolysis technologies will inevitably be reduced with availability of low cost electricity and changes in electricity (*e.g.* ancillary participation) and hydrogen markets.

3.2.2.2 Increasing the lifetime/durability

PEM technology has low durability compared to AWE. The acidic environment tend to reduce the stability of the metal and has been a major bottleneck hindering the potential use of non-noble metals in the PEM technology.[120] Currently, PEM technologies demand extensive control and management to also prevent Nafion® membrane fouling and degradation.[121] Ir is also not stable in the oxygen evolution reaction.[119] Improvement in durability will greatly reduce the stack replacement costs.[118] More work is needed to increase the durability of the PEM, including finding corrosion resistant separator plates and current collectors, and research investigation must keep track of changes in durability with changes in loading of the Ir and Pt, particularly under intermittent conditions.

3.2.2.3 Increasing efficiency and flexibility

Although many factors (*e.g.* the combination of electricity sources) are at play influencing the efficiency of the PEM, developing improved catalysts materials with capability of breaking the scaling relations (*i.e.* linear relationship between the binding energy of the intermediates) for the oxygen evolution reaction side will pay a great deal by reducing overpotential and as a consequence improve the efficiency of the technology. Concerning flexibility, low temperature (LT-PEM) PEM has shorter start-up and shut down times and hence a relatively higher flexibility. A recent study by Schnuelle *et al.*[94] compared performance of the PEM and AWE technologies under dynamic conditions, taking into account their flexibility and hydrogen production. Their results showed that although PEM has a higher flexibility, the hydrogen production rate for this technology may be lower depending on the electricity source and efficiency. The findings from these authors show that the advantageous flexibility of the PEM, though very important, cannot be treated in a manner to suggest that PEM is an all-round solution for application in variable renewable energy storage. Ultimately, hydrogen production rate, production cost, investments and stack replacement costs become major factors to incorporate in deciding on the choice of the electrolyser. This points to an important synergy between flexibility and durability, such that highly flexible technologies (capable of increasing hours of operation) must have a relatively higher durability and hence lower frequency of stack replacement. To what extent will the flexibility of PEM change with changes say from using noble to using non-noble catalysts, remains an open question especially considering the latter synergy.

3.2.2.4 Modeling of the PEM

The interesting features of the PEM electrolyser has drawn several attentions to evaluate its performance against a set of applications, primarily based on variable renewable energy. As a consequence, there is a growing number of model-based studies and model development pertaining this technology. Table 5 summarizes the models concerning the PEM technology. Similar to AWE, the PEM electrolysis is characterised by two-phase flow which tends to have a strong effect of performance of the technology, for example, formation of hot spots is linked to misdistribution of two-phase flow and current density.[123] When considering the solids such as electrodes, the model then features three phases. Models considering the aspects of PEM control and monitoring are also available in literature.[121,124,125] With variation of operating conditions, it will be necessary to interrogate the accuracy of the PEM models and further develop and validate these model under dynamic conditions. A more recent study by Sood *et al.*[126] focused on developing a generic model for the PEM taking into account auxiliaries and dynamic conditions. The model also simulate the losses and real-time efficiency under dynamic conditions, and it forms a good base for prognosis and diagnosis related to PEM.[126] The authors represented the system based model using modular bond graph and deduce that their model predicts the experiment well (with error percentage <5%). Additionally, comparative analysis of mass transfer models for the PEM is still required to ascertain the model with best predictive capabilities. Most of the authors in literature neglect the concentration losses which are best accounted for by considering elaborate mass transfer equations. The rationale for the latter neglect is that the electrolyser operates at lower current densities, however, in future the ball game may change and the current density for the PEM is expected to increase (>1.6 A cm^{-2}), thus developing model that take into consideration the overpotentials due to mass transfer diffusion is needed. Besides, it is necessary to consider mass transfer effect when designing novel cells configurations and materials. Effective models considering two-phase flow mass and heat transport aspects can be developed and tested using CFD platforms.[127] Limited models deals with cross-over and bubbles formations issues which forms part of the two-phase flow in PEM; thus more investigations are needed in this direction including experimental validations.[123,128–131] On the other hand, most model developers do not consider pressure effects correlation in their formulations. Moreover, experimentally validated universal degradation model is missing for the PEM electrolyser. The degradation model developed by Chandesris *et al.*[131] is mainly focused on membrane. VoltaChem and TNO[105] have also announced their target to develop the advanced degradation model for PEM. Additionally, few multiscale models have been reported in literature and as a consequence, more work is still needed in this direction. Ultimately, collaboration among researchers and engineers in the field to develop a universal electrolyser model (more especially multi-scale) *via* using a dedicated open source platform is required.

Table 5

PEM electrolysis models

Applications	Model type	Typical assumptions	Advantages	Disadvantages/limitations	Ref.	Possible improvements
Stack to system level	Lumped Parameters	- Uniform stack temperature	- Easy to use and feature control aspects and losses (real time)	- Experimentally dependent	122, 132 and 133	- Increase validation range under unsteady conditions
		- Ideal gas laws and 0D to quasi-1D	- Model can be formulated as dynamic model	- Complex interactions and non-linearity in the models are not simulated in details		- Consider elaborate losses taking into account auxiliaries and concentration gradients
		- Typically based on equivalent circuits or empirical or semi-empirical	- Can couple some auxiliaries such as converters and other power management electronics and assess topology	- May neglect some other domains such as the fluidic domains		
		- Equivalent circuit model is typically based on electrochemical impedance spectroscopy (EIS)				
	Distributed dynamics	- Constant charge transfer coefficient: 0.5 and typically 1D	- Relevant for evaluation of the technology under extremely varying conditions	- Geometry is oversimplified to generate usable model, without imposing excessive computational effort	94, 124, 126, 134	- Consider elaborate mass transfer *e.g.* water
		- Bulter–Volmer equation	- Useful for sizing and	- Less developed and less validated under unsteady		- Consider incorporating the

Level	Model type	Assumptions	Characteristics	Limitations	Ref.	Recommendations
		used to describe the kinetics	analysis of transport phenomena *i.e.* the multiphysics	state conditions	and 135	degradation model of the electrolyser to improve diagnostics and control
		- Water and gas flow simultaneously in the same speed. Stack repeating unit (SRU)-All cell same	- Models take into considerations the auxiliaries and control	- Each cell depending on its position in the system may behave differently from the assumed representative cell		- Consider prognostics and elaborate control (*e.g.* multi-timescale) models featuring auxiliaries
		- Homogenous temperature, uniform distribution of water and current	- Simulates real time efficiency	- Some system parameters are considered as lumped		- Consider additional channel dynamics and pressure drop and high temperature validation
			- Other models use simple graphical approach			- Consider multizonal modelling formulation to reduce model complexity
	Input–output	- Constant charge transfer coefficient: 0.5	- Predicts stack voltage, gas production flowrate and stack efficiency with reasonable agreement to experimental performance	- When model is purely empirical, the physical meaning may be lacking	136	- Consider non-linearity *e.g.* in variation of hydrogen production rate with input power, and pressure effect on voltage
		- Bulter–Volmer equation used to describe the activation losses				- Consider robust artificial intelligence algorithms to predict the missing level data
		- Uniform stack temperature	- Relevant for sensors and safety monitoring in the system	- Limited by the electrolyser design and experimental conditions		- Consider incorporating a simplified but robust degradation model
		- Ideal gas laws and 0D				
		- Empirical and semi-empirical				- Consider elaborate thermal models with cooling and water management
		- SRU-All cell same				
		- Ohm's law is used for ohmic losses				
Stack level	Lumped parameters	- Uniform stack temperature (stack is considered as lumped thermal capacitance)	- Simple model, easy to adapt to system level	- Experimentally dependent	122 and 132	- Increase validation range under unsteady conditions
		- Ideal gas laws and 0D	- Model can be formulated as dynamic model	- Complex interactions and non-linearity in the models are not simulated in details		- Consider elaborating losses in the model
		- Typically based on equivalent circuits and EIS	- Models consider losses such ohmic losses	- May neglect some other domains such as the fluidic domains		
			- Model considers double layer capacitance			
	Distributed dynamics	- Constant charge transfer coefficient: 0.5	- Semi-empirical distributed dynamics thermal models are growing and encompasses data fitting derived from dynamic experiments	- Charge transfer coefficient tend to vary with temperature	126 and 127	- Consider additional experiments to confirm an accurate exchange current density co-efficient
		- Bulter–Volmer equation used to describe the activation losses	- Takes into consideration the geometry	- Complex and computational expensive		- Consider developing and incorporating accurate temperature-dependent model and/or Lagrange multiplier technique for charge transfer coefficient
		- Ohm's law is used to describe ohmic losses		- Less developed and less validated under unsteady state conditions		- Consider different ancillaries and the associated losses and coupling simplified elementary kinetics and elaborate thermal model
		- Water and gas flow simultaneously in the same speed	- Useful for sizing and analysis of transport phenomena	- Each cell depending on its position in the system may behave differently from the assumed representative cell		- Consider more elaborate two phase flow model development on CFD platforms
		- Uniform distribution of water, current, and homogenous temperature distribution				- Consider additional channel/fluidic dynamics, pressure drop and variable water distribution
		- 1D to quasi-3D				
		- All cells are represented by 1 cell				
	Input–output	- Constant charge transfer coefficient: 0.5	- Predicts stack voltage, gas production flowrate and stack efficiency with reasonable agreement to experimental performance	- By virtue, the empirical features of the models are limited by experimental validation range	136	- Consider non-linearity *e.g.* in variation of hydrogen production rate with input power, and pressure effect on voltage
		- Bulter–Volmer equation	- Relevant for sensors, safety			- Consider extended validation

Level	Model type	Assumptions	Advantages/Uses	Limitations	Ref.	Recommendations
			monitoring and control in the stack			range *i.e.* in terms of temperature and pressure
		- Uniform stack temperature				- Consider incorporating a simplified degradation model
		- Ideal gas laws and 0D, (semi-)empirical	- Easy to use and to obtain real time polarization curves			
		- Ohm's law is used to describe ohmic losses. Water and gas flow simultaneously at the same speed. All cells are represented by 1 cell				- Consider water management model
Cell Level	Lumped parameters	- Uniform stack temperature	- Simple model and easy to adapt to stack and system level	- All physical domains are not completely taken into account	132, 137 and 138	- Increase validation range under unsteady conditions
		- Ideal gas laws	- Useful for studying global impedance of the cells	- Limited by the experimental validation range		
		- Typically based on equivalent circuits	- Useful power conversions and losses are taken into account and linked to operating conditions	- Experimentally dependent		- Consider more elaborate losses such as those based on current and pressure driven cross-over
		- Follows the Faraday's Ohm's and Kirchhoff's law	- Usually experimentally validated	- Complex interactions and non-linearity in the models are not simulated in details		
		- Double layer capacitance	- Accurate voltage description (error 1–2%)			
	Distributed dynamics	- Constant charge transfer coefficient: 0.5	- Features elaborate mass transfer at the membrane and electrodes interfaces *e.g.* electro-osmotic drag of water and the diffusivity of gas	- Models are complex and computationally expensive	120, 123, 127 and 134	- Consider more experimental validation of the model
		- Bulter–Volmer equation used to describe the activation losses	- Good for optimization of membrane thickness *i.e.* gas-crossover and ohmic resistance of the membrane	- Models are less developed and less experimentally validated		- Consider coupling simplified elementary kinetics models
		- Ohm's law is used to describe ohmic losses	- Some models considers non-ideal behavior of hydrogen *via* compressibility factor			- Consider establishing consistency in model formulations and assumption depending on the geometry and design of the electrolyser
		- 1D to 3D	- Semi-empirical thermal models are growing and encompasses data fitting derived from dynamic experiments	- Excludes the non-ideal behavior of hydrogen gas		- Consider developing an elaborate fluidic model taking into account pressure variations effects e especially unbalanced pressure conditions
		- Water and gas flow simultaneously in the same speed				- Consider multizonal modelling technique to reduce the complexity of the model
		- Balanced pressure operation	- Some models take into considerations different ancillaries			- Consider elaborate mass transfer *e.g.* with water taken into account
		- Ideal gas law assumption is prominent				
		- Cell is typically operated below the boiling point of water				
		- Two-phase flow				
	Input–output	- Constant charge transfer coefficient: 0.5	- Relevant for sensors and safety monitoring in the cell level	- By virtue, the empirical features of the models are limited by experimental validation range	139	- Consider non-linearity *e.g.* in variation of hydrogen production rate with input power, and pressure effect on voltage
		- Bulter–Volmer equation used to describe the activation losses	- Easy to use and to obtain real time polarization curves			- Consider generating elaborate models that are robust and can be easily coupled to stack and system levels
		- Uniform stack temperature	- Recent models considers water managements			- Consider improving water management model
		- Ideal gas laws and 0D				
		- Ohm's law is used to describe ohmic losses				
	Degradation	- 1D polymer electrolyte membrane model	- Can be classified as input–output model	- Degradation mechanism is complex with various interplaying factors influencing it	131	- Consider elaborating degradation mechanisms using microscale models
		- Decomposition by Fenton	- Relevant for diagnosis and	- The degradation model is missing for the PEM		- Consider long hours of

		Assumptions	Uses	Limitations	Ref.	Recommendations
	reaction mechanism for formation of radicals/metal ion-impurities		control	electrolysis		operation validation and developing the models at different scales, taking into account transport effects
	- Hydrogen peroxide formation (H_2O_2)	- Takes into account the chemical degradation of the membrane, as well as the effect of temperature and current density	- Models are only validated with single cell experiments and may be difficult to integrate to stack level where multizonal operation of cells are assumed, each group of cells having different properties or operation functions			- Consider prognostics
		- Considers ionic and electronic transport				
		- Describes the gas cross-over effects and formation of hydrogen peroxide				
		- Useful to study the time evolution of membrane thickness				
Multiscale (*e.g.* atomic level to cell level)		- Elementary kinetics	- Assessment of catalysts and reactant mechanisms interactions	- Complex	140	- Consider elaborating the catalysts active sites to improve the models predictions
		- Ionomer is fully saturated with water and hence water transport is neglected	- Help in designing and optimizing the electrocatalysts	- Molecular dynamics is not suitable for simulation of larger time scale		- Consider reducing the computational time by reducing the complexity of the model
		- Isothermal and isobaric operation of the cell	- Useful for studying degradation mechanisms			- Develop these models for coupling with degradation models and operando experimental validation
		- Mechanical constraints at some interface *e.g.* electrode/membrane are neglected	- Useful for assessing catalyst–electrolyte- membrane interface	- Due to the complexity of the models at lower scale, simplified geometric assumptions are made		- Consider incorporating robust bubble formation models which is a function of operating conditions such as pressure, higher current density, *etc.*
		- Cylindrical structure is used to simplify the complex geometry of the electrode	- Microstructural description of transport phenomena			- Consider multizonal modelling technique to reduce the complexity of the model
		- Membrane is assumed to be impermeable to O_2 and H_2 (neglect gas –cross over)				

3.2.3.1 Reduction of capital and operating costs of the SOEC

Although it is widely accepted that low-cost electricity and/or waste heat is critical for the reduction of hydrogen production cost, it is also possible to achieve similar goals *via* improving the electrolyser design from material to stack to system levels. The SOEC stack is the most expensive and sensitive component in the electrolyser and its design and operation window detect the large portion of the capital and operational costs.[24] The electrolyser stack comprises individual cells joined by electrical conducting metal interconnects in a gas-tight manner.[67,141,142] The cells are either connected in series or parallel and are classified as either button/planar or (flat) tubular type.[143,144] Stack configurations are commonly designed as planar and tubular types or according to fluid flow as co-flow and counter-flow stack (both of which differ according to the active area, but can be classified as planar configurations).[81,85,141,145,146] However, each has its own limitation.

Sunfire stack is based on the planar type and parallel flow design with an open cathode optimised to achieve a favourable trade-off between the cost, performance and degradation.[76] The planar type is characterised by higher power density, but it presently has unresolved sealing problems.[146,147] While, although the tubular type has a better start-up time, thermal cycle and no sealing problems, it is nonetheless difficult to manufacture this type of stack.[81] Other configurations include flat tube, micro-tubular designs[148] and mono-block layer built type. The geometry of the stack design is also a critical factor, and it is determined by variables such as cell area, thickness of the channels, air flow rate, stack compactness, and type of interconnects. Compactness (typically measured as power density – W cm^{-3}) and durability are the most important factors of capital cost expenditure.[149] At present, the capacity of a single SOEC stack is in the range of the 3 to 15 kW scale. Literature is rich in stack design and optimisation of the solid oxide cell operating in fuel cell mode.[146] However, with cheaper materials and economies of scale, Sunfire expects the material cost of solid oxide-based technologies to reach 150 to 100 € per stack, which translates to 40–25 € per kW (calculated at 0.65 A cm^{-2}).[76] Operating costs are affected, in addition to heat and electricity costs, by the plant availability, which at times calls for the design of an electrolyser system with additional equipment (*e.g.* a battery) or different operational strategies (*e.g.* hot standby mode). Long start-up time, low ramp rates and stack degradation increases the operating cost of the SOEC. Waste heat can be used to extend the SOEC's operation hours by keeping the electrolyser on hot standby mode, but this must be available at a cheaper cost.[150] Also, system efficiency, taking into account auxiliaries such as compressors, intermediate H_2 storage tank dynamics, H_2 recycle ($\sim$10–20 mol%) to the SOEC, feed water treatment, water management and/or product purification systems, affects the operation costs of the electrolysis system.[85,151] Increasing stack/cell operation pressure can reduce downstream SOEC product compression ratios, and reduce stack temperature variation and hence cost effectiveness.[85,151] However, caution must be exercised to limit the operating pressure within the feasible operating window as permitted by the materials to prevent any mechanical failures, increased pipe thickness requirements and air turbomachinery complexities, and the excessive internal generation of methane during co-electrolysis, and reduction of system efficiency.[85,152] Wendel *et al.*[84] discussed a trade-off between the stack operational parameters and energy storage density. Nonetheless, the trade-offs between increasing the discharge pressure and other parameters such as current density, reactant utilisation, degradation rate, temperature/ambient pressure rise, *etc.* still require in-depth investigation. Sunfire uses lifecycle costs per cumulated energy production (€ per kW per h) as a key measure for stack development, and trade-off-analyses can also take this into account.[76]

3.2.3.2 Increasing the stack lifetime/durability of SOEC

Increasing the stack lifetime/durability has called for different design and operation strategies. According to Wang et al.,[24] the stack lifetime is a function of the operating temperature rather than the operating voltage, and hence effective control of the SOECs' stack temperature can be achieved by adjusting the sweep gas flow rate. Nonetheless, this compromises the system efficiency. Thermal management is critical to minimise stack temperature gradients, which can be caused by uneven flow distributions. On the other hand, the design of an electrolyser to operate in a lower temperature window is of great interest. The state-of-the-art protonic SOECs can now operate at temperatures lower than 600 °C, compared to the conventional ion-conducting SOEC type.[67,82,153] Wendel et al.,[84] however, deduced that low temperature (<600 °C) operation is not a necessity for a system configured to operate as ReSOC. This is supported by findings from Graves et al.,[152] who demonstrated that reversible cycling between the electrolysis and fuel cell modes, possible in ReSOC, is beneficial to reduce degradation. In addition, from the stack design point of view, decreasing the active surface area of each cell in the stack improves the management of thermal stress distribution and sealing quality.[154] Zhang et al.[154] observed this effect when they conducted a long-term degradation test using a stack with a reduced active area for each cell (from 60 to 45 cm^2). The authors further modified the material and microstructure on the air-side electrode to alleviate electrode delamination issues, and used stainless steel-based interconnects in their stack design – coated with spinel – to avoid oxidation and chromium vapour formation. With ongoing cell improvements and long-term stack degradation testing, Sunfire indicated, in their 2019 publication, following 3000 hours of steady-state operation, as well as power modulations and thermal/redox cycling of their improved stack, a decrease in the area-specific resistance degradation rate from 18 to 13 mΩ cm^2/1000 hours.[76] However, further assessment of the degradation rate following longer hours of operation is still required to validate the reported value.[76] Degradation under highly dynamic conditions remains an open question.

3.2.3.3 Increasing the efficiency and flexibility of SOEC

A great deal of work is currently performed to improve the efficiency, stack size, flexibility and durability of SOECs.[76] Decisions pertaining to rectification, temperature, pressure, current density, heat source, reactant compositions (including humidity and inert), reactant utilisation, sweep gas flow rate and configurations strongly influence the efficiency of the system.[65,152] However, other operational strategies to increase efficiency have been investigated, such as thermoneutral point following and thermal management. Operating electrolyser cells near the point of thermoneutral voltage has been the assumption in most studies to increase the energy efficiency, but this strategy has a challenging requirement of high current density.[65,84,85] To improve the efficiency, thermal management (e.g. via promoting an internal exothermic methanation reaction during co-electrolysis at intermediate temperatures (500–750 °C) and elevated pressure up to 20 bar, or the use of heat-storage technologies such as phase change materials, etc.) has been discussed as a critical strategy.[152,155–158] For the effective implementation of heat storage in the ReSOC system, the key requirement is that the operating temperature in the SOFC mode (T_{fc}) must be higher than both the heat storage temperature (T_m) and the electrolyser temperature in SOEC mode (T_{ec}). The temperature difference between the heat storage and SOFC/SOEC modes, expressed by eqn (1), has a critical influence on the roundtrip efficiency; the roundtrip efficiency marginally decreases (1–2%) with an increase in the temperature difference (ΔT).

$$T_{fc} - T_{hs} = \Delta T = T_{hs} - T_{ec}$$

1

Flexibility can be divided into three aspects: scalability, operational flexibility (e.g. at various part loads, etc.) and tolerance to different fuels.[62,159–162] Both SOEC and ReSOC can be scaled up and down without significant loss in thermodynamic performance.[62,76] The ability to perform co-electrolysis reaction in the HT-SOEC, and operate the system in reversible mode are unique and well-known flexibilities offered by solid oxide cell technology, thus pointing to its tolerance to different fuels. This flexibility provides potential for thermal management.[66] In terms of operational flexibility, short start-up and shut-down times are other key factors, for which a micro-tubular SOEC have been proposed.[148] Sanz-Bermejo et al.[159] considered different SOEC thermodynamic operation modes, i.e. constant cell inlet temperature vs. thermoneutral point following, the influence of dependency of the ionic conductivity of the electrolyte on temperature in the overall system, and operation strategies such as constant steam conversion (60%) vs. constant steam flow rate to optimise the SOEC design and operation under part-load.

Thermoneutral point following was observed to have constant cell efficiency, whereas constant inlet cell temperature depicted higher cell efficiency at low current density (endothermic operation) than at higher current density (exothermic operation).[159] Higher area-specific resistance variation resulted in lower temperature variations.[159] On the other hand, higher system efficiency corresponded to constant steam utilisation at points below reference power load and constant steam flow rate at points above the reference power load.[159] Andika et al.[66] and Wang et al.[24] discussed the benefit of a SOEC system to improve the efficiency and design flexibility of the PtMeOH process. At this stage, it is crucial to point out that a trade-off exists between the electrolyser's operational flexibility and the requirements of externally coupled processes.

3.2.3.4 Models for SOEC and further optimisation opportunities

Numerous modelling studies on SOEC (not so much for ReSOC) exist, and recent focus has been on combining both stack- and system-level models towards analyses and the optimisation of the SOEC.[70,80,144,151,162–165] The reaction is either assumed to be instantaneous with constant conversion or fitted to match the experimental data.[166] García-Camprubí et al.[166] discussed fitting experimentally derived electrochemical parameters (such as pre-exponential coefficients, exponents and the forward and backward transfer coefficients) in the computational modelling of an SOEC as an important challenge in ensuring model accuracy. It is usually assumed that electrodes have a negligible electronic resistance. Stempein et al.[70] gave a good review of SOEC modelling work from the 1970s to 2013 taking into account both steady-state and transient models from 0D to 3D. Even though electrolysis models have been developed in the past years, electrolysis model development is still an active research field, especially since the technology is still improving. A major trend in the literature is to adapt the SOFC models to represent the solid oxide electrolysis process with key distinction between SOEC- and SOFC-derived models, among others, being the kinetics used. However, numerous studies are emerging and are focusing on the development of electrolysis-based models. It is not recommended to simply adapt SOFC models to SOEC processes, especially (semi-) empirical-based models as the behaviour of the cell under each underlying process is different. In addition, heat transfer in the SOEC (i.e. endothermic, exothermic or thermoneutral) is more complex than in the SOFC.[167] Wang et al.[165] developed a combined stack and system model for a SOEC, coupled with the power-to-methane process. Moreover, increased modelling efforts are directed towards electrolyser cell investigations, e.g. the modelling of electrode and electrolyte configurations and their associated performance.[70,80,168–170] Wang et al.[170] developed a three-dimensional model for a single cell to predict the performance of the cell in a cathode-supported planar SOEC and taking into account H_2O/CO_2 co-electrolysis, internal reforming reaction and multi-component diffusion. They proposed a novel and structurally optimised flow-field porous material, which improved the electrolysis efficiency (4.78% at 2.5 A cm^{-2}), uniform thermal and concentration distribution, and further lowered the cell voltage (~0.026 V at 2.5 A cm^{-2}). Other modelling and optimisation efforts are directed towards the hierarchical combination of both cell and stack models.[149,171–173]

Nevertheless, there is still a need to improve these models, e.g. by incorporating detailed cell degradation models/mechanisms and validating them experimentally over wide temperature ranges and dynamics.[162,166,169,173]

Since degradation models tend to be empirical, their accuracy will be improved by long-term field testing of the SOEC or ReSOC. A degradation-based model was developed and evaluated by Parhizkar and Hafeznezami.[174] Table 6 summarises the types of models (lumped parameters, distributed dynamic, input–output), their applications (cell level, stack level, system level and detailed multiscale and kinetics), typical assumptions, advantages and disadvantages/limitations, along with possible

areas of improvements. Among other required improvements, validation of the models considering most recently developed experimental findings and recent knowledge/performance improvements in SOEC system or SOEC materials are required. In addition, most dynamic models are validated with steady-state generated experimental data. However, for dynamic models, dynamic experiments are required. Dynamic modelling will provide valuable information for decision making, and process design and optimisation.

Table 6

Overview of SOEC models and exemplary studies

Application	Model type	Typical assumptions	Advantages	Disadvantages/limitations	Exemplary ref.	Possible improvements
Stack to system level	Lumped parameters	- Gases flow at the same speed and are ideal	- Applicable in evaluation of overall system (including stack) with its auxiliaries	- Excludes some physical domains (*e.g.* typically temperature distribution) and non-linearity involved in the electrolysis cell/stack	175–178	- Consider elaborate thermal effects, mass transfer and fluid dynamics
		- Homogenous state variables, 0D to quasi-1D	- Easy to solve/converge	- Validation with experimental data		- Consider degradation
		- Can be formulated based on equivalent circuits/kinetics/impedance elements	- Every/most parameters have physical interpretation *i.e.* no empirical efficiencies used	- Possibility of over/under-estimation and prone to numerical robustness challenges		- Consider incorporating error control ability in the model
		- Can also be formulated as a surrogate model	- Good calculation of ions and electrons flows			
		- In case the equivalent circuits kinetics are used, the voltage is determined based on Ohm's and Kirchhoff's laws		- Geometry is often neglected in these models		
	Distributed dynamic model	- Uniform temperature distribution	- Better describes the electrical response	- Increased complexity and computational time	80 and 179–184	- Consider further development and validation of models with dynamic experimental data
		- Gases are assumed to be ideal	- Fits impedance parameters and links irreversibility	- Requires a robust numerical solver		- Consider dynamic behaviour in H_2 production and feed distribution, and pressure gradients
		- Iterative calculations based on area-specific resistance (ASR)	- Couples other ancillaries such as converters	- Currently less developed		- Consider all/multiple ancillaries (anode, cathode, voltage, flow channels, *etc.*) dynamics, responses and losses, and multizone modelling strategy
		- Typically 1D, 2D, quasi-3D	- Considers non-homogeneity in state variables	- Challenges associated with modelling some additional balance of plant equipment *e.g.* actuators		- Consider elaborate thermal effects (*e.g.* conduction and convention, radiation) and degradation
		- Uniform distribution of the feed across the cells/laminar flow	- Describes geometry	- Each cell hence stack may behave differently depending on its position in the stack		- Reduction in computational time (<10 minutes)
		- Instantaneous electrochemical reaction (fast kinetics)		- Geometry may be simplified to a certain extent		- Consider additional factors affecting the current density such as coordination number of ionic and electronic particles, *etc.*
		- Repetitive unit of stack (*i.e.* one cell, interconnect and frame)	- Relevant for assessing variable energy integrated electrolysis	- Some models are validated with steady-state derived experimental data		- Consider distributed charge-transfer
		- Stack heat losses to the environment negligible				
		- One-directional flow of electric current				
	Input–output	- Butler–Volmer equation for kinetics (modified or unmodified)	- Predict performance easily especially thermodynamic performance	- Care must be taken with value of charge transfer coefficient (*e.g.* a value unique to 0.5)	163, 165, 182, 185 and 186	- Consider additional non-linearity such as in the activation potential without imposing severe complexity in the model
		- Black box and considers mostly flow	- Reduced complexity (model is generally linear)	- The typically assumed single step, single electron reaction does not give good predictions of SOEC polarisation curves		- Consider artificial intelligence techniques to train some input parameters and better predict SOEC operation
		- Either empirical or semi-empirical/analytical	- Useful in operation (input–output) optimisation of the electrolyser	- May be limited by conditions in which they are experimentally (empirically) developed and thus yield errors beyond. Thus demand careful fitting methods		- Consider widening the operating conditions of ASR models
		- Zero-dimensional (0D)		- Some models are validated with old experimental data, which may not be representative of the current SOEC		- Consider two-rate limiting steps mechanism involving adsorption of water

Level	Model type	Characteristics	Advantages	Disadvantages	Ref.	Recommendations
		- Isothermal operation and single charge-transfer reaction		performance and mostly neglect spatial configuration, and contact resistances		- Consider improving robustness of the models
		- Equilibrated Nernst equation to calculate the open circuit voltage and linear relation of voltage and current				- Consider distributed charge-transfer
		- Area-specific resistance used *e.g.* to calculate polarisation losses				
Stack level	Lumped parameters	- Homogeneous temperature and fluid	- Offers additional performance and control parameters	- Typically excludes electrode/electrolyte microstructure	162, 176 and 178	- Include safety control, prognostic and diagnosis aspects
		- Equivalent electric circuit and ideal gases	- Reduced complexity	- Auxiliary losses are neglected		- Consider thermal effects
		- Repetitive unit of cell (all cells the same)				
	Distributed dynamic model	- Repetitive unit of stack (*i.e.* one cell, interconnect and frame, called SRU)	- Offers additional performance and control parameters (*e.g.* electrode porosity and size)	- Each cell hence stack may behave differently depending on its position in the stack	187–191	- Consider validation of models with dynamic experimental data
		- Isothermal operation and 1D to 3D	- Best predicts the thermal behaviour of the cell	- Long computational time		- Consider dynamic behaviour in H_2 production and pressure drop, and reduce computational time
		- Equilibrated Nernst equation to calculate the open circuit voltage and linear relation of voltage and current	- Describes geometry	- Available models are limited to oxygen ion-conducting SOEC and therefore not adapted to proton-conducting SOEC		- Consider all/multiple ancillaries (anode, cathode, voltage, interconnects, *etc.*) dynamics and losses
		- Area-specific resistance used to iteratively calculate cell potential				- Consider elaborate thermal effects (*e.g.* radiation, *etc.*) and degradation and control aspects
	Input–output	- Area-specific resistance used to calculate cell potential	- Useful in obtaining the polarisation curve	- Limited to few parameter analyses	24 and 192	- Consider additional non-linearity such as in the activation potential without imposing severe complexity in the model
		- All cells have same behaviour as a single cell and 1D to quasi-2D	- Models have been improved overtime	- Available models are limited to oxygen ion-conducting SOEC and therefore not adapted to proton-conducting SOEC and isothermal assumption neglects the effects of heat transfer		- Consider validity of models with scale-up
		- Isothermal				- Consider incorporating a simplified stack degradation model and homogeneous medium to replace SRU
Cell-level	Lumped parameters	- Can be formulated based on equivalent circuit kinetic modelling or surrogate models	- Includes multiple cell-level ancillary dynamics and microstructure	- Excludes certain ancillaries (*e.g.* interconnects) thus rendering over-estimation if linearly scaled to stack level	162, 169, 175, 178 and 193–196	- Consider thermal effects, losses, mass transfer and fluid dynamics
		- In case the equivalent circuit kinetics are used, the voltage is determined based on Ohm's and Kirchhoff's laws	- Offers additional performance and control parameters (*e.g.* electrode porosity and size, cell efficiency)	- Care must be taken with value of charge transfer coefficient (*e.g.* typical unique to 0.5 and non-symmetrical)		- Consider more cell-level experimental validation
		- Ideal gases and no pressure drop	- Typically encompasses electrode/electrolyte modelling			
	Distributed dynamic model	- Either Darcy's law or Dusty gas model is used for anode diffusion modelling	- Offers additional performance and control parameters (*e.g.* electrode porosity and size)	- Not significantly developed	81, 169 and 197	- Consider developing these models along with continued experimentation and demonstrations
		- Charge transfer is assumed to take place at triple-phase boundaries and ideal gases	- Best predicts the thermal behaviour of the cell	- The hydrogen may behave non-ideal and must be corrected		- Consider incorporating the models to safety control, prognostic and diagnosis aspects and flow-field design
		- Homogenous physical parameters	- May better describe geometry	- Deviations in mass transfer diffusion may occur and best model needs further investigation		- Consider properties such as tortuosity factor, three-phase boundary densities, permittivity of electrolyte, *etc.* and other elaborate microstructure, morphological parameters
		- Convective flux, radiative heat transfer and pressure drop are neglected				
	Input–output	- Area-specific resistance is used to calculate cell potential and homogeneous temperature	- Simple to use *e.g.* in platform such as computational fluid dynamics (CFD) modelling	- Models may be empirical and lack physical meaning	198 and 199	- Consider active area thickness calculations
		- Fick's Law is used to calculate	- Useful to calculate the	- Predictive capabilities are prone to		- Consider detailed electro-kinetics

		concentration over-potential and/or simplified Butler–Volmer equation to calculate the activation overpotential polarisation behaviour, and empirical/semi-empirical	charge transfer and current density, which are typically not known prior	quality of fitting method (*e.g.* charge transfer co-efficient and current density are calculated by fitting experimental data)		mechanisms
	Degradation	- Simplified electrolyte model	- Assists in improving the prediction of SOEC performance under varying environments	- Empirical thus limited by apparatus and experimental conditions	172, 174, 195 and 200–205	- Consider more long-term experimentation and use of advanced characterisation methods to understand failure criteria and assess coupled phenomenon
		- Temperature is assumed uniform or modelled in the direction of flow or cross-section of the cell as 1D/2D to quasi-3D	- Considers thermal effects	- Degradation mechanism is still illusive and therefore the underlying physical phenomena		- Consider elaborate thermal effect models (with *e.g.* chemical reaction entropy, chemical component thermodynamics, Joule effect, *etc.*) and thermo-mechanical physical field
		- Typically uses ASR degradation rate measured per 1000 hours	- Permits detailed description of the over-potential through cell thickness and consider geometry	- Physical meaning may be missing if the model is purely empirical		- Consider validation of model in wide experimental parameters (*e.g.* temperature, high current density) ranges and making models convergence faster
		- Models can also be derived based on equivalent circuit kinetics		- Typically one degradation phenomenon is considered at a time, *e.g.* carbon deposition, but in reality multiple phenomenon are cross-coupled		
Cell to stack level	Multi-scale	- Butler–Volmer expression used to formulate kinetics of the interfacial charge transfer, and models are 1D to 3D	- Considers multiple ancillary interactions and transients	- Reaction mechanism remains unclear in particular for co-electrolysis	80, 149, 171, 192, 206 and 207	- Consider elaborate thermal effect models and diffusion and incorporation of artificial intelligence techniques to predict missing data, and multizones
		- Temperature gradients in solid components assumed to be constant	- Assist in analysis for scale-up from lab-scale cell-level to stack-level and the associated optimisation	- Limited validity range and models tend to be highly dependent on the material		- Consider properties such as tortuosity factor, three-phase boundary densities, permittivity of electrolyte, *etc* and flow-field
		- Constant charge carrier concentration		- Some diffusions are neglected (*e.g.* axial pore diffusion)		
Cell to system level	Multi-scale	- 2D–3D solid oxide cell stack model with 0D models of balance of plant components	- Gives more detailed performance and therefore permits effective control and reduces degradation	- Increased complexity and computational time	80 and 207	- Consider properties such as permittivity of electrolyte, *etc* and validation with dynamic experiments
		- 1D + 1D thermo-fluidic transport along the thickness and the flow direction at repeating unit level	- Considered 3D stack temperature distribution and combined multiple ancillaries (electrode-cell-stack)	- Difficulties in obtaining convergence		- Consider incorporation of artificial intelligence techniques to predict missing data, and multizones
		- Butler–Volmer used		- Not significantly developed		- Consider data-driven approach, along with robustness and reduced amount of data/sampling points
				- Model only focused on steady-state evaluation		
Atomic to cell level	Multi-scale	- Couples Density Function Theory (DFT), transition state and electrochemical theory at different scales	- Effect of temperature and manufacturing aspects on the characteristics can be studied and predicts electrode design aspects	- Model validated for a limited experimental range	208 and 209	- Consider detailed experiments on different microstructure performance and possible microstructure reconstructions
		- Atomistic, meso and continuum scales		- Less developed		- Advance the models by coupling to different scale
				- Complex		
Co-electrolysis kinetics	Elementary kinetics	- RWGS catalysed by nickel	- Good prediction of the experimental data and typically validated	- Limited experimental/validity range *e.g.* pressure ~2 bar	192, 210 and 211	- Consider wide experimental conditions and carbon deposition effects and all relevant aspects of the mechanism, deeper investigation of possible electrochemical reduction of CO_2, active area thickness and thermal/chemical effects
		- Butler–Volmer is used to describe the kinetics of the electrochemical reaction		- Lack of understanding of reaction mechanism		
				- Not significantly explored, including other potential catalysts		

Further developments of steady-state and dynamic models considering electrolyser stack, cell-level models, reaction kinetics, different loss mechanisms, flow field designs and the integration of electrode, electrolyte, current collectors and interconnects to form multi-physics and multi-scale models are still required.[98] Moreover, improvements of SOEC technology regarding ramping flexibility, start-up time and system integration in a global power-to-methanol process are still needed.[66,80,170,212]

Other improvements are required in the areas of strategies for thermal management, water separation from the product stream, control of reactant utilisation, H_2 and/or oxidant tank storage, and the reduction of balance of plant (BOP) power consumption considering practical operating windows. The focus should also be directed towards the integration and optimisation of this technology in a power-to-methanol process, with detailed analysis and the investigation of various system configurations, off-design conditions and dynamics. The integration and optimisation of HT-SOEC and/or ReSOC for H_2O/CO_2 co-electrolysis and pure H_2O electrolysis for application in methanol synthesis represent a new and growing field of R&D. Evaluation of trade-offs between the energy efficiency and capital cost, at variable electrolysis (*i.e.* load-dependent) efficiency, as will be introduced by the variation in the load, must be investigated.

4. CO₂ as a precursor: sources, capture technologies and synergies with (co-)electrolysis.

The CO_2 sources differ in terms of their process chemistries; hence, the composition and purity of the CO_2 stream and the dedicated CO_2 capture methods and economics will also differ.[213] The sources of CO_2 include fossil fuel-based electricity/heat production processes, cement plants and chemical plants such as fermentation, incineration

processes, iron/ferric reduction, pulp production and CO_2 already in the atmosphere. Table 7 shows the different sources and their respective concentration of CO_2. Each of these processes allows for the integration of thermal energy and components, such as H_2 and O_2 (see Fig. 3).[213,214] In this section, we qualitatively discuss the synergy. However, a quantitative assessment of advantageous synergistic factors still deserves further investigation and must be coupled to downstream methanol synthesis. Components such as O_2 and H_2 are often needed in the CO_2-producing sources as oxidant or combusting and reducing agents, respectively. For example, the O_2 that originates from the electrolysis can be used as an oxidant during ferric reduction, the incineration of municipal waste, the gasification of biomass, calcination, black liquor combustion and biogas upgrading to remove the hydrogen sulfide (H_2S).[213]

Table 7

CO_2 sources and typical capture methods.[12,215,224,236] Modified from Ghiat & Al-Ansari[215], Roode-Gutzmer *et al.*[12] and Roussanaly *et al.*[236] Only the typically used methods' highlights are presented in this table

CO_2 source	Waste CO_2 stream compositions[a] (%)	% contribution to globally available CO_2[a]	Typical capture method	Estimated capture cost [\$ per ton-CO_2-captured][a]	Highlights on challenges of the typically used capture method
Flue gas					
Gas turbine plants	3–10	40–60	Amine-based chemical absorption	\$70–100	- Regeneration of amine is energy intensive - Amine (or amine-composite) degradation, evaporation and corrosion
Coal power plants	12–15		Amine-based chemical absorption	\$35–202	
Steel production	20–30	7–19[b]	Post-combustion capture (amine based)	~\$59–83	
Cement process	20–33	6.97	Amine-based chemical absorption	~\$70–178	
Fired boiler of oil refinery and petrochemical plant	~8	~1.5–2	Adsorption method (*e.g.* zeolites)	~\$71–166	- Adsorption methods are characterised by low CO_2 uptake and high sensitivity to moisture
Natural gas-fired boilers	7–10	~2.5–5.52	Amine-based chemical absorption	—	- Regeneration of amine is energy intensive, degradation, evaporation and corrosion.
Oil-fired boilers and ethylene production	11–13	—	—	—	—
Hydrogen production	15–60	~2	Pre-combustion	—	—
Aluminium production	1–2	—	—	—	—
Others					
Iron reduction	20–30	—	Water condensation	—	—
Biogas	35–55	—	Pressure swing adsorption (PSA), water scrubbing chemical absorption (*via* organic solvents)	<\$23	- Water scrubbing uses a significant quantity of water, features hazardous chemicals, biological contaminants, and electrical and cooling requirements. - PSA requires notable maintenance and H_2S pre-removal, and higher loss of methane *via* off-gas.
Biomass gasification/combustion	3–8	—	Calcium looping, chemical absorption	—	- Uncertainties in biomass deployment and land availability, poor mechanical stability of CaO.
CO_2 from the atmosphere	≥400 ppm	—	Direct air capture (*e.g.* organic, metal carbonates or sorbents)	\$300–1500	- Costly and challenging due to low concentration of CO_2. - Energy intensive
Bioethanol plant (fermentation)	Up to 100	—	Water condensation	—	- Volumetric amount of CO_2 is low
Urea/ammonia synthesis	Up to 100	~0.84	Water wash process	< \$23	—

Table Footnotes

[a] Since it is difficult to obtain the exact numbers as different sources gives different values obtained in different years, we present mostly a range for the CO_2 composition in each source, the % contribution to global CO_2 and capture costs. In addition, different assumptions and methods may yield different cost estimates.

[b] Values may overlap with iron industry, as the steel production and iron industry are typical combined together.

Fig. 3
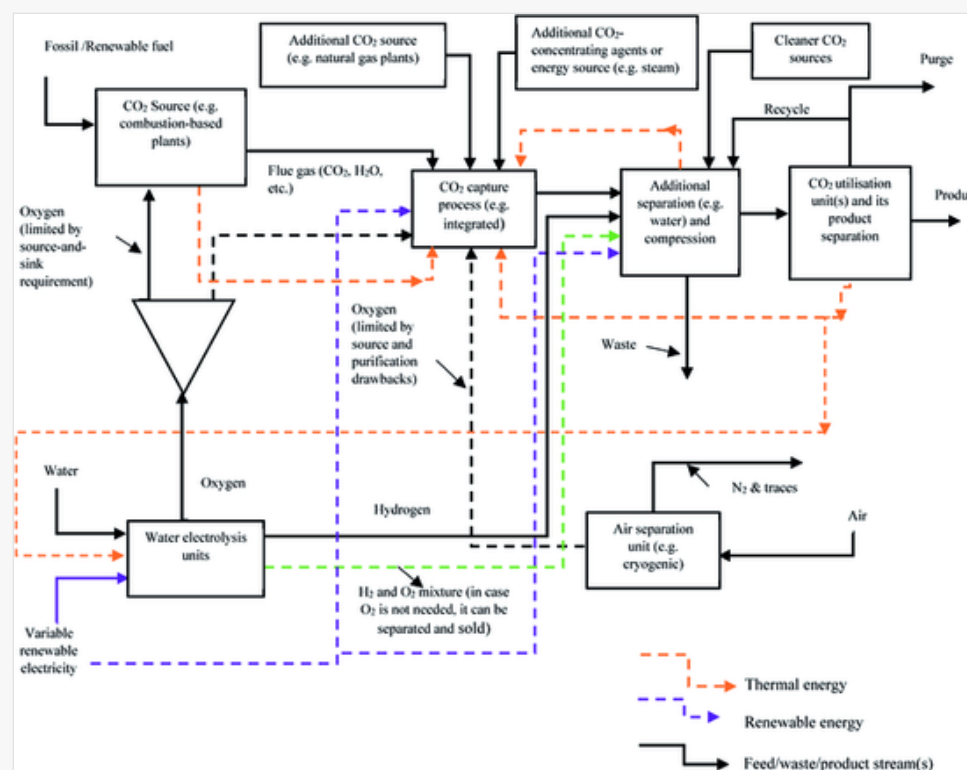
A simplified generic superstructure showing synergies of renewable energy, electrolysis products, capture and subsequent CO_2 utilisation. Modified from Dwivedi *et al.*[214]

The use of this ultrapure O_2 eliminates or reduces the composition of the inert components in the reactant stream. Furthermore, the availability of O_2 from the electrolysis may eliminate the need for a costly air separation unit.[213,214] In addition, to concentrate the CO_2 stream, dilution with water can be performed since CO_2 is soluble in water. However, the latter may require further separation of water, which may come at a cost. Excess thermal energy from the CO_2-producing processes such as black liquor combustion can be used, for example, in steam generation for the electrolysis process. Capture technologies are also largely influenced by the concentration or pressure of CO_2 inlet stream to the capture system, sorption efficiency or capacity and catalyst materials, which strongly influence the technology's energy penalty and cost. However, in case oxygen from the variable renewable electrolysis is used in the CO_2 source and in the absence of storage, the associated dynamics may cascade to the capture process, resulting in a varying flow rate of CO_2 output.

Several review papers have been published in literature concerning CO_2 sources, capture technologies, storage and utilisation. Among the most recent review papers, few consider a holistic view on the CO_2 source, capture technologies and cross-sectoral linkages with other processes. Most recently, Ghiat & Al-Ansari[215] briefly reviewed different CO_2 sources, the capture methods and technologies, and major carbon capture and utilisation projects that focus on their *trans*-sectoral symbiosis within the energy, water and food nexus. Koytsoumpa *et al.*[50] discussed CO_2 emissions and their separation methods from various industries, and assessed the potential CCU pathways with the emphasis on CO_2 conversion to fuels and chemicals. Mikulčić *et al.*[216] evaluated various CCU pathways and their potential for integration with renewable energy systems. This section extends to briefly assess the synergies of the renewable energy, electrolysis, CO_2 sources and their corresponding carbon capture technologies, as well as the integrated CO_2 capture technologies and capture process flexibility.

4.1 CO_2 sources with high-cost capture methods

4.1.1 CO_2 production from power and cement plants (flue gas)

Fossil fuel power and cement plants are the largest CO_2 emitters (see Table 5). The capture of CO_2 from flue gases occurring on these plants can mainly be accomplished with processes based on absorption, adsorption and membrane technologies.[2,12,217] These include different process flow sheets such as capture processes that occur before (pre-combustion) and after combustion (post-combustion), respectively, in the case of coal-fired plants. Pre-combustion capture involves the removal of CO_2 from a gas stream from a gasification process prior to combustion. Post-combustion consists of CO_2 capture after combustion (coal fired) with air.[218] Absorption processes that involve amine-based scrubbing using chemical absorption and regeneration simultaneously are considered the most mature capture technology, particularly the technology based on mono- and di-ethanolamine (DEA) solvents.[2,219] Extensive research involving advanced sorbents and process modelling is currently in progress.[220–223] However, these processes are characterised by high energy usages (3886–6480 kJ per t per CO_2 and corresponding to 30 wt% (for lower cost) to 15 wt% (for higher cost bend) mono-ethanolamine (MEA) solvent concentration) for the regeneration step, and corrosion of the MEA solvent is prevalent when its concentration is higher than 30 wt%.[224] Dry and semi-dry adsorption (physical and chemical) methods are also currently being developed, which involve sorbents such as activated carbons, zeolites, metal organic frameworks, amine-based solid sorbents, carbon nanotubes, potassium and sodium carbonates.[225,226] Fixed-bed and circulating fluidised beds with simultaneous regeneration (temperature-swing) are currently used and are being investigated.[227] Membrane technology can easily be applied to the separation of CO_2 from flue gas as a result of the inherent permeating properties of the favourable CO_2.[228] Membranes such as glassy and rubbery polymers, molecular sieves and several inorganic materials are excellent for CO_2 separation.[228,229] The oxy-combustion process which consists of the combustion of coal with pure oxygen has been found to produce high-purity (99.7 mol%) CO_2. Due to the use of pure oxygen usually obtained from cryogenic air separation, the method is expensive. However, by-product oxygen from the electrolysis process can be coupled to this method.

4.1.2 CO_2 from the atmosphere

The CO_2 in the atmosphere has been increasing steadily.[229] Capturing and recycling CO_2 from the atmosphere presents a potential sustainable and economic avenue for chemical production.[2] Direct air capture (DAC) technology can be used to capture CO_2 from the atmosphere. The advantage of direct air capture lies in the fact that it can be deployed anywhere; hence it does not need to be in a location near the point source, and it is not compromised by the presence of SOx and NOx.[2] An extremely low concentration is present in the atmosphere (slightly above 400 ppm) relative to the other gases.[2,229] This makes DAC technology expensive due to its higher energy penalty, resulting from using a large volume of air in the capture system.[2,12,229] This challenges the integration of this process with CO_2 conversion processes. However, Climeworks, Switzerland, is commercialising DAC technology.[12,229] Metal hydroxide solutions have been used to capture CO_2 from the atmosphere by a start-up company called Carbon Engineering, Canada. Other technologies include the amine-based capture technology that has been commercialised by Global Thermostat. Alternatively, adsorption-based methods can also be suitable for CO_2 capture from the atmosphere.[229]

4.1.3 CO_2 from steel production

The production of steel makes use of carbon-based fuels and reductants. It is an energy-intensive process with various by-products such as methane, hydrogen, CO_2, CO, sulphur, NOx, metals, chlorine-containing compounds, polycyclic aromatic hydrocarbons, benzene, toluene, ethylbenzene and xylenes. However, the concentration of CO_2 in the waste stream is higher (20–30%) than the normal flue gas.[12,230] Post-combustion capture is the typically used method for capturing CO_2 from this process. Membrane-based technologies are currently being developed for commercial application.[230]

4.1.4 CO_2 from natural gas-based plants with chemical cooping

Natural gas-based plants emit 7–10% CO_2.[215,231] Although the CO_2 can be captured from natural gas-based processes using amine-based technologies, chemical looping is also gaining interest.[215] The chemical looping combines both fuel conversion and capture technology, and is gaining interest due to its potential to reduce the energy penalty. Depending on the application, chemical looping can be classified as chemical looping combustion, chemical looping reforming and chemical looping water splitting.[213] Chemical looping was originally proposed for use with gaseous fuels, especially natural gas.[215,216,231] During chemical looping, oxygen – carried *via* a metal oxide, *e.g.* based on metals such as Fe, Mn, Cu, Ni – is used for the combustion of the fuel. The metal oxide forms as a product of metal redox reaction in which air is used for oxidation. The advantage of the process is that it keeps nitrogen out of the product gas stream, thereby reducing the energy cost of process capture.[215,216,229,231,232] For example, the chemical looping combustion and water splitting methods produce a mixture of CO_2 and H_2O as final product, which can easily be separated by condensation. Although the chemical looping process is gaining interest in scientific literature, it has not yet reached commercial scale. However, attractive economic incentives for the CO_2-capture technologies will likely make this process more economically attractive. Research in the modelling and optimisation of this technology is in demand.

4.1.5 CO_2 from ammonia production, biogas and the biomass gasification/combustion plant

For ammonia production, CO_2 has to be removed from the N_2 and H_2 streams. This CO_2 can be used for methanol production. With the H_2 derived from electrolysis, only N_2 purification process will be the source of CO_2 in the ammonia synthesis chain. For separating CO_2 from N_2, a water wash process can be used. Alternatively, although marred by challenges of feedstock and land availability, respectively, if implemented at a significant scale, biogas and biomass can be a sustainable source of CO_2. Usually, biogas production is based on anaerobic digestion and impurities such as hydrogen sulfides (H_2S: 0.1–3%), CO_2 and moisture are produced.[233] Water scrubbing and swing adsorption technologies are typically used for biogas upgrading. Due to its high flexibility, high auto-control degree, low investment costs, reduced energy consumption, no water requirements and zero biological impurities, swing adsorption technology (typically pressure swing adsorption) is gaining increased interest for capturing CO_2 from the biogas output stream. Hybrid technologies that combine, for example, membrane and cryogenic separation, can also be used, but they are not commercially available yet and cryogenic separation is relatively expensive. Membrane-based technologies, as well as water scrubbing for biogas upgrading, generate significant pollutants. To further reduce the separation effort, Schorn *et al.*[234] recently evaluated the potential use of oxy-fuel technology for biogas upgrading with oxygen originating from the electrolysis and energy supplied from renewables. Applying oxy-fuel separation in biogas leads to CO_2 and H_2O as waste products, which can further be easily separated by condensation to capture CO_2. Biomass gasification or combustion usually produces a stream containing H_2, CO_2, CH_4 and CO. CO_2 is captured using the calcium looping method, which uses low-cost and highly reactive CaO-based sorbents.[2] Emerging research trends are also showing the potential of integrating chemical looping combustion to biomass.[216]

4.2 Additional CO_2 sources with low-cost capture methods

4.2.1 Calcination and iron reduction

During the calcination process, which involves the use of calcium carbonate ($CaCO_3$), CO_2 is produced. Since this industrial process generally includes the elimination of inert (N_2) gas used or found in air as reagent gas, the vented product stream contains CO_2 and H_2O. CO_2 from the resulting CO_2/H_2O mixture can then be captured using condensation to eliminate water.[213] Iron-reduction using conventional blast–furnace processes converts solid carbon (coke) to CO in the presence of pre-heated air as an oxidant.[213] As a result, during the smelting process, inert (*e.g.* N_2) gas is produced. However, the use of pure O_2 produced from the electrolysis process instead of pre-heated air can eliminate inert gas from the smelting process, further producing CO_2, which can be cheaper to separate. On the other hand, H_2 from the electrolysis can also be used in the process as a reducing agent, thus resulting in a less endothermic process and hence higher energy efficiency. Moreover, in the case of co-electrolysis, a mixture of CO/H_2 from the co-electrolysis process can be used in the direct reduction of iron. The end products of direct reduction process are CO_2 and H_2O, which can again be separated using condensation, which is relatively cheaper than, for example, amine scrubbing.

4.2.2 Pulp and paper, and fermentation industries

The pulp and paper industry contributes about 1–2% of CO_2 to the globally available CO_2.[2,183] In the pulp and paper industry, air typically used to combust post-boiling liquor, which contains various by-products, such as inorganics like nitrogen. With the use of electrolysis-derived oxygen, the nitrogen can be eliminated. Thus, the main by-products from the combustion of black liquor, after recovering reagent materials, are steam and CO_2.[213] The CO_2 can then be separated from the H_2O *via* condensation. Excess oxygen can also be used in pulp bleaching.[213]

During fermentation, an oxygen-sparse environment (which can be sourced from the electrolysis) is required during metabolic glucose conversion. This produces high-purity CO_2 and bioethanol. The industrial fermentation typically uses corn, sugar cane, grapes and/or sorghum. This process produces high-purity CO_2, thus resulting in its simplified subsequent capture. However, the main challenge with this process is the annual fluctuations in the production of bioethanol (hence CO_2) and the low volumetric amount of CO_2 generated from it.[12]

4.3 Integrated capture technologies and flexibility

Each of the capture technologies has an advantage, which may be a shortcoming of another technology. Thus, a hybrid system can be created on the basis of the synergies to improve the capture efficiency and reduce cost.[229] This can be achieved by developing materials that can perform multiple functions (a one-pot solution), *e.g.* absorption and adsorption, or staging different methods in series or in parallel.[229] For example, the combination of membrane and absorption in a staged manner (series), whereby the membrane can serve to concentrate the CO_2 stream on the upstream, thereby reducing the energy penalty during downstream absorption and desorption. On the other hand, a one-pot process may combine two or more capture methods in one unit (using dedicated materials) and/or a combination of capture and conversion in one step (*e.g.* amine-assisted capture and conversion to methanol).[235] A one-step capture and conversion process offers process intensification by removing the desorption, compression, transportation and storage of CO_2, and thereby showing potential for improving the energy efficiency and profitability if it is technically feasible.[229,235] A recent review by Wang & Song[176] covers these topics.

However, integrated capture deserves further investigation and optimisation, in particular the assessment of trade-off between the operating and capital costs.[236] This must be tied to the further assessment of the flexibility in the CO_2 capture technologies, which will also be critical, considering the case of the high penetration of variable

renewable energy.[216] For example, during the period of high energy demand or supply deficit and since the capture technology uses energy, the CO_2 capture technology operation will have to be reduced or halted (CO_2-containing fuel stream vented) to accommodate immediate high-priority loads and thus calling for a quick and safe response of the capture units, taking into account the variation in the loads.[216] This means that a capture system that is operated with renewable energy needs to start up or shut down quickly to avoid further energy penalty under these conditions. Similarly, during surplus renewable energy periods, the capture technology operation can be increased. This will be required to respond faster, thereby improving the economics of CO_2 capture if the energy is free, and reducing the amount of vented CO_2.

Alternatively, parts of the capture units (less energy intensive) can be operated under low-energy supply or high demand, while others, which are energy intensive, can only be operated during the period of surplus energy supply. For this purpose, the storage of intermediate products that results from each capture stage may be needed, and their viability is strongly linked to the availability of other downstream processing units. However, these aspects deserve further investigation, including how the effects of the flexible operation of the CO_2 capture cascade to influence the techno-economics of the downstream utilisation of CO_2, *e.g.* conversion to methanol and/or the capture business model(s). This will also require a detailed modelling of the capture technologies, considering the associated dynamics.[220,221]

5. Methanol synthesis

This section gives an overview of thermodynamics and reaction mechanisms, state of the art of the reactor technologies, along with their advantages and disadvantages, and developments in catalyst technologies and kinetics models that pertain to the methanol synthesis process. The section further extends to discuss the methanol synthesis reactor design, the associated modelling assumptions and key optimisation requirements. Studies and aspects critical for the application of catalysts, reactor technology design and modelling in the power-to-methanol chain are also highlighted.

5.1 Overview of thermodynamics and reaction mechanisms

Historically, methanol synthesis from syngas operating conditions changed from high pressure (>300 bar) and temperature (350–400 °C) to low pressure (<100 bar) and temperature (200–300 °C). Recently, the focus is on changing the synthesis feed gas composition to pure CO_2/H_2. The reactions of syngas to methanol (Syn2MeOH) and pure CO_2/H_2 to methanol (dCO$_2$-MeOH), eqn (2) and (3), respectively, are exothermic and proceed by a reduction in the number of gas moles, hence low temperature and high pressure favour these reactions. Nonetheless, temperatures above 200 °C are used, with current industrial $Cu/ZnO/Al_2O_3$ catalysts, to enhance the reaction kinetics. [237–239] The reactions are also limited by equilibrium at higher temperature, and the occurrence of side reactions such as the endothermic RWGS reaction (eqn (4)) may jeopardise product selectivity.[240]

$$CO + 2H_2 \leftrightarrow CH_3OH, \Delta H^{\circ}_{298\,K} = 90.8 \text{ kJ mol}^{-1}$$

(2)

$$CO_2 + 3H_2 \leftrightarrow CH_3OH + H_2O, \Delta H^{\circ}_{298\,K} = 49.2 \text{ kJ mol}^{-1}$$

(3)

$$CO_2 + H_2 \leftrightarrow CO + H_2O, \Delta H^{\circ}_{298\,K} = 41.6 \text{ kJ mol}^{-1}$$

(4)

The equilibrium methanol yield is higher for Syn2MeOH than for dCO$_2$-MeOH.[239,241,242] The activation energy of a CO_2 hydrogenation reaction is higher (~68 kJ mole^{-1}) compared to that of CO hydrogenation over a commercial $Cu/ZnO/Al_2O_3$ catalyst.[239,242] The carbon source of methanol is controversially argued to be either from CO or CO_2 or both. The lack of agreement on the reaction mechanism over a $Cu/ZnO/Al_2O_3$ surface is a big debate in literature.[243–256] Earlier, it was adopted that CO is the source,[257] then with isotope labelling, it changed to CO_2,[243,246,249,256,258–262] and more recently to both depending on a Cu^+/Cu^0 ratio.[250,256,263–265] Literature also recently agreed on the presence of the RWGS reaction in the reaction mechanism even though the roles of its products (CO and H_2O) remain a point of debate. Whether these reactions proceed stepwise or simultaneously, on which active sites (and their state *i.e.* either oxidised or reduced and the number or mechanism *i.e.* competitive or dual, *etc.*) and role of each product or intermediate represent crucial points to be explored further.[266]

A recent study by Nielsen *et al.*[267] deduced that CO is detrimental to the methanol formation rate at low conversions, while at high conversion (leading to ≥1 mol% of methanol at the effluent), it serves to scoop water *via* the water gas shift reaction (see illustration in Fig. 4 and Fig. 5(a and b)). Nielsen *et al.*[267] further concluded that CO_2 is at-least the major carbon source of methanol over Cu-based catalysts. Fig. 5 shows the relative methanol formation rate variation with the percentage concentration and the partial pressure of CO_2, plotted using experimental data. Methanol formation increases fast in the presence of CO_2 (see Fig. 5(c)) even at low CO_2 partial pressure.[267] However, it would be key to reconcile this with theoretical models which seems to predict CO hydrogenation as having the fast methanol formation rate[268,269] than CO_2 hydrogenation, contrary to experimental findings such as those from Nielsen *et al.*[267] and isotope-labelling experiments which claims the rate of methanol formation to be faster for CO_2 hydrogenation.
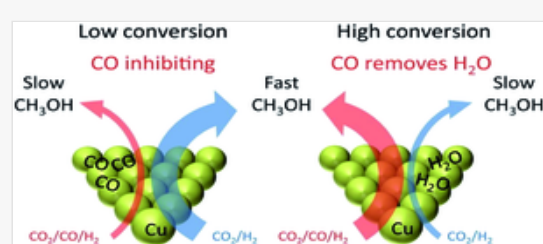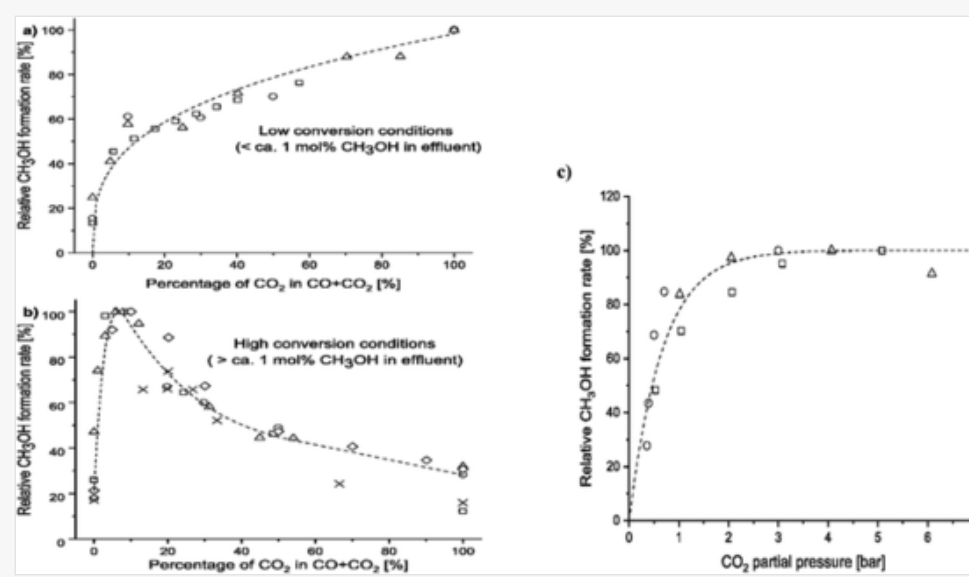

Fig. 4

Illustration of the effect of CO at low and higher conversion points as deduced by Nielsen *et al.*[267] Reproduced from Nielsen *et al.*[267] with permission from Elsevier.

Fig. 5

Variation of the methanol formation rate with the percentage and partial pressure of CO_2 over Cu–ZnO based catalysts. The experimental data ($\circ$, $\square$, Δ, $\times$) was taken several authors who performed their experiments in the temperature range, T: 496–523 K.[267,270–272] Reproduced from Nielsen *et al.*[267] with permission from Elsevier.

The intermediates for eqn (2) could be either methoxy (H_3CO^*) from the formyl route or hydroxyl considering the hydrocarboxyl route, however methoxy is mostly reported as a stable intermediate. On the other hand, eqn (3) seems to proceed either *via* a formate (formate or methoxy intermediate) or carboxyl route or hydrocarboxyl (hydroxyl or hydroxymethylene), but mostly formate hydrogenation has been observed on different catalysts and surface measurements shows that both methoxy and formate are the mostly abundant intermediates.[262,273,274] Conversely, the hydrocarboxyl route has also been shown to be kinetically favoured due to its lower energy barriers. However, studies on reaction mechanisms and hence intermediates are not concluded.[266,275] Other intermediates, mechanisms and side reactions are possible and may be a function reaction conditions, feed composition and catalyst sites.
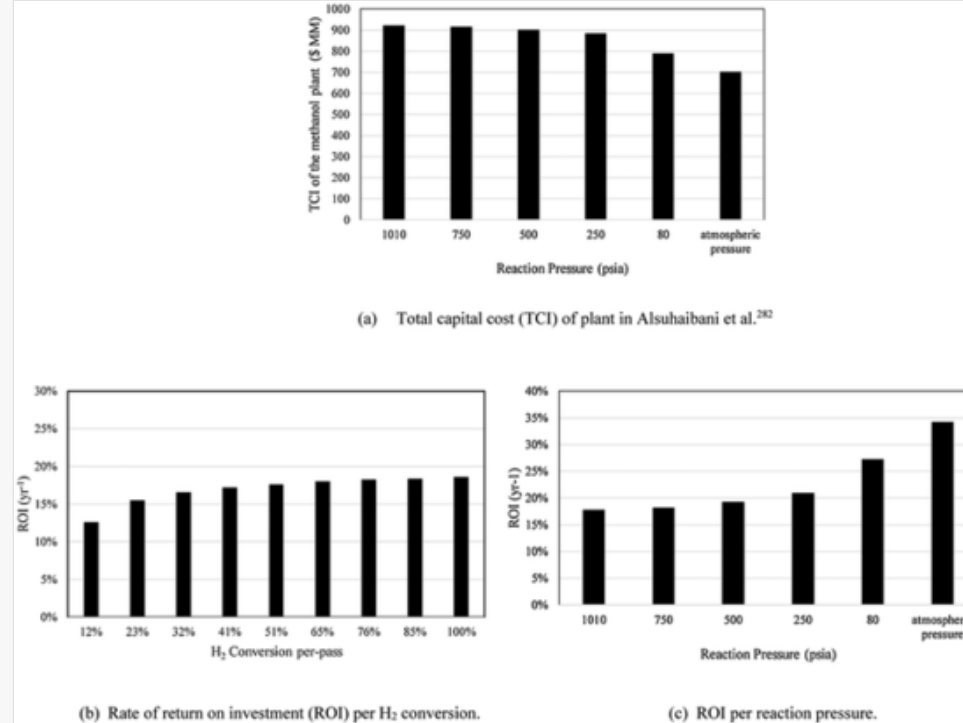
5.2 Catalysts and kinetic models

5.2.1 Catalysts for methanol synthesis using pure syngas (CO/CO$_2$/H$_2$), CO/H$_2$ and CO$_2$/H$_2$ as a feed

Methanol can be produced from both homogenous and heterogeneous catalysts. Heterogeneous catalysts based on Cu–ZnO–Al$_2$O$_3$ are industrially applied.[276,277] Homogenous catalysts are receiving growing interest due to their ability to operate at lower temperatures (<150 °C).[277] The main limitations of homogeneous catalysts are their problematic recovery from products and required additives to achieve high catalytic activity.[247,278] Heterogeneous catalysts are preferred in terms of stability, separation, handling, reuse, and with them, lower costs of reactor design are possible.[276] Many good reviews are available in the literature that compare recent progress on heterogeneous catalysts for methanol synthesis.[11,263,276–281] The catalyst affects the process energy efficiency, productivity and economics.[282]

Alsuhaibani *et al.*[282] investigated the impact of catalyst development concerning the methanol reaction system on the entire profitability of the plant and hence identified the catalytic performance metrics that could enhance the profitability of the plant more significantly as shown in Fig. 6. They observed that synthesising the catalyst with higher single pass conversion, although important to increase yield, has a smaller effect on the entire plant's profitability (measured by ROI), but reducing the methanol synthesis reaction pressure to less than 5.4 atm, with an efficient catalyst capable of operating in that window, can significantly increase the profitability of the plant. The reduction in the capital cost is due to a reduction in the number of compression units, whereas the operating cost is mostly influenced by a reduction in the input energy requirements for compression (hence improved energy efficiency). The savings improves the ROI by a factor of about two.

Fig. 6

(a) Total capital cost (TCI) of plant in Alsuhaibani et al.[282]

(b) Rate of return on investment (ROI) per H₂ conversion.

(c) ROI per reaction pressure.

Variation of methanol plant costs (a), and ROI (in (b) and (c)) with H_2 conversion and reaction pressure, respectively. Reproduced from Alsuhaibani et al.[282] with permission from Elsevier.

Table 8 summarises the performance of the catalysts emanating from the most recent studies that have been tested and found to be best performing. Special reference is made herein to the key research activities and new directions in the aspect of catalyst development. Heterogeneous catalysts can be metal-based (e.g. Cu, Au, Ag, In, Pd, Fe, Ce and Pt) or metal-oxides with various support materials.[239] Industrial Cu−ZnO−Al$_2$O$_3$-based catalysts were originally optimised for syngas hydrogenation reactions.[282] When the feed is changed to a pure CO/H$_2$ mixture, the industrial catalyst performs very poorly. In addition and owing to debates about reaction mechanisms, and the advantages of syngas and CO$_2$/H$_2$ reactions as highlighted in Section 2, limited work focuses on the development of catalysts suitable for methanol synthesis using a feed with pure CO/H$_2$.[238,244,279,283–286] High CO concentrations in the feed promote reactions that form undesirable by-products such as carbonyls over commercial Cu/ZnO/Al$_2$O$_3$. Seidel et al.[286] also discussed that long-term operation with pure CO/H$_2$ feed is unreasonable due to significant reduction in activity. However, a pure CO/H$_2$ reaction to methanol does not form water, which is an advantage of this reaction. Crucially, Van de Water et al.[284] and Zhang et al.[285] presented Cu/CeO$_2$ and Rh/MoO$_3$/SiO$_2$, respectively, as candidate catalysts for methanol synthesis from a pure CO/H$_2$ feed.

Table 8

Catalysts for methanol synthesis from mostly CO_2/H_2 feed, and pure CO/H_2 feed

Catalyst	Temp. (°C)	Pressure (bar)	Feed ratio[f]	Feed	GHSV	CO$_2$ or CO conversion [a] (%)	MeOH selectivity (%)	MeOH yield (%)	Space time yield (MeOH)	Average pore diameter (nm)	BET surface area (m^2 g^{-1})	Reactor	Ref.
Cu/ZnO/Al$_2$O$_3$	250	50	3 : 1	CO$_2$/H$_2$	—	27	28	—	—	—	—	Zeolite membrane	1
Cu/AlCeO – prepared by co-precipitation	200–280	30	3 : 1	CO$_2$/H$_2$	14.4 L g$_{cat}^{-1}$ h^{-1}	2.9–23.7	85–33[b]	7.4[c]		22.7	80	Vertical fixed bed	290
Cu/ZnO/Al$_2$O$_3$ – prepared by co-precipitation	160–220	7	9 : 1	CO$_2$/H$_2$	2.4–22.5 L g$_{cat}^{-1}$ h^{-1}	13[d]	23 [e]	2.7	11.9 mmol g$_{cat}^{-1}$ h^{-1}		65.54	Fixed-bed	305
Cu/CeO$_2$ – prepared by deposition–precipitation	195	25	33%	CO/H$_2$	—	—	—	—	—	—	—	Six parallel fixed-bed micro reactor	284
Cu/In/Zr/O – prepared by co-precipitation	250	25	—	CO$_2$/H$_2$	18 L g$_{cat}^{-1}$ h^{-1}	1.48	79.7	1.18	0.079 g g$_{cat}^{-1}$ h^{-1}	—	—	Fixed-bed	307
Pt/film/In$_2$O$_3$ – prepared by cold	30	1.013	3 : 1	CO$_2$/H$_2$	—	37.0	62.6	23.2	0.355 g	—	63.6	Dielectric	314

Catalyst	T (°C)	P	Ratio	Feed	GHSV/Flow	Conv.	Sel.	Yield	STY			Reactor	Ref.
plasma/peptide-assembly									g_{cat}^{-1} h^{-1}			barrier discharge plasma reactor	
Cu/ZnO/Al$_2$O$_3$ – prepared by polyol	240	1.013	9 : 1	CO$_2$/H$_2$	—	14	86	12.0	—	23	30	Tubular	306
CuO/ZnO/CeO$_2$ – prepared by polyol	240	1.013	9 : 1	CO$_2$/H$_2$	—	20	90	18	—	22	38	Tubular	306
Cu/ZnO – prepared by co-precipitation	200–260	28	3 : 1	CO$_2$/H$_2$	3.05 L g_{cat}^{-1} h^{-1}	20.3	63.2	12.8	—	23.5	128	Fixed-bed	315
In$_2$O$_3$ – prepared by calcination	330	40	3 : 1	CO$_2$/H$_2$	15 L g_{cat}^{-1} h^{-1}	7.1	39.7	2.82	3.69 mol kg_{cat}^{-1} h^{-1}	—	—	Tubular	316
In$_2$O$_3$ – prepared by calcination	270	40	3 : 1	CO$_2$/H$_2$	15 L g_{cat}^{-1} h^{-1}	1.1	54.9	~0.65	0.78 mol kg_{cat}^{-1} h^{-1}	—	—	Tubular	316
Cu/ZnO/ZrO$_2$ – prepared by co-precipitation microfluidics	280	50	3 : 1	CO$_2$/H$_2$	10 000 h^{-1}	21.0	34	7.14	486 g kg_{cat}^{-1} h^{-1}	20	40	Fixed-bed	317
Re/TiO$_2$ – facile impregnation method	<150	60	—	CO$_2$/H$_2$	—	—	82	—	—	—	—	—	278
CuO/ZnO/ZrO$_2$ – prepared by polymeric precursor	240	30	3 : 1	CO$_2$/H$_2$	1.8–6 L g_{cat}^{-1} h^{-1}	16.1	42	7.0	—	9.2	58.5	Tubular fixed-bed reactor	274
CuIn/SiO$_2$ – prepared by a solvo-thermal method	280	30	3 : 1	CO$_2$/H$_2$	20 L g_{cat}^{-1} h^{-1}	9.8	78.1	7.65	13.7 mmol g_{cat}^{-1} h^{-1}	4.9	161.6	Tubular fixed-bed reactor	318
Rh/MoO$_3$/SiO$_2$ – prepared by atomic layer deposition	250	40	1 : 1	CO/H$_2$	—	1.4	61	0.85	215.8 ± 21.6 μmol g_{cat}^{-1} min^{-1}	—	—	Fixed-bed	285
CoGa – prepared by incipient wetness impregnation	250	30	3 : 1	CO$_2$/H$_2$	—	1	63	0.63	—	—	290	Fixed-bed	319
PdZn/(carbon-activated nanotubes) – prepared by impregnation	250	30	3 : 1	CO$_2$/H$_2$	1.8 L g_{cat}^{-1} h^{-1}	6.30	99.6	6.3	37.1 mg g_{cat}^{-1} h^{-1}	—	121	Fixed-bed	320
Cu/ZnO – prepared by solid phase grinding	250	30	2.9 : 1	CO$_2$/H$_2$	2.16 L g_{cat}^{-1} h^{-1}	29.2	83.6	24.4	—	~3.04	34.7	Tubular fixed-bed	321
Pd/(rod Ga$_2$O$_3$) – prepared by impregnation	250	50	3 : 1	CO$_2$/H$_2$	6 L g_{cat}^{-1} h^{-1}	11.80	45.78	5.31	—	—	16.69	Tubular fixed-bed	322
Pd/plate Ga$_2$O$_3$ – prepared by impregnation	250	50	3 : 1	CO$_2$/H$_2$	6 L g_{cat}^{-1} h^{-1}	17.33	51.62	8.93	—	—	21.87	Tubular fixed-bed	322
Pd/In$_2$O$_3$ – prepared by calcination	300	50	4 : 1	CO$_2$/H$_2$	>21 L g_{cat}^{-1} h^{-1}	>20.0	~70.0	—	0.89 g g_{cat}^{-1} h^{-1}	—	—	Tubular micro-reactor	323
Pd/Ga$_2$O$_3$ – prepared by co-precipitation	250	50	3 : 1	CO$_2$/H$_2$	18 L g_{cat}^{-1} h^{-1}	19.6	51.5	10.1	—	—	—	Fixed-bed	324
Cu/ZnO – prepared by co-precipitation	250	50	3 : 1	CO$_2$/H$_2$	18 L g_{cat}^{-1} h^{-1}	11.7	36.1	4.2	—	—	—	Fixed-bed	324
Pd/SiO$_2$ – prepared by co-precipitation	250	50	3 : 1	CO$_2$/H$_2$	18 L g_{cat}^{-1} h^{-1}	0.05	100	0.05	—	—	—	Fixed-bed	324
Pd/Zn/TiO$_2$ – prepared by solvent-free chemical vapour impregnation method	250	20	3 : 1	CO$_2$/H$_2$	0.916 L g_{cat}^{-1} h^{-1}	10.3	61	6.3	2040 mmol kg^{-1} h^{-1}	—	—	Tubular	325
Pd/Zn/(ZnO + CdSe) – prepared by heterojunction method	270	45	3 : 1	CO$_2$/H$_2$	18 L g_{cat}^{-1} h^{-1}	14.4	64.9	9.3	0.60 g g_{cat}^{-1} h^{-1}	—	—	Tubular fixed-bed	325
Pd/Zn/ZIF-8 – prepared by calcination	270	45	3 : 1	CO$_2$/H$_2$	21.6 L g_{cat}^{-1} h^{-1}	~22	~50.0	11	0.65 g g_{cat}^{-1} h^{-1}	—	38	Fixed-bed continuous-flow micro reactor	326
ZnO/ZrO$_2$ – prepared by co-precipitation	315–320	50	(3–4):1	CO$_2$/H$_2$	24 L g_{cat}^{-1} h^{-1}	>10	86–91	—	730 mg g_{cat}^{-1} h^{-1}	—	44.3	Fixed-bed	327
CuNi$_2$/CeO$_2$-NT – prepared by impregnation	260	30	3 : 1	CO$_2$/H$_2$	6 L g_{cat}^{-1} h^{-1}	17.8	78.8	14.0	18.1 mmol g_{cat}^{-1} h^{-1}	—	33.6	Tubular fixed-bed	328
Cu/ZnO/Al$_2$O$_3$/Y$_2$O$_3$ – prepared	230	50	3 : 1	CO$_2$/H$_2$	10 L	20.2	69.3	14.0	0.39 g g_{cat}^{-1}	—	108	Fixed-bed	329

Catalyst	Temp (°C)	Pressure (bar)	Ratio	Feed	GHSV/WHSV	Conv.	Sel.	Yield	Loading			Reactor	Ref.
by co-precipitation					g_{cat}^{-1} h^{-1}								h^{-1}
Cu/ZnO/Al$_2$O$_3$/Y$_2$O$_3$ – prepared by co-precipitation	230	90	3 : 1	CO$_2$/H$_2$	10 L g_{cat}^{-1} h^{-1}	29.9	89.7	26.8	0.57 g g_{cat}^{-1} h^{-1}	—	108	Fixed-bed	[329]
Cu/SBA-15 – prepared by impregnation	210	22	3 : 1	CO$_2$/H$_2$	—	13.9	91.3	12.7	—	6.99	458	Micro fixed-bed	[330]
Cu/Zn/Ga/LDH – prepared by co-precipitation	270	45	3 : 1	CO$_2$/H$_2$	18 L g_{cat}^{-1} h^{-1}	18.8	47.8	9.0	0.60 g g_{cat}^{-1} h^{-1}	—	—	Tubular fixed-bed	[331]
CuO/ZnO/ZrO$_2$/WO$_3$ – prepared by co-precipitation	240	30	2.7 : 1	CO$_2$/H$_2$	2.4 L g_{cat}^{-1} h^{-1}	19.7	49.3	9.7	—	13.8	128	Fixed-bed	[332]
Cu/ZnO/Al$_2$O$_3$ – prepared by co-precipitation	250	50	3 : 1	CO$_2$/H$_2$	18 L g_{cat}^{-1} h^{-1}	19.7	48.1	9.5	0.637 g g_{cat}^{-1} h^{-1}	—	—	Flow reactor	[333]
PtW/(SiO$_2$) – prepared by bimetal carbonyl hydride	200	30	3 : 1	CO$_2$/H$_2$	—	2.6	92.2	2.4	0.10 mol g_{cat}^{-1} h^{-1}	—	—	Fixed-bed	[334]
Cu/ZnO@m-SiO$_2$ – prepared by solvothermal treatment and impregnation	250	50	3 : 1	CO$_2$/H$_2$	6 L g_{cat}^{-1} h^{-1}	9.8	66.6	6.53	136.6 g kg_{cat}^{-1} h^{-1}	4.0	589	Fixed-bed	[335]

Table Footnotes

[a] Depending on the feed the conversion either refers to CO or CO$_2$ conversion.

[b] In the order of increasing temperature from 200 to 280 °C.

[c] The yield increased up to 260 °C and then stated to decrease (thus this value reported is the highest yield obtained at 260 °C).

[d] The value as measured at 200 °C for a Cu/ZnO/Al$_2$O$_3$ with compositions of 45/45/10 mol%.

With its potential for large CO$_2$ utilisation, significant research is focused on finding better catalysts favouring the direct CO$_2$ hydrogenation reaction (CO$_2$/H$_2$) to produce methanol.[238] Cu–ZnO–Al$_2$O$_3$-based catalysts exhibit low selectivity (<90%) and conversion (<40%) for the direct CO$_2$ hydrogenation reaction under normal conditions (temperature: 200–300 °C, pressure: 30–80 bar, and a H$_2$/CO$_2$ ratio of 3 : 1).[11,276,279,287,288] The thermodynamic equilibrium conversion of CO$_2$ is said to be around 25.78% at 473 K and 30 bar following the Benedict–Webb–Rubin equation.[287,288] Candidate catalysts based on Pd/In$_2$O$_3$, In$_2$O$_3$/ZrO$_2$, CeO$_2$ support, Cu/ZnO/Al$_2$O$_3$/Y$_2$O$_3$ and Cu–ZnO–ZrO$_2$ are promising for selective CO$_2$ hydrogenation to methanol, but are also characterised by low conversion (<30%). An In$_2$O$_3$/ZrO$_2$ catalyst was tested by Martin *et al.*[289] and found to have reduced activity loss (8% in 400 hours) due to water-induced sintering. Ceria oxide (CeO$_2$) is attractive due to its ability to strengthen the CO adsorption on active Cu sites, thereby inhibiting the progress of RWGS and methanol decomposition reactions, ultimately enhancing the selectivity to methanol.[290,291]

To overcome challenges such as deactivation at higher temperatures and/or catalytic particle agglomeration, bimetallic catalysts such as Pd–Cu/SiO$_2$, Pd–Zn/TiO$_2$, Pd–Ga, Pd–Zn, Cu–Fe, In–Pd, Cu–Co, Co–Ga, Ni–Ga, carbides, lanthanum oxides (Cu/LaO$_x$) and nickel (*e.g.* Cu–Ni)-based catalysts are proposed.[287,290–293] A Ni–Ga-based catalyst developed as Ni$_5$Ga$_3$/SiO$_2$ shows promising performance since it remains active and selective at temperatures as high as 300 °C.[293] Pd-based (*e.g.* Pd–Zn, Pd–Ga) catalysts show attractive performance under low pressure operations.[292,294,295] For example, a PdZn/TiO$_2$ catalyst developed by Bahruji *et al.*[296] achieved a CO$_2$ conversion of 10.1% and methanol selectivity of 40% at 20 bar and 250 °C. Other tested catalyst materials include Cu–ZrO$_2$, Cu–ZnO/SiO$_2$, Cu–SiO$_2$, Cu–Ni, Cu–TiO$_2$ and the metal–organic frameworks (MOFs) as the porous support to anchor/stabilise the Cu/ZnOx catalyst.[297,298]

From an industrial point of view, the methanol catalyst should improve to fulfil the following requirements:[16,278,279,282,290,299–304]

• Low pressure drop and moderate diffusion restrictions, *i.e.* a factor of pellet size and shape design (*e.g.* daisy shape highlighted as optimal[304]).

• High activity and selectivity, which decreases by-product formation.

• High thermal and mechanical stability.

• Tolerance to poisons (*e.g.* water, sulphur, chlorine, nickel/iron, carbonyls) and process dynamics (*e.g.* intermittent power supply) – which reduces feed purification requirements and cost, and improves process efficiency.

• High activity at low pressure (<50 bar) and low temperature (≤150 °C or Huttig temperatures) compared to industrial conditions (temperature ≥200 °C and pressure ≥50 bar).

The industrial Cu/ZnO/Al$_2$O$_3$ catalyst will likely remain a benchmark catalyst for several years to come due to its superior activity, stability and economic advantages compared to other catalysts.[9,247,282] However, the findings from Lo and Wu,[305] based on Cu/ZnO/Al$_2$O$_3$ with different compositions, give hope that reasonable selectivity and conversion can be achieved at low temperature and pressure conditions (180–200 °C and 7 bar, respectively). Opportunities exist to further decrease the temperature and pressure with the use of different materials and/or preparation methods (*e.g.* Allam *et al.*[306]) or use of plasma catalysis.[287] There is developing literature that approached this indirectly by investigating the interaction between Cu and ZnO (or any other promoter of concern) and morphological changes that probe further insight into how the catalyst and its preparation methods can be optimised.[266,298,307–312] For example, the Cu–Zn and/or Cu–ZnO synergy model developed by Kuld *et al.*[313] can be utilised to optimise catalysts by developing predictions that can be further tested with experiments. Wang *et al.*[309] also combined experiments and DFT calculations to study the metal synergistic interaction of a Cu–ZnO–ZrO$_2$ catalyst.

Limited work investigates the performance of catalysts under dynamic conditions as they will be prevalent in power-to-methanol processes using solar and wind as the energy sources.[299–301,336] These dynamics could also be introduced by the consequence of failure in the performance of the balance of plant equipment such as imperfect mixing. Kalz *et al.*[299] highlighted the importance of considering dynamic conditions when designing catalysts systems, and further assessed implications and key actions needed to ensure that chemical systems are best adapted (resilient and flexible) for highly dynamic conditions, *e.g.* at time scales between a few milliseconds for heat and

mass transfer changes and a few hours typical for catalysts restructuring *e.g. via* morphological changes or sintering processes. The potential negative influences that can be introduced by dynamic operating conditions on catalysts include sintering, oxidation, the formation of carbides, dissolution or leaching, composite formation, formation of metal complexes, and – ultimately – the loss in product quality.[337]

On the other hand, the potential positive effects that can be introduced by this mode of operation include the regeneration of active sites, *etc.*, depending on the process conditions and catalyst materials.[249,291] For example, as cited by Kalz *et al.*,[299] Topsøe[300] performed the *in situ* characterisation under dynamic variations of the feed-to-methanol reactor from $H_2/CO/CO_2$ to CO_2 free synthesis and back, which depicted a positive change in the methanol yield. In contrast, Zurbel *et al.*,[~~326~~336] using an integral reactor and $Cu/ZnO/Al_2O_3$ as a catalyst, reported a loss of 4.5% and 4.7% in CO_2 conversion and methanol yield, respectively, under dynamic operating conditions, even though the temperature inside the reactor and catalyst stability remained less affected. However, more discriminating experiments in aspects of long-term catalyst stability and kinetics under dynamic operating conditions are required to confirm potential the benefits.[300,338] Therefore, dynamic operation may either reactivate or deactivate the catalyst. Future studies must investigate this from an atomic to bulk catalyst and reactor scales. Spectroscopic methods will be critical in this regard.

5.2.2 Kinetic models

Four categories of kinetic models for methanol synthesis exist.[264] Category 1 assumes reactions 2–4 to occur, hence CO_2 and CO as sources of methanol.[241,261,339,340] Category 2 assumes reactions 2 and 3, but not the RWGS reaction.[249,341] Category 3 assumes reactions 3 and 4, but excludes CO hydrogenation, hence only CO_2 as the carbon source of methanol.[255,264,342] Lastly, Category 4 assumes reactions 2 and 4, but excludes CO_2 hydrogenation, hence only CO as the carbon source of methanol.[257] The most used are the models of Bussche and Froment[255] and Graaf *et al.*[261] Although recent literature suggests an Eley–Rideal mechanism, these models are based on Langmuir–Hinshelwood (LH) or Langmuir–Hinshelwood–Hougen–Watson (LHHW) by nature, which requires knowledge about the reaction mechanism. These models have different validity windows (pressure, feed and temperature). They also differ on assumptions regarding active sites (*e.g.*, Graaf *et al.*[261] two-active sites, Park *et al.*,[241] Seidel *et al.*[339] and Slotboom *et al.*:[264] three-active sites, while Bussche and Froment:[255] one-active site) and rate-determining steps.

Additionally, the models are outdated and exclude the latest developments, such as catalyst morphological changes.[264] The model of Graaf *et al.*[261] is partially physically sound and tends to predict one surface concentration twice.[255,264,343] Earlier, the source of this dual prediction of the same species concentration was thought by Bussche and Froment[255] to emanate from assuming all three reactions (2–4). However, with the use of different active sites, this was debunked by Seidel *et al.*[339] Regardless, the use of reactions 3–4 (noting that reaction 2 is a summation of 3 and 4) only in the model formulation is convenient and reduces parameters, hence helps attain model simplification as a critical driver. From a reactor modelling perspective, Leonzio[344] compared the kinetic models of Graaf *et al.*[261] and Bussche and Froment,[255] and deduced the model of Bussche and Froment[255] as being better in describing the industrial methanol reactor.

Recently, Slotboom *et al.*[264] used similar data sets compared to the model of Graaf *et al.*,[261] Bussche and Froment,[255] Seidel *et al.*,[339] Villa *et al.*,[257] and Ma *et al.*,[345] along with the six and ten parameter models they proposed. Fig. 5 shows the performance comparison of their six-parameter model (Np = 6) with the model of Graaf *et al.*,[261] Bussche and Froment,[255] Seidel *et al.*,[339] and experiments. Slotboom *et al.*[264] screened different rate-determining steps using a regression method.

From their study, it emanates that the original model of Graaf *et al.*[261] performs poorly compared to that of Bussche and Froment,[255] as shown in the plot of CO_2 conversion and methanol selectivity depicted Fig. 7. However, it performs better when regressed. The authors attributed this to be potentially from the use of data obtained using an older MK-101 catalyst in the regression of the original model of Graaf *et al.*[261] Both models of Graaf *et al.*[261] and Bussche and Froment[255] do not accurately predict data outside their training sets. Besides, Category 2 and Category 4 models represent the system more poorly. Moreover, at pressures higher than 30 bar, the model of Bussche and Froment[255] predicts a constant response on CO_2 conversion, and the model of Seidel *et al.*[339] best predicts the experimental data with reduced standard errors (see Fig. 8), but their model is complex. Nonetheless, the model of Seidel *et al.*[339] is developed for unsteady-state conditions, while that of Slotboom *et al.*[264] is focused on steady-state operation and Seidel *et al.*[346] recently issued a correction to their original model *i.e.* Seidel *et al.*[339] Furthermore, Slotboom *et al.*[264] deduced that the best-fitting rate-determining step is the HCOOH* dissociation to OH* and HCO* for CO_2 hydrogenation (* means adsorbed), while for RWGS, it is the CO_2 dissociation to CO and O. Nonetheless, more discriminating experiments are needed since the statistical differences were minor on the tested dataset and the six-parameter model, which was the simplified version of their 10-parameter model, which best predicted the data. However, their proposed model is characterised by a large error in the activation energy of RWGS reaction 4.3, errors in methanol and water concentration for which the authors advocated for more experimental data collection and formulation of experiments with water and/or methanol in the feed to improve the model.

Fig. 7
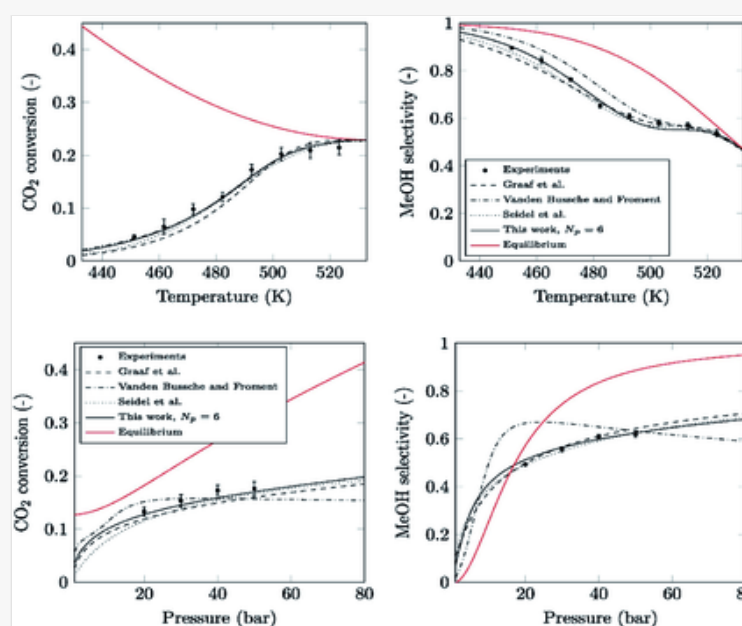
A plot of CO_2 conversion and methanol (MeOH) selectivity *versus* temperature (at a pressure = 40 bar, GHSV = 3000 h^{-1}) and pressure (at a temperature = 493 K, GHSV = 3000 h^{-1}) considering a stoichiometric feed ($H_2 : CO_2$ ratio of 3 : 1) over the commercial (Johnson Matthey-CP-488) $Cu/ZnO/Al_2O_3$ catalyst. Reproduced from Slotboom *et al.*[264] with permission from Elsevier.

Fig. 8
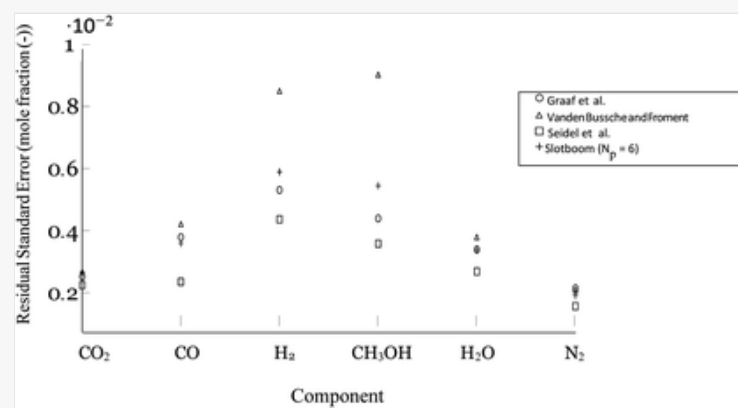
Residual standard errors of each component mole fraction per kinetic model. This depicts large errors and difficulties in predicting for hydrogen and methanol mole fraction. Reproduced from Slotboom *et al.*[264] with permission from Elsevier.

Table 9 gives a summary of the kinetics models (steady state and dynamic) with a focus on the most recently developed (2014–2020) and most used models derived over Cu-based commercial catalysts, their rate expressions, validity range, key assumptions, strengths and weaknesses. From an evaluation of these studies, assumptions based on three active sites (*i.e.* the oxidised and reduced centers separated) have become the recent trend as model developers seem to claim that this approach best predicts the experimental data. However, it is still not very clear which assumption is really the best as some researchers still assume two active sites and still find their models to fit their experimental data points very well. In addition, there is still no clear distinction in performance when different rate-determining steps are assumed. Most of the global kinetics presented in literature lump elementary steps together. On the other hand, care must be taken when selecting the rate-determining step of the RWGS reaction. Moreover, some authors do not tend to disclose the entire validity range of the models, with prominent exclusions being the carbon oxide ratio (COR) and stoichiometric number (SN) ranges, while other models are only validated for limited range. Interestingly, most recent models tend to take the limiting effect of water into account and are mostly developed for pure CO_2 hydrogenation. Nestler *et al.*[347] proposed that future experiments should consider high CO_2 feed content (in syngas feed), fibre optics for hot spot detections and improved kinetic model formulation. Considering the latter, Nestler *et al.*[348] extended their previous model given in Nestler *et al.*[347] to study the temperature profile of non-isothermal-polytropic miniplant reactor. They compared their updated model with that of Graaf *et al.*,[261] and Bussche and Froment,[255] and deduced that all models poorly predicts temperature profile. On the other hand, operations under hydrogen deficit (contrary to the excess or stoichiometric which is usual considered) may be possible in the context of power-to-methanol and therefore experiments with low partial pressures of these components are needed to adjust the models. In addition, parameter identifiability (*e.g.* considering both additional independent measured information and reducing the number of unknown parameters while ensuring that the model is physically sound and with minimal correlations) and/or kinetic inverse and sensitivity problems deserve further attention in order to improve model predictive capabilities and variance, and this must be coupled to the development of dynamic kinetics models for methanol synthesis.[349] Furthermore, deactivation models and probable side reactions must be included. Even though Siedel *et al.*[286] attempted to correct their model by including the probable deactivation and side reactions, the model is still marred by the fact that it was validated with experiments beyond the interesting kinetic range (<500 K) and its lack of improved identifiability. Furthermore, Seidel *et al.*[286] failed to detect some side components in the gas chromatography with ion-molecular-reaction mass spectrometry that they used, while Park *et al.*[241] considered dimethyl ether (DME) kinetics developed from a different catalyst. Outcomes from most recent studies such as Svitnic *et al.*[350] can provide valuable insights in the aspect of by-product formation. To support model developments, further detailed experiments on catalyst intermediates and/or adsorption constants, axial/radial temperature profile, and deactivation are needed. Nonetheless, a number of studies[351–353] consider formulating kinetic models using non-commercial catalysts and provide valuable insights on the reaction mechanism and potential reduction of apparent activation energy, thus helping scientists and engineers understand and improve the performance of the non-commercial catalyst in question. Validation of kinetic models in semi-pilot and pilot plants under relevant industrial conditions is required. Other models are formulated based on power law, artificial neural networks, micro-kinetics with DFT and kinetic Monte-Carlo.[273,354–357] Power law represents numerous possibilities to fit the experimental data, which can yield inaccurate predictions if not handled with care, and are valid for a limited range of conditions.

Table 9

Most used kinetic models and most recent (2014–2020) kinetic models based on Cu-containing commercial catalyst

Key assumptions	Validity range	Strength(s)	Weaknesses	Ref.
Steady-state kinetic models				
- Two active/adsorption sites	T: 483–518 K	- Measured both sub- and over-stoichiometric conditions	- Yields two concentration of the same species at once	
- Stepwise hydration of CO and CO_2 as mechanism	P: 15–50 bar	- Better predict most experimental data after regression	- Limited validity range	
- Both CO/H_2 and CO_2/H_2 to methanol, and RWGS are considered	COR: 0.1–1		- Based on outdated catalyst data	261
- Competitive adsorption	SN: 1.5–8.5	- Wide SN range	- Poor activity obtained from this model probably due to the less active catalyst used to develop the model	
			- Poor prediction of hot spot temperature	
			- Poor prediction of data beyond the training set	
			- Too many parameters in this model	
			- Probable deactivation neglected	
- One active site (CO_2 and heterolytic decomposition of H_2)	T: 453–553 K	- Best predict the methanol synthesis reactor	- Limited validity range (pressure ≤ 50 bar)	255
- Carbonate species mechanism	P = 15–51 bar	- Accounts for the limiting effect of water formation	- Fails to predict data beyond the training sets (extrapolation leads to significant errors)	
- Only CO_2/H_2 to methanol and RWGS	COR: 0.2–1		- Catalyst data used for model validation may be outdated/old	
			- No data on the stoichiometric number was provided	

			- for this model	
			- Model not validated COR<0.2	
			- Too many parameters	
			- Cannot predict data generated from feed containing pure CO	
			- Predict a constant CO_2 conversion at higher pressure (>51 bar)	
- Three active sites	T: 503–613 K		- DME kinetics used were developed from another catalyst	241
- Original reaction mechanism of Graaf *et al.*	P: 50–90 bar	- Accounts for the rate-limiting effects of high water content	- Parameter set not completely presented	
- Both CO/H_2 and CO_2/H_2 to methanol, and RWGS	COR: 0–1		- H_2 shortage (SN < 2) is not investigated for this model and thus renders stoichiometric validity range questionable	
- DME kinetics included (side reaction)	SN: 2–6		- Deactivation neglected	
- Three active sites	T: 503–533 K	- Better predictive capabilities and identifiability	- Complex with highly correlated parameters	339 and 346
- Both CO/H_2 and CO_2/H_2 to methanol, and RWGS	P: 30–60 bar	- Takes into account the most recent catalyst and knowledge developments	- Adsorption isotherms are assumed to be constant	
- Lumped elementary steps	COR: 0–1		- Experimental data fitted excludes kinetically relevant low temperatures (<500 K)	
			- Deactivation aspect of the catalyst not considered	
- Three active sites	T: 450–573 K	- Reduces the parameter identifiability problem (simplified to six parameters)	- Few and thus non-discriminating data sets are used and thus more experiments are needed	264
- Formate mechanism (elementary reaction adapted from Bussche and Froment)		- Fitted on new experimental data sets	- COR and SN not stated	
- Only CO_2/H_2 to methanol and RWGS	P: 20–70 bar	- Better predict beyond the boundaries/outside training sets	- Model is based only on surface abundant species (hydroxyl, methoxy and formate groups)	
- Lumped fitting parameters		- Considers latest catalysts developments and knowledge of reaction mechanism	- Contains large errors at low pressure and low hydrogen concentration	
		- Valid for different industrial catalyst	- Prediction errors in methanol and water concentrations	
- Two active sites	T: 473–593 K	- High accuracy towards measured data	- Kinetic expression not finalised	347
- Based on mechanism of Graaf *et al.* with exclusion of CO hydrogenation path	P: 50–80 bar	- Accounts for limiting effect of water	- Better description of diffusion and heat transfer is still required for this model and further experimental test to ascertain its accuracy	
- Only CO_2/H_2 to methanol, and RWGS	SN = 2	- Consistent behaviour towards SN and valid for higher pressures	- Parameter identifiability not considered	
	COR: 0.001–1.0		- CO hydrogenation not considered	

Dynamic kinetic models

- Both CO/H_2 and CO_2/H_2 to methanol, and RWGS	T: 503–533 K	- Avoids prediction of one surface concentration twice	- Experimental data fitted excludes kinetically relevant low temperatures (<500 K)	
- Three active sites (oxidised centres for CO, reduced centres for CO_2, and active centres for heterolytic decomposition of H_2) and varying depending on the gas composition	P: 30–60 bar	- Includes the most recent physical effects descriptions/developments	- Probable deactivation of the catalyst and side reactions are neglected	
		- Identifiability is considered and thus reduces the kinetic model	- Complex with highly correlated parameters	339, 346 and 349
- Lumped elementary steps	COR: 0–1	- Accounts for catalyst morphological changes and therefore changes in active sites	- Low hydrogen partial pressure/hydrogen deficit not considered and therefore model is prone to errors under these conditions	
			- Limited validity range and deactivation aspect of the catalyst not considered	
			- Dynamic experiments were performed over constant temperature and pressure and space velocity	
			- Most kinetic parameters are generated from steady-state experiments and therefore less improved identifiability	

Micro-kinetics and kinetic Monte-Carlo give insights about the reaction mechanisms, but are characterised by severe complexity and longer computational time.[273,354,357] In addition to gathering more data, future work should focus on simplification of the model, while incorporating the latest and most relevant insights for better predictions.[252,254,256,358,359] For example, the incorporation of synergetic effects and surface morphological changes (*e.g.* incorporating the kinks, steps and other defects, the Zn

substituted Cu such as in the work of Jo *et al.*[360] and Ovesen *et al.*[361] is advocated and must not compromise model simplification. As the accuracy improves, insights beyond what can be experimentally tested will be gained and this will scale to reactor modelling, designs and optimisation.

5.3 State-of-the-art reactor technologies with their advantages and disadvantages

Three categories of reactors, using solid catalyst for methanol synthesis exist: gas-phase, three-phase and membrane reactors.[254,362,363] Quasi-isothermal fixed-bed reactors, operated in the gas phase, are the most-used technology for methanol synthesis. The work of Dieterich *et al.*[10] and Bozzano and Manenti[254] gives detailed summaries of different types of commercial and semi-commercial methanol synthesis reactors and their advantages and limitations, and schematic diagrams. About 60% of the worldwide methanol is produced from the adiabatic quench reactor from Johnson Matthey, while 27% is generated through Lurgi technology.[12,362] Johnson Matthey quench reactors suffer from faster catalyst deactivation due to irregular flow distribution and the formation of variable hot and cold regions, hence more by-product formation.[12,254,281,364] They also have low per pass conversion. The Lurgi reactor has higher per pass conversion ($\sim$40%), but still features a recycle that can make it slightly costly and the reactor design complex.[12,34,38,254,281] Packed bed reactors typically have less effective heat recovery (in particular at higher heat transfer rates or highly exothermic reactions), which is a limitation to the exothermically characterised methanol synthesis process that requires good temperature control.[254,362,363] Membrane reactor technologies are unfortunately very expensive at present. Novel reactors, known for high heat transfer and fast kinetics, which have not reached commercial scale, include micro (channel and monolith-structured) reactors and non-thermal dielectric plasma reactors.[365–367] These reactors are still subject of intensive research (*e.g.* to alleviate flow distribution challenges, catalyst loading/replacement, scalability issues, *etc.*).[368–378]

5.4 Reactor design principles

Three underlying principles are key drivers for methanol synthesis reactor design: effective heat-removal and enhancing single-pass conversion, reducing pressure drop, and flexibility and economics.[379,380]

5.4.1 Effective heat removal and increasing single-pass conversion

Due to the exothermic nature of the methanol synthesis reactions, effective heat removal or transfer is required for safety, reduction in the number of pieces of physical equipment (*e.g.* heat exchangers) and to enhance selectivity and yield.

To achieve this, common large-scale synthesis reactor design features two stages: the water-cooled section where low, medium or high pressure (36–43 bar) steam is generated, removing heat from the reaction zone, and the gas-cooled section where the fresh feed gas is heated in the tube side and synthesis product from the water-cooled reactor reacts further in the catalyst loaded shell side.[35,254,381,382] Contrary to this conventional design, Mirvakili *et al.*[381] proposed, as the best, a configuration in which the total recycle from both gas-cooled and water-cooled reactors is heated *via* a heat exchanger unit and fed to the shell side while only fresh feed gas (not mixed with recycle) is heated on the tube side of the gas-cooled reactor. The key design parameter is the heat transfer coefficient or rather shell side and coolant temperatures.[382–384] However, undesirable gas flow maldistribution inside the gas-cooled reactor often results in non-uniform temperature distribution and hence gas condensation within the reactor, which, in effect, lowers the single-pass conversion.[45,385,386] Increasing the single-pass conversion (limited by equilibrium) is also a critical driver in synthesis reactor design.[45] Leonzio[344] evaluated parameters such as recycle ratio, global heat exchange coefficient, temperature, pressure and tube diameter on carbon conversion and specific heat flux, and deduced that increasing reaction temperature and recycle ratio decreases the carbon conversion.[383]

Mirvakili *et al.*[385] investigated the cause of flow maldistribution and attributed it to poor design of the gas distributor in the shell and tube side of the reactor. They proposed three different configurations: with partial condenser prior to the gas-cooled reactor, the injection of hot synthesis gas at 2 m near the exit of the reactor, and warming the shell side of the reactor with steam in a jacket within the last 2 m of the reactor to address the effective heat removal and enhance single-pass conversion. The configuration with partial condenser, which separates methanol and water in the inlet of the gas-cooled reactor, provides the most effective strategy with a 7.9% increase in the methanol production rate. They further used self-heat recuperation technology. The concept of a multistage indirect intercooling and radial flow reactor is also applied industrially.[387] The other strategy is typically referred to as liquid-out gas-in (LOGIC) and has been demonstrated using a laboratory-scale reactor by Bos and Brilman[45] to achieve near (99.5%) full conversion. Following the LOGIC principle, the reactor designs differ in their cooling strategy, *i.e.* adiabatic single bed, adiabatic multi-bed reactors with external cooling, adiabatic multi-bed reactors with direct cooling (*e.g.* quench reactor), multi-tubular cooled reactor, *etc.* Cui and Kær[35] compared single-bed adiabatic reactors with water-cooled and gas-cooled reactors considering syngas to methanol and direct CO_2 hydrogenation routes. They deduced that the water-cooled reactor has efficient heat removal, low hot spots temperature and a wider inlet temperature control range than the gas-cooled and single-bed adiabatic reactor, especially for the direct CO_2 hydrogenation route. Other designs use a temperature gradient between the cold and hot plate or heat exchanger like reactors and retrofits such as tube-cooled with metal inserts or using different catalysts layers within the reactor,[386,388,389] and others couple the exothermic methanol synthesis reaction with endothermic reaction, *e.g.* in the so-called ring network/simulated moving bed reactor network, but all, at present, still fail to achieve full single pass conversion.[390,391]

Other reactor designs take advantage of a reduction in reactor volume to gain effective control of reaction heat such as micro (channel or structured) reactor technology.[392,393] Their modular nature is relevant for distributed application of power-to-methanol as energy storage technologies, and in the case of adiabatic or gas-cooled operation.[35] Modular reactors have significant economic, safety and flexibility advantages.[299,371,394–397]

5.4.2 Pressure drop within the reactor

Pressure drop is generally dominant at larger reactor scales (>5000 tons per day, P_{loss}: 2.4–7.5 bar).[10] To reduce pressure drop within the reactor, and hence compression requirements, radial flow and fluidised bed designs are proposed as solutions. Adiabatic, radial, spherical, packed bed reactors are significantly researched in literature, particularly for syngas to methanol.[398–403] These reactors also exhibit higher conversions. Recently, Parvasi and Mohammad Jokar[403] presented a novel radial flow, cylindrical packed-bed reactor with tube-cooled configuration and evaluated its performance for methanol synthesis. They deduced that the reactor provides a greater cross-sectional area than conventional axial flow, tubular, packed-bed reactors, and thus reduces the pressure drop (<0.5 bar) or the gas passing through the catalytic bed and permits a larger inlet gas flow rate. Furthermore, the reactor volume can be increased vertically without drastically increasing the pressure drop, while the non-adiabatic nature of the reactor avoids heat accumulation. One other strategy is to design compact reactor(s) with short catalyst bed lengths.[22]

5.4.3 Flexibility and economics principle

The flexibility of the reactor refers to its scalability, part-load or periodic operation capabilities. Using intermittent renewable energy supply to produce hydrogen or syngas from electrolysis means reactors will have to start up and shut down quite often, and must be flexible to handle variable inlet conditions such as feed flow rate, molar ratio, adaptive coolant temperature/flow rate, *etc.*, while protecting the catalyst from deactivation and ensuring cost-effective production.[22,242,299,337,379,404,405] The Lurgi reactor is said to be capable of part-load (10–15%), quick response to load changes (1.5 minutes) and easy start up, but more discriminating dynamic experiments are

required to confirm.[254,406] The economics of the methanol plant is partly dependent on the methanol reactor design, flexibility and size.[379,405,407] Increasing flexibility (in terms of high turn-down ratio and ramp-up and down rates), capacity utilisation and the operating hours of the plant (including reduction of plant down times) are important factors. Related to flexibility and capacity utilisation is the question of the extent of coupling the variable energy profiles to the methanol reactor and associated limiting factors, which deserves further detailed exploration to assess the capabilities of electrolysis and reactor technologies. Table 10 gives the advantages and disadvantages of each extent of coupling, *i.e.* fully coupled, partially coupled and fully decoupled.[405] Huesman[405] compared a scenario where the methanol synthesis step is decoupled (operating at steady state) from inlet fluctuations using a large battery to a scenario in which it is fully coupled (meaning a highly dynamic operation with a small or no battery). The authors deduced that the fully coupled scenario is economically preferred and reduced operational flexibility increases the production cost of methanol by at least 20%.[380]

Table 10

Comparison of the merits and demerits of extent of coupling [modified from: Heusman[405]]

Extent of coupling	Advantages	Disadvantages
Fully decoupled	- Known operation (conventional processes operated at steady state provides a wealth of experience)	- Typically uses (large) battery storage/hydrogen storage facility, which increases the costs of the plant
	- High equipment utilisation *i.e.* design capacity/average capacity ≈1	- Lower overall efficiency, *e.g.* with addition of battery (discharge efficiency <100% and lower voltage during discharge) and/or compression necessary for intermediate tank storage of hydrogen
Partially coupled/decoupled	- May be relevant for operation where, *e.g.* standby mode is relevant; in case certain equipment cannot be shut down due to longer start-up time	- Not yet explored significantly
	- Reduced battery capacity	- Battery may still be needed and therefore increase costs and reduce efficiency
Fully coupled	- No battery storage and/or no high level of rectification of variable energy sources required	- Clarity on the best operation mode is limited as conventional plants are typically operated under steady state
	- Higher overall efficiency	- Reduced process equipment utilisation, *i.e.* design capacity/average capacity >2
		- Not yet explored significantly

On the other hand, input fluctuations offer an opportunity for forced periodic operation. Forced periodic operation, implementable with proper actuation, sensors and scheduling, can deliver desirable modulations and therefore desirable outputs.[22] Modular reactors are argued as having a potential to offer flexibility, for example tolerating low feed rate, since they can be connected as multiple reactors in series and independently from each other to achieve the desired plant capacity, and therefore making such serial connections easy to bypass.[22,299] However, trade-offs exists between the reasonable number of reactors (ultimately, capital costs) and desired production rate, *etc.* Limited work is available in literature that investigates the dynamic or flexible operation of the methanol synthesis reactors.[337,379,405,408–410] A key related requirement is that the system must be easy to design, control and/or manage without incurring unreasonable operating and capital costs. However, in the case of the power-to-methanol process and its achievable flexibility ranges, it would be necessary to question the attractive economics and scales (*e.g.* size and number of modular reactors) for various energy system applications, along with the associated challenges they may pose. Closely related is the reduction of plant down times, *e.g.* with designs capable of easy catalyst loading and removal. The scalability (*e.g.* in terms of space-time yield) of new and better-performing reactor designs, such as the reactor with condensation presented by Bos and Brilman,[45] and microchannel reactors deserve further investigation. In addition, the effects of disturbances on the temperature of solid and fluid phases, space-time-yield, and comparison of flexibility of commercial reactor designs and other types of fixed-bed reactors deserve further investigation including their different thermal management strategies under varying load.

5.5 Reactor models

Large efforts in the modelling of methanol synthesis reactors are directed to packed-bed reactors (PBRs). Table 11 highlights critical modelling efforts and model types. Reactor modelling is intrinsically non-linear and complex, *e.g.* stiffness in the partial differential equations. Two types of steady-state modelling approaches are prominent, *i.e.* pseudo-homogenous and heterogeneous models. Most of the literature work assumes pseudo-homogenous models.[383,392,411–413]

Table 11

Highlights of reactor modelling efforts in the context of power to methanol, and as a stand-alone (refer to reference Bozzano and Manenti[254] and Riaz *et al.*[418] for more details)

Model type	Process units considered	Comment (s)	Ref.
Pseudo-steady state	SOEC, adiabatic fixed-bed reactor	No deactivation	30
Pseudo-homogenous, one-dimensional	Various reactor configurations	No mass and heat transport limitations and no deactivation	374
—	SOEC-based process	—	24
Heterogeneous, four dimensions	Fixed-bed reactor	—	415
Dynamic model	Fixed-bed reactor	—	417
Heterogeneous and homogeneous dynamic models with deactivation	Fixed-bed reactor	Compared the two models	419
Pseudo-homogenous, one-dimensional	Radial flow cylindrical fixed-bed reactor	—	403
3D CFD model	A two-step configuration of gas- and water-cooled shell and tubular fixed-bed reactors	Impact of maldistribution on the reactor performance	385
Pseudo-homogeneous	Multi-tubular fixed-bed reactor		383

These are applied to one-dimensional (1D) or two-dimensional (2D) reactor modelling, even though the chemical-physical phenomena within the reactor exist in at least four dimensions (*e.g.* the axial and radial directions of the reactor, catalyst particle radius and time).[411,414–416] Pereta *et al.*[415] developed an algorithm to solve a multi-scale model (with four dimensions) of the fixed-bed reactor. Most of the literature work is focused on 1D modelling of the methanol reactor, hence 2–4D modelling is limited in literature.[383,411,412] PBRs have axial and radial gradients, and gradients along the radius of single catalytic pellets and temporal dynamics.[254] The 1D heterogeneous and 2–4D models (pseudo-homogenous and heterogeneous) capture these gradients.[411,412] These gradients and dynamics cannot be neglected in industrial-scale reactors and will be more pronounced in variable power-to-methanol processes. Accurate modelling is critical for reactor design and optimisation.

5.5.1 Steady-state models

Common assumptions in the modelling of the methanol synthesis reactor under steady state are negligible axial diffusion, negligible radial diffusion, constant radial velocity, constant temperature and pressure in the catalyst, negligible catalyst deactivation, absence of side reactions, and Thiele modulus applied to a representative single-catalyst particle to evaluate the effectiveness factor and thus the intra-particle mass transport.[35,254] The model basis is either mole or mass balance, with mass balance formulation taking into account variations of moles in the axial direction described by Manenti *et al.*[414] being more accurate. Pseudo-homogeneous models based on mole balances, in addition, neglect axial variations in molar flows and gradients between the gas and solid phases, but the rates are expressed as a function of the solid phase temperature and concentration profiles. Pseudo-homogenous models based on mass balances consider molar variation along the axial direction, but still neglect the gradient between the gas and solid phases. Pseudo-homogenous models treat both gas and solid phase as a single entity (pseudo phase) and consider the average properties of the two phases, but neglect the solid and fluid phase gradients, at times expressing rates as a function of fluid phase temperature and concentration. Pseudo-homogenous models work well under high inlet gas velocity.

In pseudo-heterogeneous models, heat and mass transports between the particles and the gas phases are considered, and each phase's mass balance is treated separately. Heterogeneous models are advantageous to best describe the reactor performance. Bozzano and Manenti[254] highlighted that pseudo-homogeneous models can accurately describe the reactor performance, with lower computational time demand in cases where conditions such as feed flow rate, shell temperature (in shell and tube reactors), *etc.* are close to nominal conditions (*e.g.* at high inlet gas velocities). The necessary details to achieve high accuracy are typically not very clear in model formulations and hence, at present, researchers use problem formulation as the critical first guiding step to what assumptions may be prevalent. Kaiser and Freund,[413] using a pseudo-heterogeneous model, deduced that there are considerable concentration and temperature gradients, for example within the catalyst, and thus neglecting them can lead to a violation of the allowable range of operating conditions for the catalyst.

5.5.2 Dynamic models

Dynamic models based on elementary balances rather than component balances have been formulated and proved to be robust.[417] The disadvantage of dynamic models is the difficulty in convergence, which thus necessitates a robust numerical solver, typically a finite difference approach that discretises the partial differential equations and solves them as a series of ordinary differential equations.[191] Additionally, for systems with perturbations, the dynamic model would typically predict a discontinuity in the dynamic trends, which cannot be physically interpreted.[254] But considering axial dispersion, these are removable with model transformation from a hyperbolic partial differential equation system to parabolic partial differential equations Manenti *et al.*[417] demonstrated the latter along with the method to remove the numerical instabilities and maintain the minimum computational effort. Petera *et al.*[415] developed a crucial algorithm to solve the same problem. To further alleviate problems such as excessive smoothness or stiffness as sometimes introduced by finite difference methods and hence obtain the best dynamic behaviour and parametric sensitivity (*e.g.* shell temperature, inlet gas temperature, inlet mass flow rate, *etc.*), Manenti *et al.*[417] evaluated the use of adaptive grids methodology with fewer grid points to maintain minimum computational time. Besides, incorporation of response time in dynamic modelling of the reactor will be key requirements for power-to-methanol processes. Under dynamic conditions, temperature gradients (*e.g.* radial temperature) are crucial factors to consider. Typical 1D reactor models are not satisfactory in modelling this, but 2D models can be used.[383,406]

5.6 Opportunities

Although it is evident that important work has been done in the area of modelling, there is still a need to balance prediction accuracy and computational time, taking into account relevant details possible (*e.g.* the energy balance of cooling gas, mass and heat transfer, reactor hydrodynamics, thermodynamics, *etc.*). Detailed methods and analyses, particularly based on dynamic models representative of power-to-methanol processes, are needed in the context of designing flexible and resilient catalysts and reactors for methanol synthesis.[299,337,405] In addition, the efforts in this direction should include the use of advanced tools such as CFD modelling platforms and multi-scale considerations.[385] Optimisation of catalysts and reactor design for better heat removal, higher single-pass conversion, improved flexibility and cost-effectiveness are required. The continued investigation of reaction mechanisms and associated kinetic models are needed, particularly under dynamic conditions, as will be prevalent in power-to-methanol processes.

6. Process synthesis in power-to-methanol

A large body of literature is based on analyses and improvements of electrolysers,[62,420] reactors[374,385,386,403,417,421–427] and catalysts, separate from the overall process.[254] Recent research interest is directed towards the integration and optimisation of these technologies in systems such as power-to-methanol (PtMeOH).[2,24,25,30,39,66,428] Among others, the current technologies of interest include high temperature electrolysers (SOEC-based) and reactors such as fixed-bed and micro reactors. Synthesis of highly efficient and economically best-performing processes is a critical task.[41] This section discusses work on PtMeOH process synthesis *i.e.* integration, optimisation, associated methods and evaluation criteria and techno-economics. Table 12 summarises the studies on PtMeOH process integration analysis and PtMeOH integration with other processes taking advantage of synergies (*e.g.* (by-) product application). Fig. 9 illustrates the integrated process with highlights of the points of synergies.

| Table 12 | | | | | |

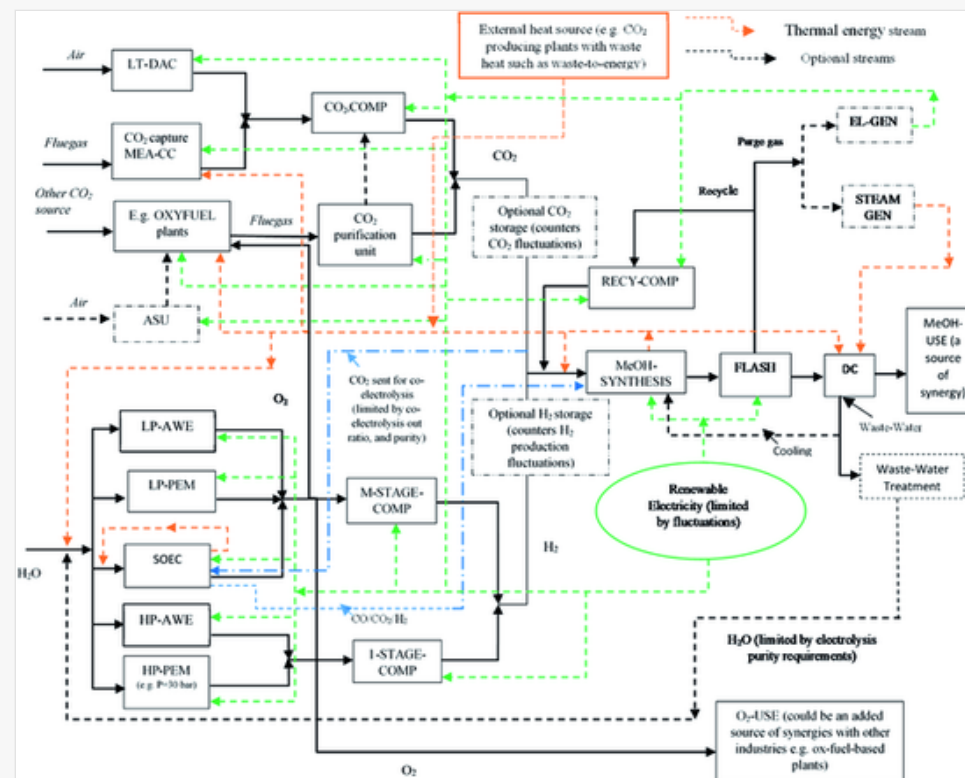Power-to-methanol process integration studies under steady-state conditions

Process	Highlights on components	Method highlights	Objective(s)	Key findings	Ref.
Steady-state (full load) integration and evaluation					
Power-to-methanol	HT-SOEC, methanol synthesis and purification	Techno-economics, pinch point analysis, 2D model for stack used for analyses of operating windows and thus select design points to be applied as basis for system comparison	- Energy integration, efficiency evaluation, techno-economics and analyses of operation window	- Co-electrolysis and increased sweep gas extend the stack operating window	24

				- that minimise stack degradation	
			- Comparison of power-to-methanol, with Fischer–Tropsch, power-to-gasoline and power-to-hydrogen	- Co-electrolysis allows better heat integration and can improve the efficiency of a mildly exothermic reaction like methanol synthesis	
Power-to-methanol	Electrolyser(s), methanol synthesis and purification	The routes compared include the following: one-step process (electrolysis and methanol synthesis combined in one reactor), direct steam electrolysis to methanol *via* CO_2 hydrogenation, separate H_2O and CO_2 electrolysers coupled with methanol synthesis *via* syngas, used black box modelling	- Compare conceptual designs of power-to-methanol from a techno-economic and life-cycle perspective	- Currently only direct steam electrolysis to methanol *via* CO_2 hydrogen is technically feasible - One-step process is still on laboratory scale - Power-to-methanol is environmentally compelling	434
Power-to-methanol coupled with its conversion to chemical intermediates and products	Electrolysis, methanol synthesis reactor, CO_2 and H_2 as feed, and chemical intermediates synthesis and purification sections	Methanol conversion to acetic acid, DMC, formalin, DME, biodiesel and MTBE are compared, a waste-reduction algorithm is used as a tool to evaluate the environmental aspects	- Compare methanol conversion to chemical intermediates highlighted and products from a technical and environmental point of view	- Conversion of methanol to biodiesel and MTBE are the most attractive routes from a technical and environmental point of view with low overall energy consumption - DMC and DME are not convenient from a technical point of view	433
Power-to-methanol to jet fuels	Alkaline electrolysis, CO_2 captured *via* absorption with monoethalamine, methanol synthesis, conversion to jet fuels and purifications	Rigorous techno-economics and environmental analysis, black-box simulations (Aspen)	- Evaluate power-to-methanol as a precursor in jet fuels from an environmental and techno-economic point of view	- Net production costs of jet fuels from this process are 2.9–4.6 times higher than the current market price - Flue gas from refineries has significant carbon capture potential and can yield 83 kt jet fuel per year - Power-to-methanol avoids 2.50 kg per CO_2 per eq. per kg	435
Power-to-methanol coupled to ethanol distilleries	Electrolysis, CO_2 is sourced from ethanol industrial distillery (~99% purity), bagasse (electricity and thermal source) and methanol production unit	Methanol synthesis is coupled with ethanol distillery, bagasse is used to co-generate energy (heat *via* boiled steam, and electricity), and factorial design is used to obtain the surface responses	- Methanol coupled with ethanol plant to generate attractive CO_2 utilisation hub - Maximise profit, energy efficiency and reduce operating costs	- Using co-generated energy, the challenge of high energy requirements mainly introduced by the electrolysis step can be overcome - In this process and considering extreme scenarios, methanol and oxygen generates 4.5 times more profits than electricity sales, and 8.8 for the sale of oxygen and hydrogen	436
Power-to-methanol integrated with larger energy-mix power grid systems (low and high flexible grids)	Power grid (with renewable solar and wind integration), water electrolysis and methanol synthesis	An agent-based model developed to explore future scenarios of deploying power-to-methanol in low and high-flexibility grid systems	- The influence of power-to-methanol in grid reliability and CO_2 reduction - The desired state in power grid is to have a constant grid balance close to zero	- Deploying power-to-methanol has a significant influence on the grid reliability - Power-to-methanol helps hold the renewable grid balance from increasing indefinitely and thus maintain better conditions for the grid - Significant CO_2 reduction can be achieved by deploying power-to-methanol - It is not recommended to invest in power-to-methanol until the grid has significant renewable power integrated	437
Power-to-methanol integrated with biomass and DME synthesis	HT-SOEC, biomass, entrained-flow gasifier, acid gas removal (CO_2 capture), water-gas shift reactor (used to generate syngas during renewable electricity downtimes), methanol synthesis, DME synthesis (*via* methanol dehydration), heat exchanger and steam turbine networks, distillation units	Aspen-based models (with black box description of some components) used to simulate the system, heat and mass integration formulated in mixed integer linear programming problem (considering electrical heater, syngas burner and steam turbine network), classical hot–cold and grand composite curves are used to evaluate heat integration	- Techno-economics, energy efficiency with consideration of system-level heat integration	- Integration of co-electrolysis-to-methanol with biomass gasification offers more operational flexibility, thus high annual production hours - Biomass- to-DME only reaches 49% efficiency, as a	430

Fig. 9

Generic process superstructure of the Power-to-methanol showing potential energy and material integrations. Modified from Kenkel *et al.*[432] (LP: low pressure, HP: high pressure, EL-GEN: electricity generating unit, DC: distillation column).

6.1 Process integration

The key system integration challenge, among others (*e.g.* flexibility and resilience), for SOEC-based processes is the need to overcome the endothermic electrolysis reaction such that the system (at feasible design or operation capacity) is energetically self-sufficient/neutral or sustaining (*e.g.* in the case of ReSOC-based processes).[24,84,85,379,428,429] The methanol synthesis reactor loop is dominated by cooling utility demand. However, pre-heating the reactor feed is typically required. Added to this are the energy requirements for distillation column(s) and CO_2 capture depending on the source and supply chain(s).[428] Electricity source(s) and heat integration are central to attain energy self-sufficiency and enhance the overall process energy efficiency.[32] Waste heat from other industries or electrical heating (less preferable) can be integrated, but the primary goals of reducing complexity and cooling exergy destruction is to efficiently integrate heat emanating from different subunits of the PtMeOH within the process or primarily subsystem of concern.[430] Reduction of more than 37% of cooling utilities can be achieved with heat integration.[4] The operating temperature of individual units, the number of utilities and the overall process configuration are decisive on the heat integration potential.[431] Wang *et al.*[24] evaluated heat integration potential for H_2O/CO_2 co-electrolysis-derived syngas to methanol (coSyn-MeOH) and steam electrolysis-derived hydrogen to methanol (*via* the direct CO_2 hydrogenation route: dCO_2-MeOH).

The coSyn-MeOH improves the process heat integration and hence energy efficiency due to the low steam feed rate requirement, since a fraction of the steam is generated internally from reverse water gas shift reaction and the fact that the CO/H_2 reaction to produce methanol is more exothermic (*e.g.* at 260 °C about ≈3.8 more heat is generated than in dCO_2-MeOH).[23] With the proper choice of the operating point of the electrolyser and heat integration, no electrical heating is required for coSyn-MeOH.[24] More than 7% of additional external heat (*e.g.* electrical heating) may be required for SOEC steam electrolysis-to-methanol, depending on the operating point, for steam generation.[24] However, Wang *et al.*[24] deduced that if no external heating is required for steam generation, then coSyn-MeOH should not be the primary choice due to its higher electrolysis voltages, which can reduce the system efficiency. Nonetheless, co-electrolysis and increased sweep gas flow rate can widen the operating windows (offering more flexibility) of PtMeOH.[24,430] Zhang and Desideri[43] also demonstrated the heat integration potential of the coSyn-MeOH process. Considering two design points, *i.e.* minimum cost design point (MCP) and maximum efficiency point (MEP), Zhang *et al.*[428] investigated the system-level heat integration for the steam electrolysis-derived hydrogen-to-methanol (SOEC-based dCO_2-MeOH) process. The SOEC was operated under highly exothermic conditions to eliminate the need for an additional external heat source, and thus the electrolyser outlet contributed a significant amount of heat energy, followed by heat from a waste (purge) boiler during steam generation. On the other hand, the heat released from the methanol synthesis step covered the distillation heat requirement. The MCP was run at a higher electrolyser current density and thus, for the same reactant utilisation, more water and heat was integrated for steam generation. Lonis *et al.*[30] integrated the ReSOC with methanol synthesis for the first time under steady-state conditions. In their study, waste heat from ReSOC in fuel cell mode was integrated into ReSOC operating in SOEC mode using thermal energy storage materials. Schwabe *et al.*[9] presented a novel process, which combines the SOEC electrolysis with methanol synthesis in one pot with potential for improved direct heat integration, kinetics and thus energy efficiency, and relevant for distributed microgrid applications. However, the prototype is still at laboratory scale, with high investment cost and technical challenges necessitating its further evaluation.

A fraction of studies considers the steady-state process integration of PtMeOH, assuming full load operation. Others extend to consider the downstream application of the PtMeOH-derived product methanol as a precursor. Petrescu *et al.*[433] evaluated and compared, in order to select the economically attractive application of product methanol, the downstream conversion of methanol to acetic acid, dimethyl carbonate (DMC), formalin, DME, biodiesel, and methyl-*tert*-butyl-ether (MTBE) processes. They showed that the conversion of methanol to biodiesel and MTBE are the most attractive routes.[433] Zhang *et al.*[406430] studied PtMeOH integrated with biomass to generate methanol and DME (*via* methanol dehydration) and showed that PtMeOH-to-DME is not heat-self-sufficient.

Wassermann *et al.*[435] assessed the techno-economics and environmental performance of PtMeOH integrated with refineries for green jet fuel production taking advantage of flue gas produced from the refinery. Whereas Rocha *et al.*[436] studied the performance of PtMeOH integrated with ethanol distilleries in which bagasse is used for the co-generation of electricity and thermal energy, while CO_2 precursor is obtained from the distilleries. They established that using co-generated energy, the challenge of high energy requirements that is mainly introduced by the electrolysis step can be overcome. While Afzali[437] considered a comprehensive evaluation of the role of integrating PtMeOH into the grid, evaluating socio–technical parameters that influence grid reliability and emission reduction. However, detailed explorations with consideration of advantageous synergies are still required. Nonetheless, studies on PtMeOH process integration are still limited, based on oversimplified flow sheets, steady state, and thus more work is required to optimise heat integration. For example, additional heat ($\approx 1/4$ of the total power consumption) can be valorised from the gas compression stages.[24] Considerations of other parameters such as pressure drop, hydrogen pinch-analysis, exergy, entropy balances and detailed water and heat exchanger networks in process integration will be relevant – in particular for small-scale PtMeOH systems (*i.e.* for distributed microgrids), which are dominated by auxiliary equipment.[24] Furthermore, possible improvements can be achieved by coupling heat integration and optimisation, simultaneously rather than in the traditional sequential approach.[431] On the other hand, only a few studies focused on PtMeOH process integration and analysis under dynamic conditions have been reported to date and the findings, summarised in Table 13, will be discussed under Section 6.2.2.

Table 13

Power-to-methanol dynamic integration and analysis under deterministic and uncertainty conditions, and optimisation-based studies

Process	Highlights on components	Method highlights	Objective(s)	Key findings	Ref.
Dynamic integration and analysis under deterministic and uncertainty conditions					
Power-to-methanol	CO_2 from air *via* direct air capture (DAC), water electrolysis for hydrogen production, battery storage decouples the system variable energy profile, methanol synthesis and purification	Simplified (lumped) dynamic model with deterministic predictions of the solar profile, and control model	- Compare the fully decoupled and fully coupled scenarios	- Fully coupled scenario is favourable - Control mode determines the economic operation mode - There is an intricate trade-off between various costs	405
Power-to-methanol to jet fuels	Wind and PV energy sources, electrolysis, Lurgi methanol synthesis reactor, CO_2 capture from point source, reactor for methanol conversion to aviation fuels, gasoline, *etc* and distillation	Integration with flexibility consideration, 1D dynamic model, 20% (w/w) increment of feed flow rate, and orthogonal collocation at spatial domain and backward difference at time domain are used as solvers	- Explore scenarios where the process becomes feasible	- System shows rapid response to disturbances, steady-state can be reached in 1.5 minutes - Increases in the amount of CO_2 in the feed up 5% (w/w) narrows the feasible region to increase methanol production	406
Power-to-methanol	Wind energy and solar energy, alkaline electrolyser, methanol synthesis reactor, purification system	Multi-period design of solar and wind-based methanol production facilities under uncertainty. Seasonality of energy resources is addressed *via* multi-period modelling, uncertainty in solar and wind energy is modelled using a two-stage stochastic approach, surrogate models are used for modelling the production process	- Design of process under uncertainty - Trade-offs related to idle equipment with large equipment cost are evaluated	- Source availability and uncertainty needs to be considered in process design - The initial tempting decision is typically to invest in the methanol capacity depending on the capacity of the solar or wind, which are variable, however, care must be ensured to minimise having equipment idle most of the time in the year - An attractive scenario for solar-based plants is to ensure that a fraction of electricity is sold while the other is used for the production of chemicals	445
Optimisation-based studies					
Power-to-methanol *via* steam electrolysis and CO_2	HT-SOEC, methanol synthesis and purification	- Bi-objective optimisation - Minimum cost design and maximum efficiency design points are used for system-level integration comparison - Pinch point analysis and black box modelling - Steady state	- Techno-economic optimisation - Process integration and energy efficiency optimisation	- There is a trade-off between the energy efficiency and methanol production cost - System efficiency high ($\sim$70%) - The choice of SOEC operating conditions affects heat management of the system	428
Power-to-methanol *via* co-electrolysis to methanol	HT-SOEC for co-electrolysis, methanol synthesis and purification	- Bi-objective optimisation - Minimum cost design and maximum efficiency design points are used for system-level integration comparison - Pinch point analysis - Black box modelling using Aspen - Steady state	- Techno-economic optimisation - Process integration and energy efficiency optimisation	- The system achieves higher efficiency ($\sim$72%) - There is a trade-off between the energy efficiency and the methanol production cost - SOEC operating in co-electrolysis and integrated with exothermic methanol has attractive heat integration performance - Large amount of heat generated from the methanol synthesis can meet steam generation demands for SOEC without requiring external heat - Excess heat can be recovered using steam turbine for the co-production of electricity	43
Power-to-methanol *via* steam	Off-shore wind, AWE, PEM and SOEC electrolyser, CO_2 cement	Simplified superstructure-based optimisation *via* bi-criterion objectives, steady state	- CO_2 emission (life cycle) and	- Utilising renewable electricity in PtMeOH contributes to positive abatement of CO_2 emission (-2.29 tCO_2/tMeOH) with	439

electrolysis and CO_2	factory, methanol synthesis and upgrading step		economics as bi-objectives	minimum net production costs of 1346 € per t of methanol	
Power-to-methanol	Electrolysis, methanol synthesis and purification	Scheduling optimisation time horizon of a year and a monthly time discretisation, with dynamics on solar and wind availability on an hourly basis, methanol is compared to ammonia, DME, *etc.*	- Assess the optimal plant and transport network, analyses of oversized capacity required under dynamic conditions	- With scheduling optimisation, a large fraction of methanol can be produced in summer (*via* solar) and consumed in winter (to meet the electricity demand)	446
Power-to-methanol with self-heat recuperators	Self-recuperative co-electrolysis, methanol synthesis, purification	- Metaheuristic rigorous optimisation vortex search strategy used to optimise benefits of recuperators as retrofits - Each objective is optimised at one point in time, *i.e.* objectives are not simultaneously optimised - Steady state	- Optimise the energy efficiency, exergy efficiency and methanol production	- Electrochemical system of co-electrolysis has the highest exergy destruction rate (~accounts for total exergy loss of 82%), followed by coolers (49% of remaining 18%) - Optimisation of self-heat recuperative-based co-electrolysis using vortex search strategy reduces the exergy loss (hence improves energy efficiency) by 61.7% and improves the methanol production	440

6.2 Optimisation-based process synthesis

Optimisation is broad, and in a simplified manner herein, is divided into design-based and operation-based optimisation with reference to the overall PtMeOH system.[254] Design-based optimisation features geometries, system topology and operating conditions. Operation-based optimisation encompasses process planning, control and safety management under dynamic conditions. Table 11 summarises these studies.

6.2.1 Design-based optimisation

In this direction, limited optimisation work is reported for both H_2O/CO_2 co-electrolysis-derived syngas to methanol[42] and steam electrolysis to methanol processes.[428] The available studies are focused mainly on operative conditions and techno-economics optimisation under steady state, but, in general, the integrated systems tend to be simplified.[43,428,432,438–440] Few studies consider the optimisation of two or more objectives.[43,428,439] Zhang *et al.*[428] considered multi-objective optimisation, *i.e.* the efficiency and production cost of PtMeOH. Kenkel *et al.*[439] and Kenkel *et al.*[432] performed a bi-objective superstructure-based optimisation of PtMeOH (*via* CO_2 hydrogenation to methanol with hydrogen derived from steam electrolysis).

The authors considered a simplified approach, with a less detailed process configuration presented, to perform economic and environmental analysis. Chaniago *et al.*[440] optimised the energy and exergy efficiency, as well as the methanol production rate and retrofitted the self-heat recuperative system of the co-electrolysis based PtMeOH process. The authors did not perform simultaneous optimisation, but optimised each of the objective functions individually under steady state conditions. From their study, optimisation of self-heat recuperative-based co-electrolysis using a vortex search strategy reduced the exergy loss (hence improving energy efficiency) by 61.7% and improved the methanol production.The work of Zhang and Desideri[43] is almost an extension of the work of Zhang *et al.*,[428] but considers H_2O/CO_2 co-electrolysis-to-methanol and uses the same subunit configuration for the methanol synthesis step, objective functions and optimisation method. A key take-away point from these studies is the existence of the trade-off between the production cost and energy efficiency, showing a slight increase in production cost with an increase in energy efficiency.

It is essential to highlight that energy efficiency is a strong function of system boundaries, *e.g.* the detailed optimisation of balance of plants and separation networks, CO_2 capture, the influence of methanol synthesis kinetics on the operating windows of the electrolyser and hence the overall process. An important factor of methanol synthesis kinetics, among others, is the stoichiometric ratio of the feed, and its effects on process operation, including the electrolyser throughput, size and electricity requirements. [36,347] Hankin and Shah,[36] using a thermodynamic model, evaluated the effects of stoichiometry on the overall energy efficiency and CO_2 conversion/emission rate (based on a stoichiometric equilibrium reactor), excluding CO_2 capture, potential deviations between kinetic models *vs.* a thermodynamic approach, and global optimisation. The authors deduced that a methanol synthesis reactor feed stoichiometry of $H_2/CO_2 = 2.5$ and $H_2/CO = 2$ yields optimal energy efficiency for direct steam electrolysis to methanol and co-electrolysis syngas to methanol, respectively. Although these studies showed promising results, opportunities for improvements exist in the SOEC-based power-to-methanol process, including its energy efficiency. The highlighted studies neglect analyses of trade-offs and 'non-trade-offs' from the simultaneous optimisation of process yields, single-pass CO_2 conversions and reactant stoichiometry (considering valid and improved kinetic models) and purity (*e.g.* CO_2 < 99 mol%), exergy efficiency, electrolyser lifetime and operating window/strategies, purge or recycle ratio, CO_2 emission, plant operating hours, and sustainability, control and safety operation objectives along with capital and production costs. Other critical factors include catalyst and electrolyser stack properties such as deactivation.

On the other hand, PtMeOH process optimisation has thus far neglected detailed optimisation and analyses of the process topology or structure, which is typically determined by the process synthesis and intensification methods.[441] Work of Zhang *et al.*,[442] Adnan and Kibria,[434] Andika *et al.*,[28] Hankin and Shah[36] and Hernandez-Perez *et al.*[443] provide good bases with important findings that can be used for the optimisation of PtMeOH process topology.

Multi-objective analyses with consideration of process topology and coupled with different process scales (multi-scale) are the required research. Thus, detailed synthesis, integration, optimisation, intensification and analysis of trade-offs and non-trade-offs *via* multi-objective analyses for the power-to-methanol system are still needed.[254,444] This must also consider the applications of the end product(s) and the incorporation of synergistic parameters to optimise the process.

6.2.2 Operational-based optimisation

Under dynamic conditions, capturing renewable energy supply intermittence, integration and optimisation of different sections of the plant can be a function of the operating period/periodic operation of each unit or subsystem.[28,305,379,405] For example, from the steady-state focused work of Lonis *et al.*,[30] the integration of different sections of the overall system was observed to be influenced by the differing operation times of different systems (in their case the ReSOEC and methanol, and the ReSOFC, *i.e.* which refers to the operation of ReSOC in fuel cell mode). Hence, the overall system of the study by Lonis *et al.*[30] was condensed into two independent subsystems (*i.e.* the production of methanol and ReSOFC for reforming methanol) and a regenerative heat exchange and thermal energy storage (TES) system was used in between. This influences the relationship between the process tasks in ways not fully understood, particularly for microgrid applications or rather when methanol has to be converted back to electricity for demand-side power management.[28,48] Varela *et al.*[406] evaluated flexible performance of the renewable energy-based PtMeOH under dynamic conditions considering scenarios with step functions of up to 20% (w/w) increments on the feed hydrogen flowrate as will be imposed by fluctuating power input (first absorbed in the electrolysis stage). They deduced that a PtMeOH system, fitted with a Lurgi reactor for methanol synthesis, shows rapid response to disturbances, reaching steady state in 1.5 minutes and that increasing the amount of CO_2 in the feed by up to 5% (w/w) limits the feasible region to increase methanol production, in particular at highest hydrogen flow rate disturbances (20%). By doing so, the authors observed that the carbon atom conversion within the reactor is not compromised and

methanol production increases with fluctuations in renewable energy sources. The authors further concluded that methanol synthesis is feasible in terms of short reaction times and smooth profiles with open loop response, and on the other hand, large recycle reduces effects of disturbances.

Most of the studies on PtMeOH under dynamic integration and optimisation (see Table 13), are focused on deterministic approaches with only Martín,[445] per author's findings, that has considered evaluation of the process under uncertainty *via* a two-stage stochastic approach. Even though the model of Martín[445] still included steady-state surrogate models for assessing the production plant and was aimed at introducing the method/tool, rendering it less oriented towards detailed evaluation of the process, but taking PtMeOH as a demonstration case study, its study offered valuable insights.

From the study of Martín,[445] which encompassed the integration of wind and solar energy resources with an alkaline-water based electrolyser, a methanol synthesis reactor and a purification system, and using multi-period as a method, Martín[445] deduced that, under uncertainty conditions, an intricate trade-off between investments and production capacity exists and, as a result, capacity utilisation and annual hours of operation become even more critical as factors to consider in design to avoid having idle/underused equipment. The work of Huesman[405] also used a simplified and deterministic dynamic model, which considered only diurnal cycles in solar energy variations.

It is also critical for the optimisation of the power-to-methanol process to take into consideration the hourly, daily and seasonal variations of renewable electricity, and uncertainties in electricity price profiles, CO_2 supply chain and carbon tax. In some instances, this will necessitate the consideration of process planning and scheduling, different designs (*e.g.* electrolyser oversizing), control and safety with flexible operation that does not constrain the economics of the process.[446] Sánchez *et al.*[446] considered design at the supply chain level and operation at the scheduling level for decision making to evaluate the storage potential of methanol relative to others (*i.e.* methane, DME and ammonia). Under the supply chain level, production and storage facilities, as well as the transportation network, are considered,[446] while under the scheduling level, the impact intermittence of solar and wind energy are evaluated, as well as the hydrogen storage.[446] These studies offer a basis to establish a more detailed evaluation. To the authors' knowledge, no detailed work has been done in this particular direction, particularly for SOEC-based processes. Ultimately, more work is required for performance analysis and optimisation of the PtMeOH process under dynamic and uncertain conditions (*e.g.* considering chance constrained optimisation). Efforts in this direction must be supported by increased electrolyser stack and reactor testing at variable load conditions.

6.3 Methods and evaluation criteria

6.3.1 Methods

Rigorous models using Aspen software with the black box treatment of the process components are commonly used for the generation of mass and energy balances. Heat integration is typically performed sequentially after the optimisation. In cases where heat integration is considered, pinch analysis methodology is used, although it is known that this method does not guarantee optimality when applied sequentially; it also fails to eliminate redundant components.[428,431,447] Heuristic methods (such as genetic algorithms) are typically used for optimisation.[43,431] Superstructure-based methods are also gaining popularity, but have mostly been used thus far in the PtMeOH for heat exchanger network, utility and techno-economics optimisation, and formulated as mixed-integer linear programming.[43,428,432,441] Few studies consider simultaneous heat integration and optimisation, and are based on separate methanol synthesis and separation steps – instead of considering the overall process.[431] Perhaps this is due to the resulting combinatorial complexity, rendering the model with mixed-integer non-linear programming; which is thus difficult to solve.

On the other hand, the direct application of pinch analysis to simultaneous optimisation is still challenging since the heat duties are decision variables and not known beforehand.[23,431] However, Schack *et al.*[431] took advantage of the idea of decoupling process-based non-linearity using the FluxMax approach to develop a method for simultaneous optimisation and integration. This method can generate alternative optimal process configurations.[431] These superstructure-based methods, coupled with multi-objective optimisation, will be key for the optimisation of complete PtMeOH processes.[448] Other computer-aided methods are available and have been recently reviewed by Martín and Adams[449] and Mencarelli *et al.*[404] These include superstructure-free methodologies such as that presented by Neveux[450] and Zhang *et al.*,[442] and the building block-based superstructure method presented by Demirel *et al.*,[451] which can be applied to achieve new and improved power-to-methanol process designs. They are particularly fitting because PtMeOH is still at an early stage of exploration with high possibilities for improved configuration(s) or topology options.[404] These methods also eliminate redundant components or the need to predefine the superstructure, since its definition may exclude the optimal alternative or include infeasible solutions.[404] Another state-of-the-art superstructure-free synthesis multi-objective optimisation methodology was presented in the work of Wang *et al.*,[452] which can be adapted and used for PtMeOH, even though it was initially devised for thermal power plants. Peng *et al.*[453] also presented a method relevant for application in the PtMeOH process based on solar and wind to treat the multiple time scale variabilities and achieve a better design, synthesis and optimisation of the system, rather than using conventional methodologies, which are based on multi-period/multi-scenario optimisation. This approach can help cater for off-design operation points and minimise the possibility of over-design.

It is important to highlight that developments in synthesis and optimisation methods will continue to play a crucial role and thus applying new methodologies for the re-evaluation of these process should not cease. These developments must be tied with realistic improvements in materials (*e.g.* catalysts) and critical components (*e.g.* electrolyser stack). It is also crucial that the simultaneous optimisation of reactor and catalyst designs *via* multiscale modelling and integration are synchronised with complete process intensification and optimisation. Multi-scale modelling will be beneficial to improve PtMeOH. A closely related study by Onel *et al.*,[454] using surrogate models, proposed a method to integrate CFD modelling, process synthesis and global optimisation to generate optimal process topology. To the best of our knowledge, no known work in this regard for overall PtMeOH optimisation has been performed. Real-life data, *e.g.* from the long-term operation of renewable energy-based plants, will play a critical role in this aspect. Again, convergence and optimum solutions must be achieved with reasonable computational power and time. An advanced open-source method/tool/code, in this field, is required.[432]

6.3.2 Evaluation criteria

Table 14 highlights the advantages and limitations of the key and commonly used evaluation criteria. Apart from energy efficiency, production efficiencies, CO_2 emissions/avoidance cost, the levelised cost of storage and conventional techno-economics criteria (*e.g.* pay-back time, *etc.*), exergy analysis is increasingly being used.[2,23,245,447,455–457] Exergy analysis can be tied to the economics of a process, hence the term 'exergo-economics'. The other versatile criteria is the entropy generation rate minimisation, which offers the opportunity to optimise designs or configurations by integrating the first and second law of thermodynamics with the constructal law. Von Storch *et al.*[458] noted the limitations of the evaluation criteria (such as energy and exergy efficiency), and proposed and tested a new evaluation criterion, *i.e.* efficiency of energy substitution (EES). The EES criterion was able to determine the practical and purpose-driven optimal configuration. Hence, the criterion was deduced as useful for hybrid processes with one or more products. Other relevant criteria are evaluated in the work of Colla *et al.*[457] Improvements in the fundamental understanding of the process, from material and equipment to the process scale (*i.e.* multi-scale), shall coincide with redefining these parameters and/or adding better expressions or new

performance criteria. Other metrics to be considered may include environmental metrics such as toxicity levels, sustainability metrics like the availability of resources, supply chain, resilience and social issues such as the potential job and economic development impact and safety with scale.[6,449,459]

Table 14

Comparison of a few process evaluation criteria

Performance parameters	Advantages	Limitations	Ref.
Energy efficiency	- Simple and useful approach in all energy using industries	- Variable definitions exist and exclude exergy efficiencies/quality of energy	245 and 458
		- With increase in process complexity, the results using this criterion may be misleading, *e.g.* when two products of different kinds (methanol and electricity) are produced in the process	
Exergy efficiency	- Expedient approach that renders it possible to compare different interactions, *i.e.* input, output, work and heat, on a common ground	- The use of a Carnot cycle results in the over-estimation of heat	455, 458 and 460
	- Considers the quality of energy	- Neglects high exergy destructive, but economically cheap units such as the valves during process synthesis and optimisation	
	- Pinpoints the thermodynamic inefficiencies within the system, processes and components with high irreversibility, which are target areas for improvement	- Still controversial if it is best applicable in processes with solar radiation and cannot optimise the design and operating variables, but only guides towards location, magnitude and source/availability of inefficiencies	
		- Challenges with estimating endogenous exergy destructions, since the theoretically operated components are treated as a black box and needs to be balanced and justified by economics	
		- Some inefficiencies are unavoidable due to physical and economic constraints	
Energy savings ratio	- Straightforward approach to compare the optimised process to the reference system	- Treats different forms of energy as one; for example, biomass-derived energy, which can be easy to store – compared to solar-derived energy, which is different due to its variability. These forms of energies will be treated as the same, and may lead to non-practical results	458 and 461
	- Easy to apply in poly-generation systems	- Requires knowledge of the reference process performance	
Exergo-economics/specific exergy costing (SPECO)	- Detailed understanding of costs related to equipment, thermodynamic inefficiencies and their interconnections	- Cannot optimise the design and operating variables, but can only guide the investigator	462, 463 and 464
	- Gives guidance on how and where to improve the efficiency and reduce the cost of the system	- Cannot automatically and algorithmically generate structural alternatives	
	- Possibility to decompose and optimise individual components of the whole system and SPECO is easily applied		
Entropy generation minimisation rate	- Versatile thermodynamics optimisation criteria for exergy analysis and its interfaces with heat transfer, thermodynamics, and fluid mechanics	- Complex compared to energy efficiency	423, 460 and 465
	- Allows the creation of realistic models that account for irreversibility, which is inherent in the systems/process		
	- Can give optimal configuration/topology/allocation of resources *via* consideration of constructal thermodynamics		
Efficiency of energy substitution	- Useful for hybrid processes with one or more products, *e.g.* heat, power and chemicals	- Requires knowledge of the fuel consumption of the reference process	458
	- Provides a better comparison of the process of interest (*e.g.* to a reference system), while being goal oriented	- Only one input is allowed to differ between the process of interest and the reference process	

6.4 Techno-economic, environmental and incentives analyses

Table 15 highlights numerous PtMeOH techno-economic studies conducted in various geographic locations and markets.[466] However, even though they are difficult to compare, they offer some insights. Most studies consider all the major process steps. However, assumptions are variant, except in a few cases, such as the annual operation hours of the plant (AOP), which assumes an almost full load operation scenario (≈7200–8000 hours per year). Based on the latter, most of these studies define or quantify technical and economically feasible scenarios, such as the selling price of methanol, electricity price, cost of major equipment (such as the electrolyser), AOP, *etc.* However, these are mostly location- and technology-dependent. Ouda *et al.*[466] and Hank *et al.*[467] evaluated scenarios to increase market adoption (in a German market) of methanol and associated ecological aspects. Four different system dynamics, as deduced in ~~Fig. 8~~Fig. 10, were considered. Electric power was derived from a wind farm, and compared to that purchased from the grid. A reduction in the cost of the electrolyser, amendment of taxation systems or policy instruments, the CO_2 from biogas or ammonia plant, credit arising from CO_2 trading, a variation in the electricity production and cost, and the temporal H_2 storage size were considered. The authors deduced that the feasibility of the process is strongly affected by electricity, H_2 production and CO_2 costs, methanol reactor dynamics (hence the H_2 storage requirements) and AOP ~~(Fig. 10)~~.

Table 15

A summary of techno-economic studies on power-to-methanol[a]

Year	Process steps considered	Key assumptions	Capacity	Net production cost	Net investment cost	Incentives considered	Quantified feasible scenario(s)	Ref.

Techno-economic Studies

Year	Process	Parameters	Scale					Ref.
2016	CO_2 capture (amine scrubbing), AWE electrolyser, two-staged methanol synthesis reactors	AOP: 75% $SP_{(MEOH)}$: 342 € per ton Lignite plant electricity cost: 6 € per MWth $SP_{(O_2)}$: 0.088 € per kg per O_2	13.791 ton per MeOH per h	PO: 421 € per ton $_{(MEOH)}$ PI: 580 € per ton $_{(MEOH)}$	PO: 421 € per ton $_{(MeOH)}$ PI: 580 € per ton $_{(MeOH)}$	CO_2 emission tax for PO: 7.44 € per ton CO_2	—	468
2016	Carbon capture units, electrolysis unit, methanol synthesis reactor, heat exchanger and multistage compression network, separators, distillation column, purge combustor	AOP: 91.3% $SP_{(MEOH)}$: 400 € per ton CO_2 conversion: 22% Price of H_2: 3090 € per ton Price of electricity: 95.1 € per MW h	440 kton per MeOH per year	295 M€ per year	496.5 € per ton $_{(MeOH)}$ per year	Emission reduction tax	CO_2 tax: 222 € per ton $SP_{(MEOH)}$: 800 € per ton (double the assumed) or H_2 price: 7725 € per ton (2.5 times the assumed)	26
2018	Electrolysis unit, methanol synthesis multi-tubular reactor, organic Rankine cycle, gas turbine (for purge stream), separators (low and high pressure), distillation unit	AOP: 8000 hours year^{-1} H_2 production energy requirement: 4.8 kW per hel per Nm^3 Electricity price: 0.06 € per kW Plant design principle: Energy Self-sufficient $SP_{(MEOH)}$: 0.4 € per kg CO_2 conversion: 30% Pressure: 80 bar	100 kton per MeOH per year	785.52 € per kg per MeOH × 10^{-3}	555.55 € per kg per MeOH × 10^{-3}	Emission reduction tax (0.01 € per kg)	CO_2 tax: 0.255 € per kg or $SP_{(MEOH)}$: 0.73 € per kg or Electricity price: 0.027 € per kW	429
2018	Electricity production source (grid *vs.* wind), PEM electrolyser, industrial gas feed rich in H_2, CO_2 capture from ammonia/biogas, H_2 storage requirement, compression of CO_2 and H_2, methanol synthesis reactor and distillation column	CO_2 credit: 365 and 430 € per t per CO_2 eq. Grid connected implies full load constant and price dependent supply H_2 storage pressure: 30–200 bar H_2 storage size: 100–50 000 kg MeOH reaction pressure: 40 bar CO_2 conversion: 90%	12 MW or 4–10 kton per MeOH per year	4.00–12.93 M€ per year	Grid connected MeOH plant: 608 and 1453 € per ton MeOH Wind connected MeOH: 1028–1067 € per ton MeOH	Credit arising from CO_2 trading	PEM cost: 440€ per kW Electricity price: 2.5 ct€ per kW h	467
2019	SOEC electrolyser, methanol synthesis reactor, heat exchanger network (details omitted), distillation column	AOP: 8000 hours year^{-1} CO_2 purchase price: 40 € per ton Stack lifetime: 48 000 hours SOE stack replacements: 3 Electricity price: 81.64 € per MW h	20 MW	—	3500–4300 € per kW LHV MeOH	—	Stack lifetime: 90 000 hours Cheap or free electricity even at an AOP of 2000 hours – process becomes competitive	24

| Year	System	Assumptions	Capacity	Production cost	Capital cost		Sensitivity	Ref
2019	SOEC electrolyser, methanol synthesis reactor, heat exchanger network, knock-out drum, distillation column	SP$_{(O2)}$: 79 $ per ton Carbon cost: 9 $ per ton Electricity cost: 30 $ per MW h AOP: 80% SOEC price: 2500 $ per kW SP$_{(MEOH)}$: 60–79 $ per MW h (LHV)	10 MW	173 487 $ per year	29 223 877 $	—	Electricity price: < 40–60 $ per MW h @ low cost SOEC SOEC price: 750–1050 € per kW Constant plant utilisation factor: 42–50%	7
2019	Hydrogen from sodium methoxide (NaOCH$_3$), multi-stage compressors, mixers, fired heaters, methanol synthesis reactor(s), (*i.e.* three configurations with recycle and purge, distillation column)	Feed H$_2$ stream from NaOCH$_3$ plant: 88 mol% H$_2$ and 12 mol% MeOH SP$_{(MEOH)}$: 496 US$ per ton H$_2$ feed rate: 800 kg h^{-1}	1122.3 kg per MeOH per h	—	—	—	SP$_{(MEOH)}$: 640 US$ per ton	473
2019	PEM electrolyser, methanol reactor, separation and distillation, power generation units (transcritical carbon dioxide gas (tCO2-GT), a supercritical carbon dioxide gas turbine (sCO2-GT), methanol steam reformer and direct methanol PEM fuel cell	Only main component of the system are modelled	50 MW	—	—	—	—	469
2019	Three methanol production routes: - Conventional coal to methanol (base case) - Solar energy coupled with coal gasification to methanol (case 1) - Solar energy, biomass-assisted CO$_2$ hydrogenation to methanol (case 3)	Electricity from PV: 0.55 RMB per kW per h Biomass price: 335 RMB per ton Feed coal: 500 RMB per ton Fuel coal: 350 RMB per ton	600 kton per MeOH per year	Base case: 1593.4 RMB per ton Case 1: 5090.7 RMB per ton Case 2: 8047.5 RMB per ton	Case 1: 3730.8 MRMB per ton Case 2: 7863.8 MRMB per ton Base case: 2875.81 MRMB per ton	—	Carbon tax: 500 RMB per ton per CO$_2$ eq PV electricity price: 72.3 RMB per MW h @zero carbon tax	474
2019	SOEC electrolyser, methanol reactor, separation units including distillation	System efficiency: 70% Electricity price: 73.16 US$ per MW h AOP: 7200 hours year^{-1} SP$_{(MEOH)}$: 504 US$ per ton SP$_{(O2)}$: 177 US$ per ton SOEC stack cost: 2000 US$ per stack Electrolyser lifetime: 48 000 hours	100 kton per MeOH per year	560 $ per ton	133.8 M$	—	Electricity price: 47–20 $ per MW h Production cost: 365–172 $ per ton Electrolyser stack cost: 1000 US$ per stack	428
2020	A stand-alone wind power system, H$_2$O electrolysis (AWE electrolyser), CO$_2$ captured from air, methanol synthesis step	System efficiency: 50% AOP: 8000 hours year^{-1} Cost of wind turbine: 3000 € per kW Cost of electrolyser: 1000 € per kW AWE efficiency: 65% CO$_2$ capture	100 MW (65 kton MeOH per year)	750–800 € per ton (including wind turbine)	500 M€ (including wind turbine)	—	—	39

		cost: 308 € per ton						
Thermo-economic/Exergo-economics and environmental studies								
2016	Energy sources (hydroelectric, wind, PV, at times non-renewable national grid), CO_2 capture/upgrading (biogas and external source), pressurised alkaline electrolyser, compressors and methanol synthesis	$SP_{(MEOH)}$: 400, 500, 600 € per ton; Electrical energy costs: 0.03–0.04–0.05 € per kW h; CO_2: 10 € per ton; $SP_{(O2)}$: 150 € per ton; Bio-methane selling price: 0.7 € per kg	1 MW	—		2.5–3.8 M€	Carbon tax; European financial incentive	Operative hours: 3000; $SP_{(MEOH)}$: 500–600	29
2018	Electricity from the renewable hydropower plant, CO_2 captured (*via* post-combustion chemical solvent) from the supercritical coal plant, PEM electrolyser (for H_2 generation), methanol synthesis *via* thermo-chemical reactor, separators, distillation column, heat exchangers, compressors, mixers and splitters	Levelised cost of H_2 production: 3.9 US$ per kg per H_2	1021.59 kton MeOH per year	1 915 558,638.7 $	138 043 862.87 $	—	$SP_{(MEOH)}$: 820 US$ per ton; $SP_{(O2)}$: 150 US$ per ton; Decrease H_2 price by 50%; CO_2 conversion: >50%	475
2017	Thermally coupled (methanol synthesis) reactors (TCRs), endothermic dehydrogenation of cyclohexane coupled to methanol synthesis, thermally coupled membrane reactor (MCR)	—	100 ton MeOH per d	—	TCR: 600 000 $, MCR: 920 000 $	—	—	462

Table Footnotes

[a] AOP: Refers to the annual operation of the plant, SP: selling price of commodity, PO: investment cost of the plant owner scenario, PI: investment cost of the private investigator scenario, RMB: Ren Min Bi (China currency).

Fig. 10
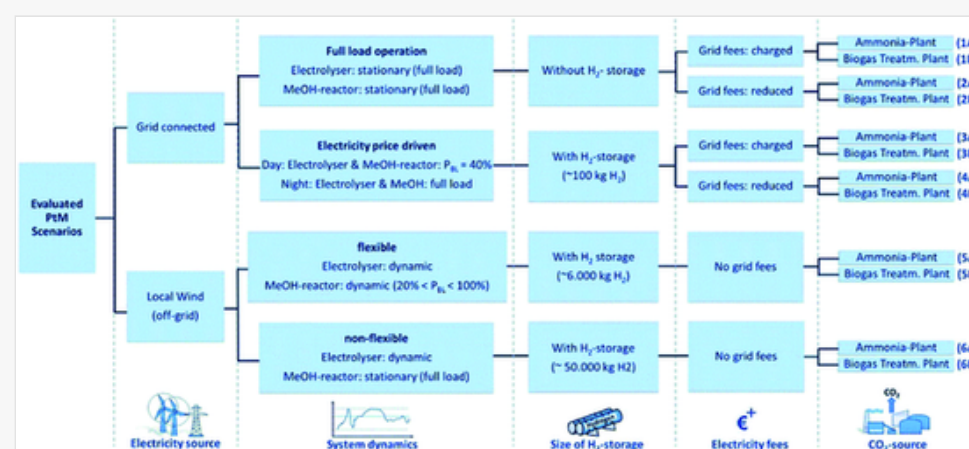
Possible scenarios of PtMeOH. Reproduced from Hank *et al.*[467] with permission from Royal Society of Chemistry.

Kourkoumpas *et al.*[468] evaluated the techno-economics of the PtMeOH and revealed that the process becomes more competitive at larger scale of the plant, longer AOP of the production, lower electricity cost, and low cost of CO_2. Baak *et al.*[469] evaluated the techno-economics of a novel, zero-emission methanol synthesis process, encompassing different power generation units (see Table 13), and deduced that the more efficient (∼30.2%) and cost-effective system is the trans-critical CO_2 gas turbine (tCO_2-GT). Pérez-Fortes *et al.*[26] deduced that the cost of compression, followed by that of a heat exchanger network, are higher for methanol synthesis. Szima and Cormos[429] evaluated the energetically self-sufficient PtMeOH process, and deduced that the heat exchanger network is the main contributor to the capital cost, followed by the compression unit. Reznicek and Braun[85] evaluated the techno-economics and trade-off designs of the ReSOC process and pointed that more work is needed to reduce the equipment capital cost, increasing unit – and hence system efficiency, and the optimisation of stack parameters such as pressure, stack current density, stack fuel utilisation and balance of plant components (*e.g.* compression), to reduce costs.

Wang *et al.*[24] evaluated the operating window of the SOEC stack and techno-economics of the SOEC-based PtMeOH process, operating on steam and co-electrolysis, and reported that the capital cost of a small-scale plant is dominated by the auxiliary equipment cost (*e.g.* compression stages). For larger plants, the SOEC contributed a large portion of the total capital cost of the system (65–75%).[24] The authors pointed out that decreasing the electricity price (or access to free electricity) and increasing the operation hours and stack life (as a function of stack operating temperature) could make the plant operation economically attractive. They emphasised access to free

electricity and, as a result, deduced that, even if the plant AOP is reduced (*e.g.* to 1000 hours per year), the plant can still be economically feasible and benefit from fewer electrolyser stack replacements. They further proposed two operation strategies. The first strategy was to set the electrolyser operating, inlet and outlet temperatures equal, and reduce the current density when required to maintain the temperature below 870 °C. The second strategy was to set the electrolyser inlet and outlet temperatures equal below 870 °C, and reduce only the electrolyser inlet temperature to 750 °C if the both outlet and inlet temperatures exceed 870 °C. The first strategy was found to be preferable since it reduced the temperature gradient between inlet and outlet temperatures, and increased the system efficiency. Zhang *et al.*[428] performed a techno-economic optimisation study for a SOEC-based power-to-methanol process, considering process integration, techno-economics and multi-objective (efficiency and production cost) optimisation. Their results showed a payback time of 13 years. The authors observed that economic performance is a strong function of the SOEC stack cost, electricity price and methanol selling price.

Taking advantage of synergies, Zhang *et al.*[430] compared the techno-economics of steam- and co-electrolysis-based PtMeOH, both integrated with methanol synthesis. They deduced that co-electrolysis-based processes are attractive from an economic point of view with higher annual operation hours and flexibility, whereas biomass-to-methanol with steam electrolysis is highly dependent on the dynamics of renewable electricity. However, the impact of limited biomass availability needs to be factored in as well. From an environmental and techno-economic perspective, interesting results from the study of González-Garay *et al.*,[470] which considered a plant-to-planet analysis of green methanol *via* using a planetary boundaries tool, discussed that the potential damage that green methanol can cause to freshwater use, nitrogen and phosphorous flow are negligible when compared to the positive effects it will have on energy imbalances, CO_2 emission reduction and ocean acidification. The authors further deduced the impact of various components on the techno-economic performance of the process, and highlighted that hydrogen production is the major economic bottleneck that is making the process unfeasible, indicating that more work and subsidies are needed in this direction. Alternatively, improving the carbon capture technologies and introducing a carbon tax of at least 430.50 US$ per t per CO_2 per eq. could make the process attractive and it is the second-most important task. The effects of catalyst improvements (*e.g.* increasing the catalysts efficiency at a pressure <50 bar) will become more dominant (~24.4% share of total costs) when PtMeOH is already economically feasible, indicating that this is less urgent in the short term than reducing both the hydrogen production and CO_2 capture costs.[470] From incentives and a policy decision perspective, Afzali[437] evaluated the role of power-to-methanol in the energy mix. From the authors' simulation and data obtained from interviewing energy experts, Afzali[437] concluded that regional incentives, including the availability of feedstock and land, are the most important factors. On the other hand, PtMeOH is affected by hard and soft institutions, *i.e.* coherence and conformity to regulatory frameworks. However, incentives from knowledge infrastructure and soft institutions have not been investigated enough. Furthermore, as Afzali[437] highlighted, incentives generated from the societal network pertaining to the technology, the structure of actors and policy conformity considering the regulatory framework of implementing PtMeOH deserve further investigation. In addition, the study pointed out that, in order to address financial and market barriers, bilateral contracts, *e.g.* taking advantage of regional incentives, in particular where multi-regions are involved, the formation of consortia between interested parties, *etc.* could be attractive incentives to push the green methanol economy and must be evaluated.[471] For the interested reader, the work of Afzali [437] and Darmani *et al.*[471] gives a good introductory and categorised analysis of these incentives and others, including incentives for actors and network incentives. It is also crucial to highlight that incentives associated with renewable power and hydrogen production, CO_2 abatements and supply chain will play a major role in making PtMeOH economically attractive. On the other hand, incentives devised specifically to support PtMeOH, considering its characteristics, could play a positive role.

PtMeOH is currently not economically feasible in most regions. However, the literature is consistent in the parameters that hold significant impact in the profitability of PtMeOH plants, *i.e.* maximise to full load AOP, lower electricity cost, increase (2 to 3.5 times more than the current) methanol selling price or introduce carbon tax, lower the electrolyser stack cost and increase its lifetime (*e.g.* >90 000 hours). Few studies consider system dynamics, and hence more work is needed here. In addition, other cost-savings from prospective services that these processes may provide to the electricity grid, such as stability, load following, *etc.*, must be incorporated and the associated operation strategies must be developed.[28] More work is required that compares the techno-economic assumptions, system dynamics, single/multiple market dynamics and the associated uncertainties/risks.[472] Integration of market models (*e.g.* for hydrogen and methanol) will improve the economics analysis, and therefore assist policy decision making by taking advantage of the potential positive (push) dynamics. In addition, PtMEOH should also be evaluated in the form of energy/CCU/H_2 hubs. Demonstration projects and transparency in data sharing are needed to improve the techno-economics of PtMeOH processes, particularly for non-mature technologies such as SOEC-based processes. These studies should also couple economics and life-cycle analysis with the explicit consideration of political, societal and environmental aspects.

7. Conclusions

Methanol will play a crucial role in future as a carbon capture and utilisation solution, variable-renewable energy chemical storage medium, and in chemical and transportation industries as an intermediate and a blend, respectively. This paper provided a thorough review of the power-to-methanol process, considering elementary aspects, technologies and system perspectives. From an elementary perspective, power to methanol is limited by exothermicity, thermodynamic equilibrium, kinetics/inconclusive reaction mechanism, large water formation, the RWGS as the main side reaction and high activation energy of CO_2. Complex limitations include low single-pass conversion (particularly for CO_2 hydrogenation to methanol), low-medium energetic efficiency, equipment flexibility requirements, poor catalyst selectivity and limited adaptation to dynamic operating conditions, high cost of attractive electrolyser stack, electrolyser stack degradation, and availability of cheap renewable electricity sources, CO_2 source and favourable incentives. This review has pointed out several research efforts and gaps related to these critical aspects.

Alkaline electrolysis technologies are relatively cheaper than other electrolysis technologies, but less adapted for integration with variable renewable energy sources. The PEM electrolyser is well adapted for integration with variable solar and wind energy sources. However, the SOEC-based technologies can be more advantageous to consider for integration with exothermic reactions such as methanol, especially with its capability to perform both H_2O and CO_2 co-electrolysis, and thus it must be optimised for integration with variable renewable energy sources. The SOEC technologies use non-noble metals, which make them further attractive relative to PEM electrolysis technologies. Continued demonstration of these technologies will play a key role, and the findings will help improve electrolyser and reactor design and modelling. It is also not concluded in literature as to which electrolysis technology is the winner in the context of PtMeOH. Besides, there exists a need for an improved understanding of electrolyser(s), CO_2 capture technology and methanol reactor and catalyst flexibilities assessing effective operation windows/strategies, start-up and shut down requirements and long-term degradations under dynamic conditions. From design perspectives, electrolysers, particularly SOEC and ReSOC, must be optimised by reducing their cost (*e.g.* from materials, cell and stack to system level), improving their stack durability, compactness, efficiency and flexibility. Improvements in the CO_2 capture technologies are also required, for example reduction in the energy penalty and assessment and optimisation of CO_2 capture technologies from sustainable sources (*e.g.* DAC) and finding cost effective sorbents and hybrid solutions. Catalyst optimisation should be directed towards increasing conversion and selectivity at lower temperature and pressure conditions, as well as tolerance to poisons, *e.g.* water and reactor inlet dynamics. Reactor design must be optimised by improving its heat dissipation capability, its flow field to enhance conversion and its flexibility at reasonable costs. Efforts in these directions must be supported by advanced (*e.g.* multiscale) modelling techniques and experimentation.

Evaluation of the overall process modelling studies showed that variable renewable energy-powered co-electrolysis-derived syngas conversion to methanol has higher energy efficiency than the direct CO_2 hydrogenation route with hydrogen derived from electrolysis (see Sections 2 and 6). However, the direct CO_2 hydrogenation route is attractive from an environmental perspective, and simplifies the reactor design (low hot spot formation) and downstream methanol separation. On the other hand, process synthesis and intensification, taking into account relevant details to perform multi-objective analyses of trade-offs and non-trade-offs, and optimisation of the topology

design of the overall power-to-methanol are required. Dynamic system operation strategies stand a chance to be beneficial to the overall system and improve the system efficiency. Therefore, they should be analysed and optimised to maximise the plant operation time and profitability, among others. It will be essential to also study this from a microgrid (especially with the ReSOC-based systems) perspective, and to consider various uncertainties. One-pot processes that combine electrolysis (steam- or co-electrolysis) and methanol synthesis in a single unit are also a new paradigm shift that is supported by process intensification goals and is attractive for distributed applications, but need further investigation, *e.g.* transport phenomena and the associated interactions, economics, *etc.* The continued model-based assessment of PtMeOH processes and subsequent demonstrations will provide valuable insight into the effects of – but not limited to – current trends in renewable energy prices, equipment cost, catalyst activity, process efficiencies and market price of methanol, social/environmental and political dynamics, on the viability of PtMeOH as a whole. It is necessary to apply life cycle thinking in process design and optimisation, and viable synergies/cohesions and diversities should be explored. Should PtMeOH become economically feasible by any means, *e.g.* government push on the subsiding cost of electrolysers, the implementation of new policies on electricity generation/pricing and carbon tax; the lack of detailed understanding of aspects such as reaction mechanisms, though a requirement for further optimisation, shall not limit the immediate application of power-to-methanol since it will provide crucial advantages both to the environment and technically to the energy systems. On the other hand, noting the variation in methanol prices, it remains a question whether developing one-pot processes in which the feed is converted to methanol, and methanol is further processed to other value-added products in one step, provided they are made technically feasible, will have a higher economic advantage and assist in responding advantageously to market sensitivities.

7.1. Further opportunities for innovations

Opportunities for attractive business cases and innovation must be explored in the following areas as well:

• Integration of power-to-methanol process into existing/new infrastructures, *e.g.* CO_2-emitting petrochemical plants and, for the purpose of reject-heat and waste-H_2 utilisation to produce methanol, *e.g.* as a combination with renewable electrolysis-derived hydrogen or during variable renewable energy downtimes, will enhance the attractiveness of implementing renewables in industry. Flexibility, resilience and reliability become key design philosophies to consider in this regard, in addition to maximising profit, as coupled system complexity and unpredictability increase. Investigation of methanol production using combination of low-cost hydrogen production methods, such as the so called Aqua-hydrogen (recently discussed in the work of Yu *et al.*[476]) and others such as biogas reforming is required.

• Coupling catalysts morphological changes to design and control the reactor in the process will be a key novelty to improve the understanding of the interaction between the catalytic activity and the reactants' flow field. In particular, the concept of catalyst shape changes, which affects its activity presents opportunities. Additionally, is the propagation of reactor dynamics *e.g.* from one stage to the next.

• Regenerative-condensing reactors that provide dual function, *i.e.* condense methanol *in situ*, while regenerating catalyst activity at a cheaper cost and using a specific solvent, which can be easily separated from the product solution and with the flexibility and resilience required for methanol synthesis, particularly under dynamic conditions, will be key, and the appropriate solvents and reactor design are required.

• On the other hand, a new and improved method of catalyst design using process synthesis or process system engineering techniques, coupled with techno-economics, optimisation and molecular level knowledge (*e.g.* of catalysts' morphology, active sites, deactivation, *etc.*) or models will be a key novelty to meet the individual process goals for different feedstocks and processes, and further offer opportunities to reduce the capital and operation costs of the processes.

• Other opportunities include utilising additive manufacturing to design 3D-structured and extended surface catalysts and reactor technologies, and use of process intensification techniques such as reactive distillation processes.[477,478]

This paper offers necessary insight and gaps in a holistic manner to researchers and engineers working in the field. Collaborations among researchers, engineers in the field, and policy makers is required to close the gap towards commercialisation.

Abbreviations

AOP:	Annual operation hours of the plant
ASR:	Area-specific resistance
AWE:	Alkaline water electrolysis/electrolyser
BOP:	Balance of plant
CCU:	Carbon capture and utilisation
CE:	Co-electrolysis syngas hydrogenation
CFD:	Computational fluid dynamics
coSyn-MEOH:	H_2O/CO_2 co-electrolysis-derived syngas to methanol
CRI:	Carbon recycling institute
dCO_2-MeOH:	Steam electrolysis-derived hydrogen to methanol *via* the direct CO_2 hydrogenation route
DAC:	Direct air capture
DEA:	Di-ethanolamine
DFT:	Density function theory
DMC:	Dimethyl carbonate
DME:	Dimethyl ether
EES:	Efficiency of energy substitution
EGRM:	Entropy generation rate minimisation
GHSV:	Gas hourly space velocity
HT-SOEC:	High-temperature solid oxide electrolyser
LH:	Langmuir–Hinshelwood
LHHW:	Langmuir–Hinshelwood–Hougen–Watson
LOGIC:	Liquid-out gas-in
MEA:	Mono-ethanolamine
MCP:	Minimum cost design point
MCR:	Thermally coupled membrane reactor
MEP:	Maximum efficiency point
MGC/MHI:	Mitsubishi gas chemical/Mitsubishi heavy industry
MHPSE:	Mitsubishi Hitachi Power Systems Europe
MOF:	Metal–organic framework
MTBE:	Methyl-*tert*-butil-ether
PSA:	Pressure swing adsorption

PBRs:	Packed-bed reactor(s)
PEM:	Polymer electrolyte membrane
PtMeOH:	Power to methanol
PV:	Photovoltaic
R&D:	Research and development
ReSOC:	Reversible solid oxide cell
ReSOFC:	Reversible solid oxide fuel cell
ROI:	Return on investment
RWGS:	Reverse water gas shift reaction
Rxn:	Reaction
SE:	CO_2 hydrogenation
SOEC:	Solid oxide electrolysis cells
SOFC:	Solid oxide fuel cell
SPECO:	Specific exergy costing
TCR:	Thermally coupled (methanol synthesis) reactors
TES:	Thermal energy storage
TRL:	Technology readiness level

Author contributions

Siphesihle Mbatha: conceptualization, investigation, formal analysis, writing – original draft, writing – review & editing. Raymond C. Everson: conceptualization, supervision, writing – review & editing. Nicholas M. Musyoka: supervision, writing – review & editing, funding acquisition, project administration. Henrietta W. Langmi: supervision, writing – review & editing. Andrea Lanzini: writing – review & editing. Wim Brilman: writing – review & editing.

Conflicts of interest

There are no conflicts of interest to declare.

Acknowledgements

References

ⓘ References can be edited in the panel that appears to the right when you click on a reference.

1 S. G. Jadhav, P. D. Vaidya, B. M. Bhanage and J. B. Joshi, Catalytic carbon dioxide hydrogenation to methanol: A review of recent studies, *Chem. Eng. Res. Des.*, 2014, **92**, 11, 2557–2567.

2 P. Esmaili, I. Dincer and G. F. Naterer, Development and analysis of an integrated photovoltaic system for hydrogen and methanol production, *Int. J. Hydrogen Energy*, 2015, **40**, 34, 11140–11153.

3 C. Panzone, R. Philippe, A. Chappaz, P. Fongarland and A. Bengaouer, Power-to-Liquid catalytic CO_2 valorization into fuels and chemicals: focus on the Fischer-Tropsch route, *J. CO2 Util.*, 2020, **38**, 314–347.

4 H. Al-Kalbani, J. Xuan, S. García and H. Wang, Comparative energetic assessment of methanol production from CO_2: Chemical versus electrochemical process, *Appl. Energy*, 2016, **165**, 1–3.

5 F. Ausfelder and K. Wagemann, Power-to-Fuels: E-Fuels as an Important Option for a Climate-Friendly Mobility of the Future, *Chem. Ing. Tech.*, 2020, **92**, 1–2, 21–30.

6 A. W. Jensen, P. Sorknæs, B. S. Bez and T. B. Nielsen, Socioeconomic Value Implementation For Power-to-X in Transportation, Aalborg University, Denmark, 2020

7 D. Parigi, E. Giglio, A. Soto and M. Santarelli, Power-to-fuels through carbon dioxide Re-Utilization and high-temperature electrolysis: A technical and economical comparison between synthetic methanol and methane, *J. Cleaner Prod.*, 2019, **226**, 679–691.

8 G. Leonzio, P. U. Foscolo and E. Zondervan, An outlook towards 2030: optimization and design of a CCUS supply chain in Germany, *Comput. Chem. Eng.*, 2019, **125**, 499–513.

9 F. Schwabe, L. Schwarze, C. Partmann, W. Lippmann and A. Hurtado, Concept, design, and energy analysis of an integrated power-to-methanol process utilizing a tubular proton-conducting solid oxide electrolysis cell, *Int. J. Hydrogen Energy*, 2019, **44**, 25, 12566–12575.

10 V. Dieterich, A. Buttler, A. Hanel, H. Spliethoff and S. Fendt, Power-to-liquid via synthesis of methanol, DME or Fischer–Tropsch-fuels: a review, *Energy Environ. Sci.*, 2020, **13**, 10, 3207–3252.

11 A. Álvarez, A. Bansode, A. Urakawa, A. V. Bavykina, T. A. Wezendonk, M. Makkee, J. Gascon and F. Kapteijn, Challenges in the greener production of formates/formic acid, methanol, and DME by heterogeneously catalyzed CO_2 hydrogenation processes, *Chem. Rev.*, 2017, **117**, 14, 9804–9838.

12 Q. I. Roode-Gutzmer, D. Kaiser and M. Bertau, Renewable Methanol Synthesis, *ChemBioEng Rev.*, 2019, **6**, 6, 209–236.

13 G. Leonzio, State of art and perspectives about the production of methanol, dimethyl ether and syngas by carbon dioxide hydrogenation, *J. CO2 Util.*, 2018, **27**, 326–354.

14 C. Bergins, E. L. Fox, K. C. Tran and P. Wuebben, Commercialization of low carbon methanol, *ATZextra worldwide*, 2016, **21**, 11, 22–25.

15 G. Harp, K. C. Tran, C. Bergins, T. Buddenberg, I. Drach, E. I. Koytsoumpa and O. Sigurbjörnson, Application of power to methanol technology to integrated steelworks for profitability, conversion efficiency, and CO_2 reduction, Proceedings of the 2nd European Steel Technology and Application Days, Duesseldorf, Germany, 2015, 15–9

16 J. Toth, S. Szlovák and R. Magda, Innovations Connected to Methanol in the Service of Blue Economy, *Visegrad Journal on Bioeconomy and Sustainable Development*, 2018, **7**, 1, 7–10.

17 A New Leading Process for CO_2 to Methanol, New Energy And Fuel, 2008, available: https://newenergyandfuel.com/http:/newenergyandfuel/com/2008/08/29/a-new-leading-process-for-co2-to-methanol/

18 A. Boretti, Renewable hydrogen to recycle CO_2 to methanol, *Int. J. Hydrogen Energy*, 2013, **38**, 4, 1806–1812.

19 D. Mignard and C. Pritchard, On the use of electrolytic hydrogen from variable renewable energies for the enhanced conversion of biomass to fuels, *Chem. Eng. Res. Des.*, 2008, **86**, 5, 473–487.

20 F. W. Speckmann, S. Bintz and K. P. Birke, Influence of rectifiers on the energy demand and gas quality of alkaline electrolysis systems in dynamic operation, *Appl. Energy*, 2019, **250**, 855–863.

21 Z. Bai, Q. Liu, L. Gong and J. Lei, Investigation of a solar-biomass gasification system with the production of methanol and electricity: Thermodynamic, economic and off-design operation, *Appl. Energy*, 2019, **243**, 91–101.

22 N. Nikačević, B. Todić, M. Mandić, M. Petkovska and D. B. Bukur, Optimization of forced periodic operations in milli-scale fixed bed reactor for Fischer-Tropsch synthesis, *Catal. Today*, 2020, **343**, 156–164.

23 L. K. Rihko-Struckmann, A. Peschel, R. Hanke-Rauschenbach and K. Sundmacher, Assessment of methanol synthesis utilizing exhaust CO_2 for chemical storage of electrical energy, *Ind. Eng. Chem. Res.*, 2010, **49**, 21, 11073–11078.

24 L. Wang, M. Chen, R. Küngas, T. E. Lin, S. Diethelm and F. Maréchal, Power-to-fuels via solid-oxide electrolyzer: Operating window and techno-economics, *Renewable Sustainable Energy Rev.*, 2019, **110**, 174–187.

25 R. Rivera-Tinoco, M. Farran, C. Bouallou, F. Auprêtre, S. Valentin, P. Millet and J. R. Ngameni, Investigation of power-to-methanol processes coupling electrolytic hydrogen production and catalytic CO_2 reduction, *Int. J. Hydrogen Energy*, 2016, **41**, 8, 4546–4559.

26 M. Pérez-Fortes, J. C. Schöneberger, A. Boulamanti and E. Tzimas, Methanol synthesis using captured CO_2 as raw material: Techno-economic and environmental assessment, *Appl. Energy*, 2016, **161**, 718–732.

27 K. Atsonios, K. D. Panopoulos and E. Kakaras, Investigation of technical and economic aspects for methanol production through CO_2 hydrogenation, *Int. J. Hydrogen Energy*, 2016, **41**, 4, 2202–2214.

28 R. Andika, Y. Kim, C. M. Yun, S. H. Yoon and M. Lee, Design of a renewable energy system with battery and power-to-methanol unit, *Korean J. Chem. Eng.*, 2019, **36**, 1, 12–20.

29 M. Rivarolo, D. Bellotti, L. Magistri and A. F. Massardo, Feasibility study of methanol production from different renewable sources and thermo-economic analysis, *Int. J. Hydrogen Energy*, 2016, **41**, 4, 2105–2116.

30 F. Lonis, V. Tola and G. Cau, Renewable methanol production and use through reversible solid oxide cells and recycled CO_2 hydrogenation, *Fuel*, 2019, **246**, 500–515.

31 P. Schmidt, V. Batteiger, A. Roth, W. Weindorf and T. Raksha, Power-to-Liquids as Renewable Fuel Option for Aviation: A Review, *Chem. Ing. Tech.*, 2018, **90**, 1–2, 127–140.

32 G. Léonard, D. Giulini and D. Villarreal-Singer, Design and evaluation of a high-density energy storage route with CO_2 re-use, water electrolysis and methanol synthesis, in Computer Aided Chemical Engineering, Elsevier, 2016, Elsevier, vol. 38, 1797–1802

33 D. S. Marlin, E. Sarron and Ó. Sigurbjörnsson, Process advantages of direct CO_2 to methanol synthesis, *Front. Chem.*, 2018, **6**, 446.

34 S. Haag, F. Castillo-Welter, T. Schuhmann, B. A. Williams, T. Oelmann, A. Guenther and M. Gorny, How to convert CO_2 to green methanol. Challenges for Petrochemicals and Fuels: Integration of Value Chains and Energy Transition DGMK Conference, Berlin, Germany, 2018

35 X. Cui and S. K. Kær, A comparative study on three reactor types for methanol synthesis from syngas and CO_2, *Chem. Eng. J.*, 2020, 124632.

36 A. Hankin and N. Shah, Process exploration and assessment for the production of methanol and dimethyl ether from carbon dioxide and water, *Sustainable Energy Fuels*, 2017, **1**, 7, 1541–1556.

37 T. Matsushita, T. Haganuma and D. Fujita, Process for producing methanol, US Pat., US20130237618A, retrieved from: https://patents.google.com/patent/US20130237618A1/en

38 B. A. Walid, B. Hassiba, H. Boumediene and S. Weifeng, Improved Design of the Lurgi Reactor for Methanol Synthesis Industry, *Chem. Eng. Technol.*, 2018, **41**, 10, 2043–2052.

39 M. J. Bos, S. R. Kersten and D. W. Brilman, Wind power to methanol: Renewable methanol production using electricity, electrolysis of water and CO_2 air capture, *Appl. Energy*, 2020, **264**, 114672.

40 M. Mehrpooya, B. Ghorbani, A. Shahsavari and A. Zaitsev, Conversion and storage of solar energy in the forms of liquid fuel and electricity in a hybrid energy storage system using methanol and phase change materials, *Energy Convers. Manage.*, 2020, **209**, 112669.

41 G. Liesche, D. Schack, K. H. Rätze and K. Sundmacher, Thermodynamic network flow approach for chemical process synthesis, InComputer Aided Chemical Engineering, Elsevier, 2018, vol. 43, 881–886

42 L. Wang, Y. Zhang, M. Pérez-Fortes, P. Aubin, T. E. Lin, Y. Yang and F. Maréchal, Reversible solid-oxide cell stack based power-to-x-to-power systems: Comparison of thermodynamic performance, *Appl. Energy*, 2020, **275**, 115330.

43

H. Zhang and U. Desideri, Techno-economic optimization of power-to-methanol with co-electrolysis of CO_2 and H_2O in solid-oxide electrolyzers, *Energy*, 2020, 117498.

44 B. Anicic, P. Trop and D. Goricanec, Comparison between two methods of methanol production from carbon dioxide, *Energy*, 2014, **77**, 279–289.

45 M. J. Bos and D. W. Brilman, A novel condensation reactor for efficient CO_2 to methanol conversion for storage of renewable electric energy, *Chem. Eng. J.*, 2015, **278**, 527–532.

46 A. A. Kiss, J. J. Pragt, H. J. Vos, G. Bargeman and M. T. De Groot, Novel efficient process for methanol synthesis by CO_2 hydrogenation, *Chem. Eng. J.*, 2016, **284**, 260–269.

47 N. Khunathorncharoenwong, P. Charoensuppanimit, S. Assabumrungrat and P. Kim-Lohsoontorn, Techno-economic analysis of alternative processes for alcohol-assisted methanol synthesis from carbon dioxide and hydrogen, *Int. J. Hydrogen Energy*, 2020.

48 F. Scheepers, M. Stähler, A. Stähler, E. Rauls, M. Müller, M. Carmo and W. Lehnert, Improving the efficiency of PEM electrolyzers through membrane-specific pressure optimization, *Energies*, 2020, **13**, 3, 612.

49 J. Burre, D. Bongartz, L. Brée, K. Roh and A. Mitsos, Power-to-X: Between Electricity Storage, e-Production, and Demand Side Management, *Chem. Ing. Tech.*, 2020, **92**, 1–2, 74–84.

50 E. I. Koytsoumpa, C. Bergins and E. Kakaras, The CO_2 economy: Review of CO_2 capture and reuse technologies, *J. Supercrit. Fluids*, 2018, **132**, 3–16.

51 P. Colombo, A. Saeedmanesh, M. Santarelli and J. Brouwer, Dynamic dispatch of solid oxide electrolysis system for high renewable energy penetration in a microgrid, *Energy Convers. Manage.*, 2020, **204**, 112322.

52 J. Brauns and T. Turek, Alkaline water electrolysis powered by renewable energy: A review, *Processes*, 2020, **8**, 2, 248.

53 P. Olivier, C. Bourasseau and P. B. Bouamama, Low-temperature electrolysis system modelling: A review, *Renewable Sustainable Energy Rev.*, 2017, **78**, 280–300.

54 A. Ursua, L. M. Gandia and P. Sanchis, Hydrogen production from water electrolysis: current status and future trends, *Proc. IEEE*, 2011, **100**, 2, 410–426.

55 J. O. Jensen, V. Bandur, N. J. Bjerrum, S. H. Jensen, S. Ebbesen, M. Mogensen, N. Tophoj and L. Yde Pre-investigation of water electrolysis, Technical University of Denmark, Lyngby, 2008, 196

56 D. Stolten and D. Krieg, Alkaline Electrolysis-Introduction and Overview, *ChemInform*, 2011, **42**, 38, 243–270.

57 K. Zeng and D. Zhang, Recent progress in alkaline water electrolysis for hydrogen production and applications, *Prog. Energy Combust. Sci.*, 2010, **36**, 3, 307–326.

58 M. Carmo, D. L. Fritz, J. Mergel and D. Stolten, A comprehensive review on PEM water electrolysis, *Int. J. Hydrogen Energy*, 2013, **38**, 12, 4901–4934.

59 J. B. Hansen, Solid oxide electrolysis–a key enabling technology for sustainable energy scenarios, *Faraday Discuss.*, 2015, **182**, 9–48.

60 S. D. Ebbesen, S. H. Jensen, A. Hauch and M. B. Mogensen, High temperature electrolysis in alkaline cells, solid proton conducting cells, and solid oxide cells, *Chem. Rev.*, 2014, **114**, 21, 10697–10734.

61 M. A. Laguna-Bercero, Recent advances in high temperature electrolysis using solid oxide fuel cells: A review, *J. Power Sources*, 2012, **203**, 4–16.

62 V. Venkataraman, M. Pérez-Fortes, L. Wang, Y. S. Hajimolana, C. Boigues-Muñoz, A. Agostini, S. J. McPhail, F. Maréchal, J. Van Herle and P. V. Aravind, Reversible solid oxide systems for energy and chemical applications–Review & perspectives, *Journal of Energy Storage*, 2019, **24**, 100782.

63 R. Küngas, Electrochemical CO_2 Reduction for CO Production: Comparison of Low-and High-Temperature Electrolysis Technologies, *J. Electrochem. Soc.*, 2020, **167**, 4, 044508.

64 S. S. Kumar and V. Himabindu, Hydrogen production by PEM water electrolysis–A review, *Mater. Sci. Energy Technol.*, 2019, **2**, 3, 442–454.

65 D. S. Falcão and A. M. Pinto, A review on PEM Electrolyzer Modelling: Guidelines for beginners, *J. Cleaner Prod.*, 2020, 121184.

66 R. Andika, A. B. Nandiyanto, Z. A. Putra, M. R. Bilad, Y. Kim, C. M. Yun and M. Lee, Co-electrolysis for power-to-methanol applications, *Renewable Sustainable Energy Rev.*, 2018, **95**, 227–241.

67 F. J. Wirkert, J. Roth, S. Jagalski, P. Neuhaus, U. Rost and M. Brodmann, A modular design approach for PEM electrolyser systems with homogeneous operation conditions and highly efficient heat management, *Int. J. Hydrogen Energy*, 2020, **45**, 2, 1226–1235.

68 J. Kibsgaard, P. C. Vesborg and I. Chorkendorff, Power to fuels and chemicals innovation challenge. DTU International Energy Report, 2018, 73

69 A. A. AlZahrani and I. Dincer, Modeling and performance optimization of a solid oxide electrolysis system for hydrogen production, *Appl. Energy*, 2018, **225**, 471–485.

70 J. P. Stempien, Q. Sun and S. H. Chan, Solid oxide electrolyzer cell modeling: A review, *J. Power Technol.*, 2013, **93**, 4, 216–246.

71 A. Ursúa, E. L. Barrios, J. Pascual, I. San Martín and P. Sanchis, Integration of commercial alkaline water electrolysers with renewable energies: Limitations and improvements, *Int. J. Hydrogen Energy*, 2016, **41**, 30, 12852–12861.

72 C. Lamy and P. Millet, A critical review on the definitions used to calculate the energy efficiency coefficients of water electrolysis cells working under near ambient temperature conditions, *J. Power Sources*, 2020, **447**, 227350.

73 M. Bernt, A. Siebel and H. A. Gasteiger, Analysis of voltage losses in PEM water electrolyzers with low platinum group metal loadings, *J. Electrochem. Soc.*, 2018, **165**, 5, F305.

74 A. Grimaud, J. Rossmeisl and P. Strasser, Research needs towards sustainable production of fuels and chemicals: Water splitting and sustainable H$_2$ production, 2018, retrieved from: https://www.energy-x.eu/wp-content/uploads/2019/09/Energy_X_Research-needs-report.pdf

75 S. A. Grigoriev, P. Millet, S. V. Korobtsev, V. I. Porembskiy, M. Pepic, C. Etievant, C. Puyenchet and V. N. Fateev, Hydrogen safety aspects related to high-pressure polymer electrolyte membrane water electrolysis, *Int. J. Hydrogen Energy*, 2009, **34**, 14, 5986–5991.

76 C. Geipel, K. Hauptmeier, K. Herbrig, F. Mittmann, M. Münch, M. Pötschke, L. Reichel, T. Strohbach, T. Seidel, A. Surrey and C. Walter, Stack Development and Industrial Scale-Up, *ECS Trans.*, 2019, **91**, 1, 123.

77 G. Herz, E. Reichelt and M. Jahn, Techno-economic analysis of a co-electrolysis-based synthesis process for the production of hydrocarbons, *Appl. Energy*, 2018, **215**, 309–320.

78 Y. Zheng, J. Wang, B. Yu, W. Zhang, J. Chen, J. Qiao and J. Zhang, A review of high temperature co-electrolysis of H$_2$O and CO$_2$ to produce sustainable fuels using solid oxide electrolysis cells (SOECs): advanced materials and technology, *Chem. Soc. Rev.*, 2017, **46**, 5, 1427–1463.

79 D. Ferrero, Design, development and testing of SOEC-based Power-to-Gas systems for conversion and storage of RES into synthetic methane, doctoral dissertation, Politecnico di Torino, Italy, 2016.

80 B. Chen, Modelling and optimization of solid oxide cells for energy conversion and storage, doctoral dissertation, The Hong Kong Polytechnic University, China, 2018.

81 A. Pandiyan, A. Uthayakumar, R. Subrayan, S. W. Cha and S. B. Krishna Moorthy, Review of solid oxide electrolysis cells: a clean energy strategy for hydrogen generation, *Nanomater. Energy*, 2019, **8**, 1, 2.

82 L. R. Tarutina, J. G. Lyagaeva, A. S. Farlenkov, A. I. Vylkov, G. K. Vdovin, A. A. Murashkina, A. K. Demin and D. A. Medvedev, Doped (Nd, Ba) FeO$_3$ oxides as potential electrodes for symmetrically designed protonic ceramic electrochemical cells, *J. Solid State Electrochem.*, 2020, 1–10.

83 Hydrogenics, 2020, available: https://www.hydrogenics.com/wp-content/uploads/2-1-1-industrial-brochure_english.pdf?sfvrsn

84 C. H. Wendel, P. Kazempoor and R. J. Braun, Novel electrical energy storage system based on reversible solid oxide cells: System design and operating conditions, *J. Power Sources*, 2015, **276**, 133–144.

85 E. Reznicek and R. J. Braun, Techno-economic and off-design analysis of stand-alone, distributed-scale reversible solid oxide cell energy storage systems, *Energy Convers. Manage.*, 2018, **175**, 263–277.

86 J. Mermelstein and O. Posdziech, Development and demonstration of a novel reversible SOFC system for utility and micro grid energy storage, *Fuel Cells*, 2017, **17**, 4, 562–570.

87 Y. Wang, T. Liu, L. Lei and F. Chen, High temperature solid oxide H$_2$O/CO$_2$ co-electrolysis for syngas production, *Fuel Process. Technol.*, 2017, **161**, 248–258.

88 A. Sojoudi, A. M. Sefidan, K. C. Alam and S. C. Saha, Hydrogen production via electrolysis: Mathematical modeling approach, in Bioenergy Resources and Technologies, Academic Press, 2021, 199–235

89 Ø. Ulleberg, Modeling of advanced alkaline electrolyzers: a system simulation approach, *Int. J. Hydrogen Energy*, 2003, **28**, 1, 21–33.

90 T. Holm, T. Borsboom-Hanson, O. E. Herrera and W. Mérida, Hydrogen costs from water electrolysis at high temperature and pressure, *Energy Convers. Manage.*, 2021, **237**, 114106.

91 A. C. Avci and E. Toklu, A new analysis of two phase flow on hydrogen production from water electrolysis, *Int. J. Hydrogen Energy*, 2021, DOI: https://doi.org/10.1016/j.ijhydene.2021.03.180.

92 M. T. de Groot and A. W. Vreman, Ohmic resistance in zero gap alkaline electrolysis with a Zirfon diaphragm, *Electrochim. Acta*, 2021, **369**, 137684.

93 F. W. Speckmann, D. Keiner and K. P. Birke, Influence of rectifiers on the techno-economic performance of alkaline electrolysis in a smart grid environment, *Renewable Energy*, 2020, **159**, 107–116.

94 C. Schnuelle, T. Wassermann, D. Fuhrlaender and E. Zondervan, Dynamic hydrogen production from PV & wind direct electricity supply–Modeling and techno-economic assessment, *Int. J. Hydrogen Energy*, 2020, **45**, 55, 29938–29952.

95 J. Rodríguez and E. Amores, CFD Modeling and Experimental Validation of an Alkaline Water Electrolysis Cell for Hydrogen Production, *Processes*, 2020, **8**, 12, 1634.

96 M. Hammoudi, C. Henao, K. Agbossou, Y. Dubé and M. L. Doumbia, New multi-physics approach for modelling and design of alkaline electrolyzers, *Int. J. Hydrogen Energy*, 2012, **37**, 19, 13895–13913.

97 J. Schillings, O. Doche and J. Deseure, Modeling of electrochemically generated bubbly flow under buoyancy-driven and forced convection, *Int. J. Heat Mass Transfer*, 2015, **85**, 292–299.

98 J. Vanhanen, Mathematical modelling of an electrolyser, University of Technology, Department of Technical Physics, 1990

99 P. S. Kauranen, P. D. Lund and J. P. Vanhanen, Development of a self-sufficient solar-hydrogen energy system, Int. J. Hydrogen Energy, 1994, 19, 1, 99–106; S. Santhanam, Process systems analysis of reversible Solid Oxide Cell (rSOC) reactors for electricity storage and sector coupling, University of Stuttgart, Stuttgart, Germany

100 Z. Abdin, C. J. Webb and E. M. Gray, Modelling and simulation of an alkaline electrolyser cell, *Energy*, 2017, **138**, 316–331.

101 A. Ursúa and P. Sanchis, Static–dynamic modelling of the electrical behaviour of a commercial advanced alkaline water electrolyser, *Int. J. Hydrogen Energy*, 2012, **37**, 24, 18598–18614.

102 L. Abdelouahed, R. Hreiz, S. Poncin, G. Valentin and F. Lapicque, Hydrodynamics of gas bubbles in the gap of lantern blade electrodes without forced flow of electrolyte: Experiments and CFD modelling, *Chem. Eng. Sci.*, 2014, **111**, 255–265.

103 M. Schalenbach, G. Tjarks, M. Carmo, W. Lueke, M. Mueller and D. Stolten, Acidic or alkaline? Towards a new perspective on the efficiency of water electrolysis, *J. Electrochem. Soc.*, 2016, **163**, 11, F3197.

104 P. Haug, B. Kreitz, M. Koj and T. Turek, Process modelling of an alkaline water electrolyzer, *Int. J. Hydrogen Energy*, 2017, **42**, 24, 15689–15707.

105 Voltachem and TNO, Modeling aging and degradation of stacks for a gigawatt electrolyzer, 2020, https://www.voltachem.com/news/modeling-aging-and-degradation-of-stacks-for-a-gigawatt-electrolyzer

106 J. P. Vanhanen and P. D. Lund, Computational approaches for improving seasonal storage systems based on hydrogen technologies, *Int. J. Hydrogen Energy*, 1995, **20**, 7, 575–585.

107 J. Milewski, G. Guandalini and S. Campanari, Modeling an alkaline electrolysis cell through reduced-order and loss-estimate approaches, *J. Power Sources*, 2014, **269**, 203–211.

108 G. Matute, J. M. Yusta, J. Beyza and L. C. Correas, Multi-state techno-economic model for optimal dispatch of grid connected hydrogen electrolysis systems operating under dynamic conditions, *Int. J. Hydrogen Energy*, 2021, **46**, 2, 1449–1460.

109 Ø. Ulleberg and S. O. Mørner, TRNSYS simulation models for solar-hydrogen systems, *Sol. Energy*, 1997, **59**, 4–6, 271–279.

110 S. Kélouwani, K. Agbossou and R. Chahine, Model for energy conversion in renewable energy system with hydrogen storage, *J. Power Sources*, 2005, **140**, 2, 392–399.

111 J. J. Hwang, W. R. Chang and A. Su, Dynamic modeling of a solar hydrogen system under leakage conditions, *Int. J. Hydrogen Energy*, 2008, **33**, 14, 3615–3624.

112 A. Roy, S. Watson and D. Infield, Comparison of electrical energy efficiency of atmospheric and high-pressure electrolysers, *Int. J. Hydrogen Energy*, 2006, **31**, 14, 1964–1979.

113 C. Henao, K. Agbossou, M. Hammoudi, Y. Dubé and A. Cardenas, Simulation tool based on a physics model and an electrical analogy for an alkaline electrolyser, *J. Power Sources*, 2014, **250**, 58–67.

114 E. Amores, J. Rodríguez and C. Carreras, Influence of operation parameters in the modeling of alkaline water electrolyzers for hydrogen production, *Int. J. Hydrogen Energy*, 2014, **39**, 25, 13063–13078.

115 C. Lei, Y. Wang, Y. Hou, P. Liu, J. Yang, T. Zhang, X. Zhuang, M. Chen, B. Yang, L. Lei and C. Yuan, Efficient alkaline hydrogen evolution on atomically dispersed Ni–N x Species anchored porous carbon with embedded Ni nanoparticles by accelerating water dissociation kinetics, *Energy Environ. Sci.*, 2019, **12**, 1, 149–156.

116 J. Wang, Y. Gao, H. Kong, J. Kim, S. Choi, F. Ciucci, Y. Hao, S. Yang, Z. Shao and J. Lim, Non-precious-metal catalysts for alkaline water electrolysis: operando characterizations, theoretical calculations, and recent advances, *Chem. Soc. Rev.*, 2020, **49**, 9154–9196, DOI: https://doi.org/10.1039/D0CS00575D.

117 D. Franzen, M. C. Paulisch, B. Ellendorff, I. Manke and T. Turek, Spatially resolved model of oxygen reduction reaction in silver-based porous gas-diffusion electrodes based on operando measurements, *Electrochim. Acta*, 2021, **375**, 137976.

118 Z. Taie, Accelerating Power-to-Gas Energy Storage Through PEM Electrolyzer Development and Technoeconomic Forecasting, 2021.

119 J. Kibsgaard and I. Chorkendorff, Considerations for the scaling-up of water splitting catalysts, *Nat. Energy*, 2019, **4**, 6, 430–433.

120 H. Kim, M. Park and K. S. Lee, One-dimensional dynamic modeling of a high-pressure water electrolysis system for hydrogen production, *Int. J. Hydrogen Energy*, 2013, **38**, 6, 2596–2609.

121 M. E. Lebbal and S. Lecœuche, Identification and monitoring of a PEM electrolyser based on dynamical modelling, *Int. J. Hydrogen Energy*, 2009, **34**, 14, 5992–5999.

122 B. Yodwong, D. Guilbert, M. Hinaje, M. Phattanasak, W. Kaewmanee and G. Vitale, Proton Exchange Membrane Electrolyzer Emulator for Power Electronics Testing Applications, *Processes*, 2021, **9**, 3, 498.

123 A. C. Olesen, S. H. Frensch and S. K. Kær, Towards uniformly distributed heat, mass and charge: A flow field design study for high pressure and high current density operation of PEM electrolysis cells, *Electrochim. Acta*, 2019, **293**, 476–495.

124 M. B. Abdelghany, M. F. Shehzad, D. Liuzza, V. Mariani and L. Glielmo, Optimal operations for hydrogen-based energy storage systems in wind farms via model predictive control, *Int. J. Hydrogen Energy*, 2021.

125 R. Maamouri, D. Guilbert, M. Zasadzinski and H. Rafaralahy, Proton exchange membrane water electrolysis: Modeling for hydrogen flow rate control, *Int. J. Hydrogen Energy*, 2021, **46**, 11, 7676–7700.

126 S. Sood, O. Prakash, M. Boukerdja, J. Y. Dieulot, B. Ould-Bouamama, M. Bressel and A. L. Gehin, Generic Dynamical Model of PEM Electrolyser under Intermittent Sources, *Energies*, 2020, **13**, 24, 6556.

127 Z. Ma, L. Witteman, J. A. Wrubel and G. Bender, A comprehensive modeling method for proton exchange membrane electrolyzer development, *Int. J. Hydrogen Energy*, 2021, **46**, 34, 17627–17643.

128 F. Arbabi, H. Montazeri, R. Abouatallah, R. Wang and A. Bazylak, Three-dimensional computational fluid dynamics modelling of oxygen bubble transport in polymer electrolyte membrane electrolyzer porous transport layers, *J. Electrochem. Soc.*, 2016, **163**, 11, F3062.

129 B. Han, J. Mo, Z. Kang and F. Y. Zhang, Effects of membrane electrode assembly properties on two-phase transport and performance in proton exchange membrane electrolyzer cells, *Electrochim. Acta*, 2016, **188**, 317–326.

130 J. K. Lee, C. H. Lee and A. Bazylak, Pore network modelling to enhance liquid water transport through porous transport layers for polymer electrolyte membrane electrolyzers, *J. Power Sources*, 2019, **437**, 226910.

131

M. Chandesris, V. Médeau, N. Guillet, S. Chelghoum, D. Thoby and F. Fouda-Onana, Membrane degradation in PEM water electrolyzer: Numerical modeling and experimental evidence of the influence of temperature and current density, *Int. J. Hydrogen Energy*, 2015, **40**, 3, 1353–1366.

132 O. Atlam and M. Kolhe, Equivalent electrical model for a proton exchange membrane (PEM) electrolyser, *Energy Convers. Manage.*, 2011, **52**, 8–9, 2952–2957.

133 M. G. Dozein, A. Jalali and P. Mancarella, Fast Frequency Response from Utility-Scale Hydrogen Electrolyzers, *IEEE Transactions on Sustainable Energy*, 2021, **12**, 3, 1707–1717.

134 B. Flamm, C. Peter, F. N. Büchi and J. Lygeros, Electrolyzer modeling and real-time control for optimized production of hydrogen gas, *Appl. Energy*, 2021, **281**, 116031.

135 I. Holmes-Gentle, S. Tembhurne, C. Suter and S. Haussener, Dynamic system modeling of thermally-integrated concentrated PV-electrolysis, *Int. J. Hydrogen Energy*, 2021, **46**, 18, 10666–10681.

136 M. Sartory, E. Wallnöfer-Ogris, P. Salman, T. Fellinger, M. Justl, A. Trattner and M. Klell, Theoretical and experimental analysis of an asymmetric high pressure PEM water electrolyser up to 155 bar, *Int. J. Hydrogen Energy*, 2017, **42**, 52, 30493–30508.

137 Á. Hernández-Gómez, V. Ramirez, D. Guilbert and B. Saldivar, Cell voltage static-dynamic modeling of a PEM electrolyzer based on adaptive parameters: Development and experimental validation, *Renewable Energy*, 2021, **163**, 1508–1522.

138 A. Beainy, N. Karami and N. Moubayed, Simulink model for a PEM electrolyzer based on an equivalent electrical circuit, International Conference on Renewable Energies for Developing Countries 2014, Ieee, 2014, 145–149

139 F. Aubras, M. Rhandi, J. Deseure, A. J. Kadjo, M. Bessafi, J. Majasan, B. Grondin-Perez, F. Druart and J. P. Chabriat, Dimensionless approach of a polymer electrolyte membrane water electrolysis: Advanced analytical modelling, *J. Power Sources*, 2021, **481**, 228858.

140 L. F. Oliveira, C. Jallut and A. A. Franco, A multiscale physical model of a polymer electrolyte membrane water electrolyzer, *Electrochim. Acta*, 2013, **110**, 363–374.

141 F. Ramadhani, M. A. Hussain, H. Mokhlis and S. Hajimolana, Optimization strategies for Solid Oxide Fuel Cell (SOFC) application: A literature survey, *Renewable Sustainable Energy Rev.*, 2017, **76**, 460–484.

142 C. Bienert, M. Brandner, S. Skrabs, A. Venskutonis, L. S. Sigl, S. Megel, W. Becker, N. Trofimenko, M. Kusnezoff and A. Michaelis, CFY-stack technology: the next design, *ECS Trans.*, 2015, **68**, 1, 2159.

143 A. Lindermeir, C. Immisch, C. Szepanski, J. Hamje, A. Bentaleb and L. Dörrer, New SOFC-Stack Design with Parallel-Connected Cells–Basic Concept and Joining Aspects, *Fuel Cells*, 2015, **15**, 5, 703–710.

144 V. Menon, Q. Fu, V. M. Janardhanan and O. Deutschmann, A model-based understanding of solid-oxide electrolysis cells (SOECs) for syngas production by H_2O/CO_2 co-electrolysis, *J. Power Sources*, 2015, **274**, 768–781.

145 Y. Luo, Y. Shi, Y. Chen, W. Li and N. Cai, In-situ thermal integration between H_2O/CO_2 co-electrolysis and thermochemistry by heat-flow design for efficient direct power-to-methane, International Heat Transfer Conference Digital Library, Begel House Inc, 2018

146 Y. Naumovich, M. Błesznowski and A. Żurawska, Contemporary approaches to planar SOFC stack design and performance characterization, inModeling, Design, Construction, and Operation of Power Generators with Solid Oxide Fuel Cells, Springer, Cham, 2018, 49–96

147 L. Peigat, M. Reytier, F. Ledrappier and J. Besson, A leakage model to design seals for solid oxide fuel and electrolyser cell stacks, *Int. J. Hydrogen Energy*, 2014, **39**, 13, 7109–7119.

148 M. A. Laguna-Bercero, R. Campana, A. Larrea, J. A. Kilner and V. M. Orera, Performance and Aging of Microtubular YSZ-based Solid Oxide Regenerative Fuel Cells, *Fuel Cells*, 2011, **11**, 1, 116–123.

149 A. Banerjee, Y. Wang, J. Diercks and O. Deutschmann, Hierarchical modeling of solid oxide cells and stacks producing syngas via H_2O/CO_2 Co-electrolysis for industrial applications, *Appl. Energy*, 2018, **230**, 996–1013.

150 M. Seitz, H. von Storch, A. Nechache and D. Bauer, Techno economic design of a solid oxide electrolysis system with solar thermal steam supply and thermal energy storage for the generation of renewable hydrogen, *Int. J. Hydrogen Energy*, 2017, **42**, 42, 26192–26202.

151 C. Wang, M. Chen, M. Liu and J. Yan, Dynamic modeling and parameter analysis study on reversible solid oxide cells during mode switching transient processes, *Appl. Energy*, 2020, **263**, 114601.

152 C. Graves, S. D. Ebbesen, S. H. Jensen, S. B. Simonsen and M. B. Mogensen, Eliminating degradation in solid oxide electrochemical cells by reversible operation, *Nat. Mater.*, 2015, **14**, 2, 239–244.

153 T. M. Gür, Review of electrical energy storage technologies, materials and systems: challenges and prospects for large-scale grid storage, *Energy Environ. Sci.*, 2018, **11**, 10, 2696–2767.

154 X. Zhang, J. E. O'Brien, R. C. O'Brien, J. J. Hartvigsen, G. Tao and G. K. Housley, Improved durability of SOEC stacks for high temperature electrolysis, *Int. J. Hydrogen Energy*, 2013, **38**, 1, 20–28.

155 V. T. Giap, Y. D. Lee, Y. S. Kim and K. Y. Ahn, A novel electrical energy storage system based on a reversible solid oxide fuel cell coupled with metal hydrides and waste steam, *Appl. Energy*, 2020, **262**, 114522.

156 H. Xu, B. Chen, J. Irvine and M. Ni, Modeling of CH_4-assisted SOEC for H_2O/CO_2 co-electrolysis, *Int. J. Hydrogen Energy*, 2016, **41**, 47, 21839–21849.

157 B. Chen, H. Xu, H. Zhang, P. Tan, W. Cai and M. Ni, A novel design of solid oxide electrolyser integrated with magnesium hydride bed for hydrogen generation and storage–A dynamic simulation study, *Appl. Energy*, 2017, **200**, 260–272.

158

F. Chen, L. Lei, T. Liu and S. Fang, Direct synthesis of hydrocarbons from co-electrolysis solid oxide cell, United States pat., US10336944, University of South Carolina, 2019

159 J. Sanz-Bermejo, J. Muñoz-Antón, J. Gonzalez-Aguilar and M. Romero, Part load operation of a solid oxide electrolysis system for integration with renewable energy sources, *Int. J. Hydrogen Energy*, 2015, **40**, 26, 8291–8303.

160 F. Petipas, A. Brisse and C. Bouallou, Model-based behaviour of a high temperature electrolyser system operated at various loads, *J. Power Sources*, 2013, **239**, 584–595.

161 Y. Takagi, R. Yoshimura, N. Tsuchiya, M. Yamada, H. Watanabe and T. Kameda, HTES Hydrogen Production Plant Control Methods for Fluctuating Power Sources, *Institute of Electrical Engineers of Japan Transactions on Power and Energy*, 2020, **140**, 2, 117–125.

162 K. Motylinski, M. Wierzbicki, S. Jagielski and J. Kupecki, Investigation of off-design characteristics of solid oxide electrolyser (SOE) operated in endothermic conditions, In E3S Web of Conferences, EDP Sciences, 2019, vol. 137, 01029

163 V. T. Giap, S. Kang and K. Y. Ahn, High-efficient reversible solid oxide fuel cell coupled with waste steam for distributed electrical energy storage system, *Renewable Energy*, 2019, **144**, 129–138.

164 P. Kazempoor and R. J. Braun, Model validation and performance analysis of regenerative solid oxide cells for energy storage applications: Reversible operation, *Int. J. Hydrogen Energy*, 2014, **39**, 11, 5955–5971.

165 L. Wang, M. Rao, S. Diethelm, T. E. Lin, H. Zhang, A. Hagen and F. Maréchal, Power-to-methane via co-electrolysis of H_2O and CO_2: The effects of pressurized operation and internal methanation, *Appl. Energy*, 2019, **250**, 1432–1445.

166 M. García-Camprubí, S. Izquierdo and N. Fueyo, Challenges in the electrochemical modelling of solid oxide fuel and electrolyser cells, *Renewable Sustainable Energy Rev.*, 2014, **33**, 701–718.

167 Y. Luo, Y. Shi, W. Li and N. Cai, Dynamic electro-thermal modeling of co-electrolysis of steam and carbon dioxide in a tubular solid oxide electrolysis cell, *Energy*, 2015, **89**, 637–647.

168 H. Moussaoui, J. Debayle, Y. Gavet, P. Cloetens and J. Laurencin, Particle-based model for functional and diffusion layers of solid oxide cells electrodes, *Powder Technology*, 2020, **367**, 67–81.

169 J. Xia, C. Wang, X. Wang, L. Bi and Y. Zhang, A perspective on DRT applications for the analysis of solid oxide cell electrodes, *Electrochim. Acta*, 2020, 136328.

170 Y. Wang, Y. Du, M. Ni, R. Zhan, Q. Du and K. Jiao, Three-dimensional modeling of flow field optimization for co-electrolysis solid oxide electrolysis cell, *Appl. Therm. Eng.*, 2020, 114959.

171 A. Ploner, A. Hauch, S. Pylypko, G. Di Iorio, G. Cubizolles and J. Mougin, Optimization of Solid Oxide Cells and Stacks for Reversible Operation, *ECS Trans.*, 2019, **91**, 1, 2517.

172 M. Navasa, C. Graves, C. Chatzichristodoulou, T. L. Skafte, B. Sundén and H. L. Frandsen, A three dimensional multiphysics model of a solid oxide electrochemical cell: A tool for understanding degradation, *Int. J. Hydrogen Energy*, 2018, **43**, 27, 11913–11931.

173 J. Kupecki, L. Mastropasqua, K. Motylinski and D. Ferrero, Multilevel modeling of solid oxide electrolysis. InSolid Oxide-Based Electrochemical Devices, Academic Press, 2020, 123–166

174 T. Parhizkar and S. Hafeznezami, Degradation based operational optimization model to improve the productivity of energy systems, case study: Solid oxide fuel cell stacks, *Energy Convers. Manage.*, 2018, **158**, 81–91.

175 Y. Chi, Y. Qiu, J. Lin, Y. Song, W. Li, Q. Hu, S. Mu and M. Liu, A robust surrogate model of a solid oxide cell based on an adaptive polynomial approximation method, *Int. J. Hydrogen Energy*, 2020, **45**, 58, 32949–32971.

176 P. Di Giorgio and U. Desideri, Potential of reversible solid oxide cells as electricity storage system, *Energies*, 2016, **9**, 8, 662.

177 X. Xing, J. Lin, Y. Song, Q. Hu, Y. Zhou and S. Mu, Optimization of hydrogen yield of a high-temperature electrolysis system with coordinated temperature and feed factors at various loading conditions: A model-based study, *Appl. Energy*, 2018, **232**, 368–385.

178 B. Numan, Y. S. Hajimolana, K. Motylinski, J. Kupecki, V. Venkataraman and P. V. Aravind, Dynamic modelling of reversible solid oxide cell for grid stabilisation applications, *Energy Convers. Manage.*, 2021, **228**, 113674.

179 A. Saeedmanesh and J. Brouwer, Dynamic Modeling of a Solid Oxide Electrolyzer System under Two Different Thermal Control Strategies, 13th European SOFC & SOE Forum, Lucerne, Switzerland, 2018

180 Q. Cai, C. S. Adjiman and N. P. Brandon, Optimal control strategies for hydrogen production when coupling solid oxide electrolysers with intermittent renewable energies, *J. Power Sources*, 2014, **268**, 212–224.

181 J. Laurencin, D. Kane, G. Delette, J. Deseure and F. Lefebvre-Joud, Modelling of solid oxide steam electrolyser: Impact of the operating conditions on hydrogen production, *J. Power Sources*, 2011, **196**, 4, 2080–2093.

182 S. Santhanam, M. P. Heddrich and K. A. Friedrich, Dynamic and steady state analysis of a power to methane system using a commercial solid oxide cell (SOC) electrochemical reactor, 13th European SOFC & SOE Forum, Lucerne, Switzerland, 2018

183 P. Colombo, Solid Oxide Electrolysis System: Dynamic modeling and microgrid integration, doctoral dissertation, Politecnico di Torino, Torino, Italy, 2018.

184 A. Saeedmanesh, P. Colombo, D. McLarty and J. Brouwer, Dynamic Behavior of a Solid Oxide Steam Electrolyzer System Using Transient Photovoltaic Generated Power for Renewable Hydrogen Production, *J. Electrochem. Energy Convers. Storage*, 2019, **16**, 4, 041008.

185 S. Giannoulidis, V. Venkataraman, T. Woudstra and P. V. Aravind, Methanol based Solid Oxide Reversible energy storage system–Does it make sense thermodynamically?, *Appl. Energy*, 2020, **278**, 115623.

186 C. Zhang, Q. Liu, Q. Wu, Y. Zheng, J. Zhou, Z. Tu and S. H. Chan, Modelling of solid oxide electrolyser cell using extreme learning machine, *Electrochim. Acta*, 2017, **251**, 137–144.

187 H. L. Frandsen, M. Navasa, T. T. Molla and P. V. Hendriksen, Computational efficient 3D multiphysics models to estimate the long-term mechanical behavior of SOC stacks, 12th European SOFC & SOE Forum, Lucerne, Switzerland, 2016

188 G. Botta, M. Romeo, A. Fernandes, S. Trabucchi and P. V. Aravind, Dynamic modeling of reversible solid oxide cell stack and control strategy development, *Energy Convers. Manage.*, 2019, **185**, 636–653.

189 Q. Cai, N. P. Brandon and C. S. Adjiman, Modelling the dynamic response of a solid oxide steam electrolyser to transient inputs during renewable hydrogen production, *Frontiers of Energy and Power Engineering in China*, 2010, **4**, 2, 211–222.

190 A. Cifuentes López, A. Husar, V. Roda, M. Morales, L. Bernadet, M. Torrell and M. Serra, Modelling of solid oxide electrolizer and hydrogen leak estimation, 7th Iberian Symposium on Hydrogen, Fuel Cells and Advanced Batteries. 2019

191 C. Wang, M. Chen, M. Liu and J. Yan, Dynamic modeling and parameter analysis study on reversible solid oxide cells during mode switching transient processes, *Appl. Energy*, 2020, **263**, 114601.

192 J. S. Diercks, Model-based performance analysis of a solid oxide co-electrolyzer to produce syngas for industrial applications, ~~Institut für Technische Chemie und Polymerchemie~~*Institut für Technische Chemie und Polymerchemie*, 2017.

193 Y. Tanaka, M. P. Hoerlein and G. Schiller, Numerical simulation of steam electrolysis with a solid oxide cell for proper evaluation of cell performances, *Int. J. Hydrogen Energy*, 2016, **41**, 2, 752–763.

194 E. C. Shin, P. A. Ahn, H. H. Seo, J. M. Jo, S. D. Kim, S. K. Woo, J. H. Yu, J. Mizusaki and J. S. Lee, Polarization mechanism of high temperature electrolysis in a Ni–YSZ/YSZ/LSM solid oxide cell by parametric impedance analysis, *Solid State Ionics*, 2013, **232**, 80–96.

195 S. H. Jensen, A. Hauch, R. Knibbe, T. Jacobsen and M. Mogensen, Modeling degradation in SOEC impedance spectra, *J. Electrochem. Soc.*, 2013, **160**, 3, F244.

196 V. Subotić, T. Thaller, B. Königshofer, N. H. Menzler, E. Bucher, A. Egger and C. Hochenauer, Performance assessment of industrial-sized solid oxide cells operated in a reversible mode: Detailed numerical and experimental study, *Int. J. Hydrogen Energy*, 2020, **45**, 53, 29166–29185.

197 S. Fogel, H. Kryk and U. Hampel, Simulation of the transient behavior of tubular solid oxide electrolyzer cells under fast load variations, *Int. J. Hydrogen Energy*, 2019, **44**, 18, 9188–9202.

198 R. M. Mendoza, J. M. Mora, R. B. Cervera and P. Y. Chuang, Experimental and Analytical Study of an Anode-Supported Solid Oxide Electrolysis Cell, Chemical Engineering & Technology, 2020

199 J. Han, X. Wang, L. Yan and A. Dahlak, Modelling the performance of an SOEC by optimization of neural network with MPSO algorithm, *Int. J. Hydrogen Energy*, 2019, **44**, 51, 27947–27957.

200 J. P. Neidhardt and W. G. Bessler, Microkinetic Modeling of Nickel Oxidation in Solid Oxide Cells: Prediction of Safe Operating Conditions, *Chem. Ing. Tech.*, 2019, **91**, 6, 843–855.

201 M. Navasa, Three dimensional multiphysics modeling of reversible solid oxide electrochemical cells for degradation studies, doctoral dissertation~~, doctoral dissertation, ,~~ Lund University, Sweden, 2016.

202 M. Rao, X. Sun and A. Hagen, Durability of solid oxide electrolysis stack under dynamic load cycling for syngas production, *J. Power Sources*, 2020, **451**, 227781.

203 C. Chatzichristodoulou, M. Chen, P. V. Hendriksen, T. Jacobsen and M. B. Mogensen, Understanding degradation of solid oxide electrolysis cells through modeling of electrochemical potential profiles, *Electrochim. Acta*, 2016, **189**, 265–282.

204 M. Trini, S. De Angelis, P. S. Jørgensen, A. Hauch, M. Chen and P. V. Hendriksen, Phase Field Modelling of Microstructural Changes in NI/YSZ Solid Oxide Electrolysis Cell Electrodes, In Proceedings of the 42nd International Conference on Advanced Ceramics and Composites, Ceramic Engineering and Science Proceedings, John Wiley & Sons, issue 2, 2018, 165

205 M. Nerat and Đ. Juričić, Modelling of anode delamination in solid oxide electrolysis cell and analysis of its effects on electrochemical performance, *Int. J. Hydrogen Energy*, 2018, **43**, 17, 8179–8189.

206 A. Banerjee, Y. Wang, J. Diercks and O. Deutschmann, Hierarchical modeling of solid oxide cells and stacks producing syngas via H_2O/CO_2 Co-electrolysis for industrial applications, *Appl. Energy*, 2018, **230**, 996–1013.

207 Y. Wang, A. Banerjee, L. Wehrle, Y. Shi, N. Brandon and O. Deutschmann, Performance analysis of a reversible solid oxide cell system based on multi-scale hierarchical solid oxide cell modelling, *Energy Convers. Manage.*, 2019, **196**, 484–496.

208 L. Ma, P. Priya and N. R. Aluru, A multiscale model for electrochemical reactions in LSCF based solid oxide cells, *J. Electrochem. Soc.*, 2018, **165**, 14, F1232.

209 P. Priya and N. R. Aluru, A multiscale framework to predict electrochemical characteristics of yttrium doped Barium Zirconate based solid oxide cells, *J. Power Sources*, ~~n.d.~~2021, **481**, 228969.

210 P. Thibaudeau, A. C. Roger, S. Thomas, J. Laurencin, M. Petitjean, G. Roux and J. Mougin, Kinetic Modelling of Catalytic Reactions in Solid Oxide Cells: Study of Its Coupling with Electrochemistry for Steam and CO_2 Co-Electrolysis and Steam Reforming, *ECS Trans.*, 2017, **78**, 1, 3129.

211 M. Ni, 2D thermal modeling of a solid oxide electrolyzer cell (SOEC) for syngas production by H_2O/CO_2 co-electrolysis, *Int. J. Hydrogen Energy*, 2012, **37**, 8, 6389–6399.

212 Y. Shi, N. Cai, T. Cao and J. Zhang, High-temperature Electrochemical Energy Conversion and Storage: Fundamentals and Applications, CRC Press, 2017

213 M. Ostadi, K. G. Paso, S. Rodriguez-Fabia, L. E. Øi, F. Manenti and M. Hillestad, Process integration of green hydrogen: Decarbonization of chemical industries, *Energies*, 2020, **13**, 18, 4859.

214 A. Dwivedi, R. Gudi and P. Biswas, An improved water electrolysis and oxy-fuel combustion coupled tri-reforming process for methanol production and CO_2 valorization, *J. Environ. Chem. Eng.*, 2021, **9**, 1, 105041.

215 I. Ghiat and T. Al-Ansari, A review of carbon capture and utilisation as a CO_2 abatement opportunity within the EWF nexus, *J. CO2 Util.*, 2021, **45**, 101432.

216 H. Mikulčić, I. R. Skov, D. F. Dominković, S. R. Alwi, Z. A. Manan, R. Tan, N. Duić, S. N. Mohamad and X. Wang, Flexible Carbon Capture and Utilization technologies in future energy systems and the utilization pathways of captured CO_2, *Renewable Sustainable Energy Rev.*, 2019, **114**, 109338.

217 A. Mukherjee, J. A. Okolie, A. Abdelrasoul, C. Niu and A. K. Dalai, Review of post-combustion carbon dioxide capture technologies using activated carbon, *J. Environ. Sci.*, 2019, **83**, 46–63.

218 J. D. Figueroa, T. Fout, S. Plasynski, H. McIlvried and R. D. Srivastava, Advances in CO_2 capture technology—the US Department of Energy's Carbon Sequestration Program, *Int. J. Greenhouse Gas Control*, 2008, **2**, 1, 9–20.

219 A. Veawab, A. Aroonwilas and P. Tontiwachwuthikul, CO_2 absorption performance of aqueous alkanolamines in packed columns, *Fuel Chemistry Division Preprints*, 2002, **47**, 1, 49–50.

220 S. A. Mazari, L. Ghalib, A. Sattar, M. M. Bozdar, A. Qayoom, I. Ahmed, A. Muhammad, R. Abro, A. Abdulkareem, S. Nizamuddin and H. Baloch, Review of modelling and simulation strategies for evaluating corrosive behavior of aqueous amine systems for CO_2 capture, *Int. J. Greenhouse Gas Control*, 2020, **96**, 103010.

221 X. Wu, M. Wang, P. Liao, J. Shen and Y. Li, Solvent-based post-combustion CO_2 capture for power plants: A critical review and perspective on dynamic modelling, system identification, process control and flexible operation, *Appl. Energy*, 2020, **257**, 113941.

222 R. Ben-Mansour, M. A. Habib, O. E. Bamidele, M. Basha, N. A. Qasem, A. Peedikakkal, T. Laoui and M. J. Ali, Carbon capture by physical adsorption: materials, experimental investigations and numerical modeling and simulations–a review, *Appl. Energy*, 2016, **161**, 225–255.

223 D. Y. Leung, G. Caramanna and M. M. Maroto-Valer, An overview of current status of carbon dioxide capture and storage technologies, *Renewable Sustainable Energy Rev.*, 2014, **39**, 426–443.

224 E. Adu, Y. D. Zhang, D. Liu and P. Tontiwachwuthikul, Parametric Process Design and Economic Analysis of Post-Combustion CO_2 Capture and Compression for Coal-and Natural Gas-Fired Power Plants, *Energies*, 2020, **13**, 10, 2519.

225 H. Marsh, F. R. Reinoso, Activated carbon, Elsevier, 2006

226 S. W. Park, D. H. Sung, B. S. Choi, J. W. Lee and H. Kumazawa, Carbonation kinetics of potassium carbonate by carbon dioxide, *J. Ind. Eng. Chem.*, 2006, **12**, 4, 522–530.

227 E. Abbasi and H. Arastoopour, CFD simulation of CO2 sorption in a circulating fluidized bed using deactivation kinetic model, CFD simulation of CO_2 sorption in a circulating fluidized bed using deactivation kinetic model 2011.

228 A. D. Ebner and J. A. Ritter, State-of-the-art adsorption and membrane separation processes for carbon dioxide production from carbon dioxide emitting industries, *Sep. Sci. Technol.*, 2009, **44**, 6, 1273–1421.

229 X. Wang and C. Song, Carbon Capture From Flue Gas and the Atmosphere: A Perspective, *Frontiers in Energy Research*, 2020, **8**, 560849.

230 H. Wu, Q. Li, M. Sheng, Z. Wang, S. Zhao, J. Wang, S. Mao, D. Wang, B. Guo, N. Ye and G. Kang, Membrane technology for CO_2 capture: From pilot-scale investigation of two-stage plant to actual system design, *J. Membr. Sci.*, 2021, 119137.

231 M. Osman, M. N. Khan, A. Zaabout, S. Cloete and S. Amini, Review of pressurized chemical looping processes for power generation and chemical production with integrated CO_2 capture, *Fuel Process. Technol.*, 2021, **214**, 106684.

232 S. Abuelgasim, W. Wang and A. Abdalazeez, A brief review for chemical looping combustion as a promising CO_2 capture technology: Fundamentals and progress, *Sci. Total Environ.*, 2020, 142892.

233 G. Shah, E. Ahmad, K. K. Pant and V. K. Vijay, Comprehending the contemporary state of art in biogas enrichment and CO_2 capture technologies via swing adsorption, *Int. J. Hydrogen Energy*, 2020, **46**, 9, 6588–6612.

234 F. Schorn, D. Lohse, R. C. Samsun, R. Peters and D. Stolten, The biogas-oxyfuel process as a carbon source for power-to-fuel synthesis: Enhancing availability while reducing separation effort, *J. CO2 Util.*, 2021, **45**, 101410.

235 F. M. Stuardi, F. MacPherson and J. Leclaire, Integrated CO_2 capture and utilization: A priority research direction, *Current Opinion in Green and Sustainable Chemistry*, 2019, **16**, 71–76.

236 S. Roussanaly, N. Berghout, T. Fout, M. Garcia, S. Gardarsdottir, S. M. Nazir, A. Ramirez and E. S. Rubin, Towards improved cost evaluation of Carbon Capture and Storage from industry, *Int. J. Greenhouse Gas Control*, 2021, **106**, 103263.

237 B. S. Adji, Y. Muharam and S. Kartohardjono, Simulation of Methanol Synthesis in Packed Bed Reactor for Utilization of CO_2 from Acid Gas Removal Unit, In E3S Web of Conferences, EDP Sciences, 2018, vol. 67, 03005

238 M. D. Porosoff, B. Yan and J. G. Chen, Catalytic reduction of CO_2 by H_2 for synthesis of CO, methanol and hydrocarbons: challenges and opportunities, *Energy Environ. Sci.*, 2016, **9**, 1, 62–73.

239 O. Tursunov, L. Kustov and A. Kustov, A brief review of carbon dioxide hydrogenation to methanol over copper and iron based catalysts, *Oil & Gas Sciences and Technology–Revue d'IFP Energies nouvelles*, 2017, **72**, 5, 30.

240

B. S. Adji, Y. Muharam and S. Kartohardjono, Simulation of Methanol Synthesis from CO_2 Hydrogenation in a Packed Bed Reactor using COMSOL Multiphysics, *Int. J. Eng. Res. Sci. Technol.*, 2019, **12**, 12, 2592–2599.

241 N. Park, M. J. Park, Y. J. Lee, K. S. Ha and K. W. Jun, Kinetic modeling of methanol synthesis over commercial catalysts based on three-site adsorption, *Fuel Process. Technol.*, 2014, **125**, 139–147.

242 J. Reichert, S. Maerten, K. Meltzer, A. Tremel, M. Baldauf, P. Wasserscheid and J. Albert, Shifting the equilibrium of methanol synthesis from CO_2 by in situ absorption using ionic liquid media, *Sustainable Energy Fuels*, 2019, **3**, 12, 3399–3405.

243 J. Skrzypek, M. Lachowska, M. Grzesik, J. Słoczyński and P. Nowak, Thermodynamics and kinetics of low pressure methanol synthesis, *The Chemical Engineering Journal and the Biochemical Engineering Journal*, 1995, **58**, 2, 101–108.

244 S. K. Wilkinson, L. G. Van De Water, B. Miller, M. J. Simmons, E. H. Stitt and M. J. Watson, Understanding the generation of methanol synthesis and water gas shift activity over copper-based catalysts–A spatially resolved experimental kinetic study using steady and non-steady state operation under $CO/CO_2/H_2$ feeds, *J. Catal.*, 2016, **337**, 208–220.

245 J. A. Herron, J. Kim, A. A. Upadhye, G. W. Huber and C. T. Maravelias, A general framework for the assessment of solar fuel technologies, *Energy Environ. Sci.*, 2015, **8**, 1, 126–157.

246 G. C. Chinchen and K. C. Waugh, Chemical state of copper during methanol synthesis, *J. Catal.*, 1986, **97**, 1, 280–283.

247 G. C. Chinchen, P. J. Denny, D. G. Parker, M. S. Spencer and D. A. Whan, Mechanism of methanol synthesis from $CO_2/CO/H_2$ mixtures over copper/zinc oxide/alumina catalysts: use of 14C-labelled reactants, *Appl. Catal.*, 1987, **30**, 2, 333–338.

248 G. C. Chinchen, K. Mansfield and M. S. Spencer, The methanol synthesis: How does it work?, *Chemtech*, 1990, **20**, 11, 692–699.

249 M. A. McNeil, C. J. Schack and R. G. Rinker, Methanol synthesis from hydrogen, carbon monoxide and carbon dioxide over a $CuO/ZnO/Al_2O_3$ catalyst: II. Development of a phenomenological rate expression, *Appl. Catal.*, 1989, **50**, 1, 265–285.

250 L. C. Grabow and M. Mavrikakis, Mechanism of methanol synthesis on Cu through CO_2 and CO hydrogenation, *ACS Catal.*, 2011, **1**, 4, 365–384.

251 Y. Zhang, Q. Sun, J. Deng, D. Wu and S. Chen, A high activity $Cu/ZnO/Al_2O_3$ catalyst for methanol synthesis: Preparation and catalytic properties, *Appl. Catal., A*, 1997, **158**, 1–2, 105–120.

252 S. Saeidi, S. Najari, F. Fazlollahi, M. K. Nikoo, F. Sefidkon, J. J. Klemeš and L. L. Baxter, Mechanisms and kinetics of CO_2 hydrogenation to value-added products: A detailed review on current status and future trends, *Renewable Sustainable Energy Rev.*, 2017, **80**, 1292–1311.

253 S. Saeidi, N. A. Amin and M. R. Rahimpour, Hydrogenation of CO_2 to value-added products –A review and potential future developments, *J. CO2 Util.*, 2014, **5**, 66–81.

254 G. Bozzano and F. Manenti, Efficient methanol synthesis: perspectives, technologies and optimization strategies, *Prog. Energy Combust. Sci.*, 2016, **56**, 71–105.

255 K. M. V. Bussche and G. F. Froment, A steady-state kinetic model for methanol synthesis and the water gas shift reaction on a commercial $Cu/ZnO/Al_2O_3$ Catalyst, *J. Catal.*, 1996, **161**, 1, 1–10.

256 Y. Yang, C. A. Mims, D. H. Mei, C. H. Peden and C. T. Campbell, Mechanistic studies of methanol synthesis over Cu from $CO/CO_2/H_2/H_2O$ mixtures: The source of C in methanol and the role of water, *J. Catal.*, 2013, **298**, 10–17.

257 P. Villa, P. Forzatti, G. Buzzi-Ferraris, G. Garone and I. Pasquon, Synthesis of alcohols from carbon oxides and hydrogen. 1. Kinetics of the low-pressure methanol synthesis, *Ind. Eng. Chem. Process Des. Dev.*, 1985, **24**, 1, 12–19.

258 G. H. Graaf, H. Scholtens, E. J. Stamhuis and A. A. Beenackers, Intra-particle diffusion limitations in low-pressure methanol synthesis, *Chem. Eng. Sci.*, 1990, **45**, 4, 773–783.

259 E. L. Kunkes, F. Studt, F. Abild-Pedersen, R. Schlögl and M. Behrens, Hydrogenation of CO_2 to methanol and CO on $Cu/ZnO/Al_2O_3$: Is there a common intermediate or not?, *J. Catal.*, 2015, **328**, 43–48.

260 G. Liu, D. Willcox, M. Garland and H. H. Kung, The role of CO_2 in methanol synthesis on Cu Zn oxide: An isotope labeling study, *J. Catal.*, 1985, **96**, 1, 251–260.

261 G. H. Graaf, E. J. Stamhuis and A. A. Beenackers, Kinetics of low-pressure methanol synthesis, *Chem. Eng. Sci.*, 1988, **43**, 12, 3185–3195.

262 N. D. Nielsen, A. D. Jensen and J. M. Christensen, Quantification of Formate and Oxygen Coverages on Cu Under Industrial Methanol Synthesis Conditions, *Catal. Lett.*, 2020, **150**, 2447–2456.

263 X. M. Liu, G. Q. Lu, Z. F. Yan and J. Beltramini, Recent advances in catalysts for methanol synthesis via hydrogenation of CO and CO_2, *Ind. Eng. Chem. Res.*, 2003, **42**, 25, 6518–6530.

264 Y. Slotboom, M. J. Bos, J. Pieper, V. Vrieswijk, B. Likozar, S. R. Kersten and D. W. Brilman, Critical assessment of steady-state kinetic models for the synthesis of methanol over an industrial $Cu/ZnO/Al_2O_3$ catalyst, *Chem. Eng. J.*, 2020, **389**, 124181.

265 R. Gaikwad, H. Reymond, N. Phongprueksathat, P. R. von Rohr and A. Urakawa, From CO or CO_2?: space-resolved insights into high-pressure CO_2 hydrogenation to methanol over $Cu/ZnO/Al_2O_3$, *Catal. Sci. Technol.*, 2020, **10**, 9, 2763–2768.

266 T. Fujitani, Enhancement of the Catalytic Performance and Active Site Clarification of Cu/ZnO Based Catalysts for Methanol Synthesis by CO_2 Hydrogenation, *J. Jpn. Pet. Inst.*, 2020, **63**, 2, 43–51.

267 N. D. Nielsen, A. D. Jensen and J. M. Christensen, The roles of CO and CO2 in high pressure methanol synthesis over Cu-based catalysts, *J. Catal.*, 2021, **393**, 324–334.

268 M. S. Tameh, A. K. Dearden and C. Huang, Accuracy of density functional theory for predicting kinetics of methanol synthesis from CO and CO2 hydrogenation on copper, *J. Phys. Chem. C*, 2018, **122**, 31, 17942–17953.

269 F. Studt, M. Behrens, E. L. Kunkes, N. Thomas, S. Zander, A. Tarasov, J. Schumann, E. Frei, J. B. Varley, F. Abild-Pedersen and J. K. Nørskov, The mechanism of CO and CO2 hydrogenation to methanol over Cu-based catalysts, *ChemCatChem*, 2015, **7**, 7, 1105–1111.

270 Y. Amenomiya, Infrared Study of Methanol Synthesis from CO_2+ H_2 on Supported Copper-Zinc Oxide Catalysts, in Proc. of 8th Int. Congress on Catal, 1984, vol. 2, 557–567

271 F. Le Peltier, P. Chaumette, J. Saussey, M. M. Bettahar and J. C. Lavalley, In situ FT-IR and kinetic study of methanol synthesis from CO2/H2 over ZnAl2O4 and Cu–ZnAl2O4 catalysts, *J. Mol. Catal. A: Chem.*, 1998, **132**, 1, 91–100.

272 N. Nomura, T. Tagawa and S. Goto, Titania supported copper catalysts for methanol synthesis from carbon dioxide, *React. Kinet. Catal. Lett.*, 1998, **63**, 1, 9–13.

273 K. Ahmad and S. Upadhyayula, Selective conversion of CO_2 to methanol over intermetallic Ga-Ni catalyst: Microkinetic modeling, *Fuel*, 2020, **278**, 118296.

274 K. Ahmad and S. Upadhyayula, Kinetics of CO_2 hydrogenation to methanol over silica supported intermetallic Ga3Ni5 catalyst in a continuous differential fixed bed reactor, *Int. J. Hydrogen Energy*, 2020, **45**, 1, 1140–1150.

275 W. Liu, D. Wang and J. Ren, Methanol synthesis from CO_2/H_2 on Cu (1 0 0): Two-tier ab initio molecular dynamics study, *Appl. Surf. Sci.*, 2020, **505**, 144528.

276 S. Dang, H. Yang, P. Gao, H. Wang, X. Li, W. Wei and Y. Sun, A review of research progress on heterogeneous catalysts for methanol synthesis from carbon dioxide hydrogenation, *Catal. Today*, 2019, **330**, 61–75.

277 S. Kar, J. Kothandaraman, A. Goeppert and G. S. Prakash, Advances in catalytic homogeneous hydrogenation of carbon dioxide to methanol, *J. CO2 Util.*, 2018, **23**, 212–218.

278 K. W. Ting, T. Toyao, S. H. Siddiki and K. I. Shimizu, Low-temperature hydrogenation of CO_2 to methanol over heterogeneous TiO_2-Supported Re catalysts, *ACS Catal.*, 2019, **9**, 4, 3685–3693.

279 J. Sehested, Industrial and scientific directions of methanol catalyst development, J. Catal., 2019, 371, 368–375; Matthey, available: http//:www.matthey.com//

280 K. A. Ali, A. Z. Abdullah and A. R. Mohamed, Recent development in catalytic technologies for methanol synthesis from renewable sources: A critical review, *Renewable Sustainable Energy Rev.*, 2015, **44**, 508–518.

281 J. Zhong, X. Yang, Z. Wu, B. Liang, Y. Huang and T. Zhang, State of the art and perspectives in heterogeneous catalysis of CO $_2$ hydrogenation to methanol, *Chem. Soc. Rev.*, 2020, **49**, 5, 1385–1413.

282 A. S. Alsuhaibani, S. Afzal, M. Challiwala, N. O. Elbashir and M. M. El-Halwagi, The impact of the development of catalyst and reaction system of the methanol synthesis stage on the overall profitability of the entire plant: A techno-economic study, *Catal. Today*, 2020, **343**, 191–198.

283 M. Sahibzada, I. S. Metcalfe and D. Chadwick, Methanol Synthesis from CO/CO_2/H_2 over Cu/ZnO/Al_2O_3 at Differential and Finite Conversions, *J. Catal.*, 1998, **174**, 2, 111–118.

284 L. G. Van de Water, S. K. Wilkinson, R. A. Smith and M. J. Watson, Understanding methanol synthesis from CO/H_2 feeds over Cu/CeO_2 catalysts, *J. Catal.*, 2018, **364**, 57–68.

285 L. Zhang, M. R. Ball, Y. Liu, T. F. Kuech, G. W. Huber, M. Mavrikakis, I. Hermans and J. A. Dumesic, Synthesis gas conversion over Rh/Mo catalysts prepared by atomic layer deposition, *ACS Catal.*, 2019, **9**, 3, 1810–1819.

286 C. Seidel, A. Jörke, B. Vollbrecht, A. Seidel-Morgenstern, A. Kienle. Kinetic Modeling of Methanol Synthesis-Impact of Catalyst Deactivation, in Computer Aided Chemical Engineering, Elsevier, 2018, vol. 43, 85–90

287 M. Liu, Y. Yi, L. Wang, H. Guo and A. Bogaerts, Hydrogenation of carbon dioxide to value-added chemicals by heterogeneous catalysis and plasma catalysis, *Catalysts*, 2019, **9**, 3, 275.

288 F. H. Cao, D. H. Liu, Q. Hou and D. Y. Fang, Thermodynamic Analysis of CO_2 Direct Hydrogenation Reactions, *J. Nat. Gas Chem.*, 2001, **10**, 1, 24–33.

289 O. Martin, A. J. Martín, C. Mondelli, S. Mitchell, T. F. Segawa, R. Hauert, C. Drouilly, D. Curulla-Ferré and J. Pérez-Ramírez, Indium oxide as a superior catalyst for methanol synthesis by CO_2 hydrogenation, *Angew. Chem., Int. Ed.*, 2016, **55**, 21, 6261–6265.

290 S. Li, L. Guo and T. Ishihara, Hydrogenation of CO_2 to methanol over Cu/AlCeO catalyst, *Catal. Today*, 2020, **339**, 352–361.

291 K. Sun, Z. Fan, J. Ye, J. Yan, Q. Ge, Y. Li, W. He, W. Yang and C. J. Liu, Hydrogenation of CO_2 to methanol over In_2O_3 catalyst, *J. CO2 Util.*, 2015, **12**, 1–6.

292 M. M. Li and S. C. Tsang, Bimetallic catalysts for green methanol production via CO $_2$ and renewable hydrogen: a mini-review and prospects, *Catal. Sci. Technol.*, 2018, **8**, 14, 3450–3464.

293 I. Sharafutdinov, Investigations into low pressure methanol synthesis, ~~DTU Orbit~~ *DTU Orbit*, 2013.

294 A. G. Saputro, R. I. Putra, A. L. Maulana, M. U. Karami, M. R. Pradana, M. K. Agusta, H. K. Dipojono and H. Kasai, Theoretical study of CO $_2$ hydrogenation to methanol on isolated small Pdx clusters, *J. Energy Chem.*, 2019, **35**, 79–87.

295 J. L. Snider, V. Streibel, M. A. Hubert, T. S. Choksi, E. Valle, D. C. Upham, J. Schumann, M. S. Duyar, A. Gallo, F. Abild-Pedersen and T. F. Jaramillo, Revealing the synergy between oxide and alloy phases on the performance of bimetallic In–Pd catalysts for CO_2 hydrogenation to methanol, *ACS Catal.*, 2019, **9**, 4, 3399–3412.

296 H. Bahruji, J. R. Esquius, M. Bowker, G. Hutchings, R. D. Armstrong and W. Jones, Solvent Free Synthesis of PdZn/TiO $_2$ Catalysts for the Hydrogenation of CO $_2$ to Methanol, *Top. Catal.*, 2018, **61**, 3–4, 144–153.

297 R. A. Agarwal, Methanol Synthesis from CO_2 Hydrogenation Using Metal–Organic Frameworks, In CO_2 Separation, Purification and Conversion to Chemicals and Fuels, Springer, Singapore, 2019, 79–92

298 K. Stangeland, H. Li and Z. Yu, CO_2 hydrogenation to methanol: the structure–activity relationships of different catalyst systems, *Energy, Ecology and Environment*, 2020, 1–4.

299 K. F. Kalz, I. R. Kraehnert, P. Muslim Dvoyashkin, I. R. Dittmeyer, R. Gläser, I. U. Krewer, K. Reuter and J. D. Grunwaldt, Future challenges in heterogeneous catalysis: understanding catalysts under dynamic reaction conditions, *ChemCatChem*, 2017, **9**, 1, 17.

300 N. Y. Topsøe, In situ FTIR: A versatile tool for the study of industrial catalysts, *Catal. Today*, 2006, **113**, 1–2, 58–64.

301 J. Schittkowski, H. Ruland, D. Laudenschleger, K. Girod, K. Kähler, S. Kaluza, M. Muhler and R. Schlögl, Methanol synthesis from steel mill exhaust gases: challenges for the industrial $Cu/ZnO/Al_2O_3$ catalyst, *Chem. Ing. Tech.*, 2018, **90**, 10, 1419–1429.

302 S. Kattel, P. J. Ramírez, J. G. Chen, J. A. Rodriguez and P. Liu, Active sites for CO_2 hydrogenation to methanol on Cu/ZnO catalysts, *Science*, 2017, **355**, 6331, 1296–1299.

303 H. R. Godini, M. Khadivi, M. Azadi, O. Görke, S. M. Jazayeri, L. Thum, R. Schomäcker, G. Wozny and R. Ju, Multi-scale analysis of integrated c1 (CH_4 and CO_2) utilization catalytic processes: Impacts of catalysts characteristics up to industrial-scale process flowsheeting, part i: Experimental analysis of catalytic low-pressure co2 to methanol conversion, *Catalysts*, 2020, **10**, 5, 505.

304 G. M. Karthik and V. V. Buwa, A computational approach for the selection of optimal catalyst shape for solid-catalysed gas-phase reactions, *React. Chem. Eng.*, 2020, **5**, 1, 163–182.

305 I. C. Lo and H. S. Wu, Methanol formation from carbon dioxide hydrogenation using $Cu/ZnO/Al_2O_3$ catalyst, *J. Taiwan Inst. Chem. Eng.*, 2019, **98**, 124–131.

306 D. Allam, S. Bennici, L. Limousy and S. Hocine, Improved Cu-and Zn-based catalysts for CO_2 hydrogenation to methanol, *C. R. Chim.*, 2019, **22**, 2–3, 227–237.

307 L. Yao, X. Shen, Y. Pan and Z. Peng, Synergy between active sites of Cu-In-Zr-O catalyst in CO_2 hydrogenation to methanol, *J. Catal.*, 2019, **372**, 74–85.

308 W. Wang, Z. Qu, L. Song and Q. Fu, CO_2 hydrogenation to methanol over Cu/CeO_2 and Cu/ZrO_2 catalysts: Tuning methanol selectivity via metal-support interaction, *J. Energy Chem.*, 2020, **40**, 22–30.

309 Y. Wang, S. Kattel, W. Gao, K. Li, P. Liu, J. G. Chen and H. Wang, Exploring the ternary interactions in $Cu–ZnO–ZrO_2$ catalysts for efficient CO_2 hydrogenation to methanol, *Nat. Commun.*, 2019, **10**, 1, 1166.

310 C. Tisseraud, C. Comminges, A. Habrioux, S. Pronier, Y. Pouilloux and A. Le Valant, Cu-ZnO catalysts for CO_2 hydrogenation to methanol: Morphology change induced by ZnO lixiviation and its impact on the active phase formation, *Mol. Catal.*, 2018, **446**, 98–105.

311 S. F. Tasfy, N. A. Zabidi, M. S. Shaharun and D. Subbarao, Effect of Catalyst Synthesis Parameters on the Performance of CO_2 Hydrogenation to Methanol over SBA-15 Supported Cu/ZnO-Based Catalysts, in Defect and Diffusion Forum, Trans Tech Publications Ltd, 2020, vol. 400, 159–169

312 C. Liu, B. Yang, E. Tyo, S. Seifert, J. DeBartolo, B. von Issendorff, P. Zapol, S. Vajda and L. A. Curtiss, Carbon dioxide conversion to methanol over size-selected Cu4 clusters at low pressures, *J. Am. Chem. Soc.*, 2015, **137**, 27, 8676–8679.

313 S. Kuld, M. Thorhauge, H. Falsig, C. F. Elkjær, S. Helveg, I. Chorkendorff and J. Sehested, Quantifying the promotion of Cu catalysts by ZnO for methanol synthesis, *Science*, 2016, **352**, 6288, 969–974.

314 Y. L. Men, Y. Liu, Q. Wang, Z. H. Luo, S. Shao, Y. B. Li and Y. X. Pan, Highly dispersed Pt-based catalysts for selective CO_2 hydrogenation to methanol at atmospheric pressure, *Chem. Eng. Sci.*, 2019, **200**, 167–175.

315 S. Ren, W. R. Shoemaker, X. Wang, Z. Shang, N. Klinghoffer, S. Li, M. Yu, X. He, T. A. White and X. Liang, Highly active and selective Cu-ZnO based catalyst for methanol and dimethyl ether synthesis via CO_2 hydrogenation, *Fuel*, 2019, **239**, 1125–1133.

316 K. Sun, Z. Fan, J. Ye, J. Yan, Q. Ge, Y. Li, W. He, W. Yang and C. J. Liu, Hydrogenation of CO_2 to methanol over In_2O_3 catalyst, *J. CO2 Util.*, 2015, **12**, 1–6.

317 L. Angelo, M. Girleanu, O. Ersen, C. Serra, K. Parkhomenko and A. C. Roger, Catalyst synthesis by continuous coprecipitation under micro-fluidic conditions: Application to the preparation of catalysts for methanol synthesis from CO_2/H_2, *Catal. Today*, 2016, **270**, 59–67.

318 Z. Shi, Q. Tan and D. Wu, A novel Core–Shell structured $CuIn@SiO_2$ catalyst for CO_2 hydrogenation to methanol, *AIChE J.*, 2019, **65**, 3, 1047–1058.

319 J. A. Singh, A. Cao, J. Schumann, T. Wang, J. K. Nørskov, F. Abild-Pedersen and S. F. Bent, Theoretical and Experimental Studies of CoGa Catalysts for the Hydrogenation of CO_2 to Methanol, *Catal. Lett.*, 2018, **148**, 12, 3583–3591.

320 X. L. Liang, X. Dong, G. D. Lin and H. B. Zhang, Carbon nanotube-supported Pd–ZnO catalyst for hydrogenation of CO_2 to methanol, *Appl. Catal., B*, 2009, **88**, 3–4, 315–322.

321 W. Li, P. Lu, D. Xu and K. Tao, CO 2 hydrogenation to methanol over Cu/ZnO catalysts synthesized via a facile solid-phase grinding process using oxalic acid, *Korean J. Chem. Eng.*, 2018, **35**, 1, 110–117.

322 J. Qu, X. Zhou, F. Xu, X. Q. Gong and S. C. Tsang, Shape effect of Pd-promoted Ga_2O_3 nanocatalysts for methanol synthesis by CO_2 hydrogenation, *J. Phys. Chem. C*, 2014, **118**, 42, 24452–24466.

323 N. Rui, Z. Wang, K. Sun, J. Ye, Q. Ge and C. J. Liu, CO_2 hydrogenation to methanol over Pd/In_2O_3: effects of Pd and oxygen vacancy, *Appl. Catal., B*, 2017, **218**, 488–497.

324

T. Fujitani, M. Saito, Y. Kanai, T. Watanabe, J. Nakamura and T. Uchijima, Development of an active Ga_2O_3 supported palladium catalyst for the synthesis of methanol from carbon dioxide and hydrogen, *Appl. Catal., A*, 1995, **125**, 2, L199–L202.

325 F. Liao, X. P. Wu, J. Zheng, M. M. Li, A. Kroner, Z. Zeng, X. Hong, Y. Yuan, X. Q. Gong and S. C. Tsang, A promising low pressure methanol synthesis route from CO_2 hydrogenation over Pd@ Zn core–shell catalysts, *Green Chem.*, 2017, **19**, 1, 270–280.

326 Y. Yin, B. Hu, X. Li, X. Zhou, X. Hong and G. Liu, Pd@ zeolitic imidazolate framework-8 derived PdZn alloy catalysts for efficient hydrogenation of CO_2 to methanol, *Appl. Catal., B*, 2018, **234**, 143–152.

327 J. Wang, G. Li, Z. Li, C. Tang, Z. Feng, H. An, H. Liu, T. Liu and C. Li, A highly selective and stable ZnO-ZrO$_2$ solid solution catalyst for CO_2 hydrogenation to methanol, *Sci. Adv.*, 2017, **3**, 10, e1701290.

328 Q. Tan, Z. Shi and D. Wu, CO_2 hydrogenation to methanol over a highly active Cu–Ni/CeO$_2$–nanotube catalyst, *Ind. Eng. Chem. Res.*, 2018, **57**, 31, 10148–10158.

329 P. Gao, L. Zhong, L. Zhang, H. Wang, N. Zhao, W. Wei and Y. Sun, Yttrium oxide modified Cu/ZnO/Al$_2$O$_3$ catalysts via hydrotalcite-like precursors for CO$_2$ hydrogenation to methanol, *Catal. Sci. Technol.*, 2015, **5**, 9, 4365–4377.

330 S. Tasfy, N. A. Zabidi, M. S. Shaharun and D. Subbarao, Methanol production via CO$_2$ hydrogenation reaction: effect of catalyst support, *Int. J. Nanotechnol.*, 2017, **14**, 1–6, 410–421.

331 M. M. Li, C. Chen, T. Ayvalı, H. Suo, J. Zheng, I. F. Teixeira, L. Ye, H. Zou, D. O'Hare and S. C. Tsang, CO_2 hydrogenation to methanol over catalysts derived from single cationic layer CuZnGa LDH precursors, *ACS Catal.*, 2018, **8**, 5, 4390–4401.

332 G. Wang, D. Mao, X. Guo and J. Yu, Enhanced performance of the CuO-ZnO-ZrO$_2$ catalyst for CO_2 hydrogenation to methanol by WO$_3$ modification, *Appl. Surf. Sci.*, 2018, **456**, 403–409.

333 T. Fujitani, M. Saito, Y. Kanai, M. Takeuchi, K. Moriya, T. Watanabe, M. Kawai and T. Kakumoto, Methanol synthesis from CO_2 and H_2 over Cu/ZnO/Ga$_2$O$_3$ catalyst, *Chem. Lett.*, 1993, **22**, 6, 1079–1080.

334 C. Shao, L. Fan, K. Fujimoto and Y. Iwasawa, Selective methanol synthesis from CO$_2$/H$_2$ on new SiO$_2$-supported PtW and PtCr bimetallic catalysts, *Appl. Catal., A*, 1995, **128**, 1, L1–L6.

335 H. Yang, P. Gao, C. Zhang, L. Zhong, X. Li, S. Wang, H. Wang, W. Wei and Y. Sun, Core–shell structured Cu@ m-SiO$_2$ and Cu/ZnO@ m-SiO$_2$ catalysts for methanol synthesis from CO$_2$ hydrogenation, *Catal. Commun.*, 2016, **84**, 56–60.

336 A. Zurbel, M. Kraft, S. Kavurucu-Schubert and M. Bertau, Methanol synthesis by CO$_2$ Hydrogenation over Cu/ZnO/Al$_2$O$_3$ catalysts under fluctuating conditions, *Chem. Ing. Tech.*, 2018, **90**, 5, 721–724.

337 K. L. Fischer and H. Freund, On the Optimal Design of Load Flexible Fixed Bed Reactors: Integration of Dynamics Into the Design Problem, *Chem. Eng. J.*, 2020, 124722.

338 R. Grün and C. Breitkopf, Development of transient catalyst characterization method for methanol synthesis, Technische Universität, Dresden, Germany, 2019, DGMK International Conference on Circular Economy - A Fresh View on Petrochemistry; Dresden; Germany

339 C. Seidel, A. Jörke, B. Vollbrecht, A. Seidel-Morgenstern and A. Kienle, Kinetic modeling of methanol synthesis from renewable resources, *Chem. Eng. Sci.*, 2018, **175**, 130–138.

340 M. Takagawa and M. Ohsugi, Study on reaction rates for methanol synthesis from carbon monoxide, carbon dioxide, and hydrogen, *J. Catal.*, 1987, **107**, 1, 161–172.27.

341 K. Klier, V. Chatikavanij, R. G. Herman and G. W. Simmons, Catalytic synthesis of methanol from COH$_2$: IV. The effects of carbon dioxide, *J. Catal.*, 1982, **74**, 2, 343–360.

342 J. Skrzypek, M. Lachowska and H. Moroz, Kinetics of methanol synthesis over commercial copper/zinc oxide/alumina catalysts, *Chem. Eng. Sci.*, 1991, **46**, 11, 2809–2813.

343 A. Alarifi, Modeling, Analysis and Optimization of the Gas-Phase Methanol Synthesis Process, ~~Modeling, Analysis and Optimization of the Gas-Phase Methanol Synthesis Process~~2016.

344 G. Leonzio, Mathematical modeling of a methanol reactor by using different kinetic models, *J. Ind. Eng. Chem.*, 2020, **85**, 130–140.

345 H. F. Ma, W. Y. Ying and D. Y. Fang, Study on methanol synthesis from coal-based syngas, *J. Coal Sci. Eng.*, 2009, **15**, 1, 98–103.

346 C. Seidel, A. Jörke, B. Vollbrecht, A. Seidel-Morgenstern and A. Kienle, Corrigendum to "Kinetic modeling of methanol synthesis from renewable resources", Chem. Eng. Sci., 2018, 175, 130–138 (Chem. Eng. Sci., 2020, 223, 115724).

347 F. Nestler, A. R. Schütze, M. Ouda, M. J. Hadrich, A. Schaadt, S. Bajohr and T. Kolb, Kinetic modelling of methanol synthesis over commercial catalysts: A critical assessment, *Chem. Eng. J.*, 2020, 124881.

348 F. Nestler, V. P. Müller, O. Salem, M. Hadrich, A. Schaadt, S. Bajohr and T. Kolb, A Novel Approach for Kinetic Measurements in Exothermic Fixed Bed Reactors: Advancements in Non-Isothermal Bed Conditions Demonstrated for Methanol Synthesis, *React. Chem. Eng.*, 2021.

349 C. Seidel and A. Kienle, Methanol Kinetics from Optimal Dynamic Experiments, in Computer Aided Chemical Engineering, Elsevier, 2020, vol. 48, 7–12

350 T. Svitnic, N. T. Do, T. Schuhmann, T. Renner, S. Haag and E. Örs, Data-Driven Approach for Predictive Modeling of By-Product Formation in Methanol Synthesis, in Computer Aided Chemical Engineering, Elsevier, 2020, vol. 48, 505–510

351 K. Ahmad and S. Upadhyayula, Kinetics of CO$_2$ hydrogenation to methanol over silica supported intermetallic Ga3Ni5 catalyst in a continuous differential fixed bed reactor, *Int. J. Hydrogen Energy*, 2020, **45**, 1, 1140–1150.

352

H. W. Lim, M. J. Park, S. H. Kang, H. J. Chae, J. W. Bae and K. W. Jun, Modeling of the kinetics for methanol synthesis using Cu/ZnO/Al$_2$O$_3$/ZrO$_2$ catalyst: influence of carbon dioxide during hydrogenation, *Ind. Eng. Chem. Res.*, 2009, **48**, 23, 10448–10455.

353 S. Li, L. Guo and T. Ishihara, Hydrogenation of CO$_2$ to methanol over Cu/AlCeO catalyst, *Catal. Today*, 2020, **339**, 352–361.

354 J. Park, J. Cho, Y. Lee, M. J. Park and W. B. Lee, Practical microkinetic modeling approach for methanol synthesis from syngas over a Cu-based catalyst, *Ind. Eng. Chem. Res.*, 2019, **58**, 20, 8663–8673.

355 M. S. Frei, M. Capdevila-Cortada, R. García-Muelas, C. Mondelli, N. López, J. A. Stewart, D. C. Ferré and J. Pérez-Ramírez, Mechanism and microkinetics of methanol synthesis via CO$_2$ hydrogenation on indium oxide, *J. Catal.*, 2018, **361**, 313–321.

356 I. U. Din, M. S. Shaharun, A. Naeem, M. A. Alotaibi, A. I. Alharthi and Q. Nasir, CO$_2$ Conversion to Methanol over Novel Carbon Nanofiber-Based Cu/ZrO2 Catalysts—A Kinetics Study, *Catalysts*, 2020, **10**, 5, 567.

357 A. O. Elnabawy, J. Schumann, P. Bothra, A. Cao and J. K. Nørskov, The Challenge of CO Hydrogenation to Methanol: Fundamental Limitations Imposed by Linear Scaling Relations, *Top. Catal.*, 2020, **63**, 635–648.

358 Y. CHE, T. LI and H. ZHANG, Intrinsic Kinetics of Hydrogenation of CO$_2$ towards Methanol on a Cu/ZnO/Al$_2$O$_3$ Modified Catalyst, *J. East China Univ. Sci. Technol.*, 2020, **46**, 3, 326–333.

359 S. M. Jarvis and S. Samsatli, Technologies and infrastructures underpinning future CO$_2$ value chains: A comprehensive review and comparative analysis, *Renewable Sustainable Energy Rev.*, 2018, **85**, 46–68.

360 D. Y. Jo, M. W. Lee, H. C. Ham and K. Y. Lee, Role of the Zn atomic arrangements in enhancing the activity and stability of the kinked Cu (2 1 1) site in CH$_3$OH production by CO$_2$ hydrogenation and dissociation: First-principles microkinetic modeling study, *J. Catal.*, 2019, **373**, 336–350.

361 C. V. Ovesen, B. S. Clausen, J. Schiøtz, P. Stoltze, H. Topsøe and J. K. Nørskov, Kinetic implications of dynamical changes in catalyst morphology during methanol synthesis over Cu/ZnO catalysts, *J. Catal.*, 1997, **168**, 2, 133–142.

362 G. Ferri, Modeling and design of an experimental set-up for the study of a power-to-methanol process

363 Methanol: Science and Engineering, ed. A. Basile and F. Dalena, Elsevier, 2017

364 A. Goeppert, M. Czaun, J. P. Jones, G. S. Prakash and G. A. Olah, Recycling of carbon dioxide to methanol and derived products – closing the loop, *Chem. Soc. Rev.*, 2014, **43**, 23, 7995–8048.

365 I. Iliuta and F. Larachi, Enhanced methanol synthesis process via an integrated process involving CO$_2$ hydrogenation under plasma conditions, *Ind. Eng. Chem. Res.*, 2019, **59**, 15, 6815.

366 D. Park and J. Lee, Biological conversion of methane to methanol, *Korean J. Chem. Eng.*, 2013, **30**, 5, 977–987.

367 A. Indarto, Partial oxidation of methane to methanol with nitrogen dioxide in dielectric barrier discharge plasma: experimental and molecular modeling, *Plasma Sources Sci. Technol.c*, 2016, **25**, 2, 025002.

368 H. Bakhtiary-Davijany, F. Dadgar, F. Hayer, X. K. Phan, R. Myrstad, H. J. Venvik, P. Pfeifer and A. Holmen, Analysis of external and internal mass transfer at low Reynolds numbers in a multiple-slit packed bed microstructured reactor for synthesis of methanol from syngas, *Ind. Eng. Chem. Res.*, 2012, **51**, 42, 13574–13579.

369 A. L. Tonkovich, K. Jarosch, R. Arora, L. Silva, S. Perry, J. McDaniel, F. Daly and B. Litt, Methanol production FPSO plant concept using multiple microchannel unit operations, *Chem. Eng. J.*, 2008, **135**, S2–S8.

370 H. J. Venvik and J. Yang, Catalysis in microstructured reactors: Short review on small-scale syngas production and further conversion into methanol, DME and Fischer-Tropsch products, *Catal. Today*, 2017, **285**, 135–146.

371 G. Kolb, Microstructured reactors for distributed and renewable production of fuels and electrical energy, *Chem. Eng. Process.*, 2013, **65**, 1–44.

372 F. Daly and L. Tonkovich, Enabling offshore production of methanol by use of an isopotential reactor, in Studies in surface science and catalysis, Elsevier, 2004, vol. 147, 415–420

373 X. K. Phan, H. D. Bakhtiary, R. Myrstad, J. Thormann, P. Pfeifer, H. J. Venvik and A. Holmen, Preparation and performance of a catalyst-coated stacked foil microreactor for the methanol synthesis, *Ind. Eng. Chem. Res.*, 2010, **49**, 21, 10934–10941.

374 E. Moioli, R. Mutschler and A. Züttel, Renewable energy storage via CO$_2$ and H$_2$ conversion to methane and methanol: Assessment for small scale applications, *Renewable Sustainable Energy Rev.*, 2019, **107**, 497–506.

375 H. Bakhtiary-Davijany, F. Hayer, X. K. Phan, R. Myrstad, H. J. Venvik, P. Pfeifer and A. Holmen, Characteristics of an integrated micro packed bed reactor-heat exchanger for methanol synthesis from syngas, *Chem. Eng. J.*, 2011, **167**, 2–3, 496–503.

376 H. Bakhtiary-Davijany, F. Hayer, X. K. Phan, R. Myrstad, P. Pfeifer, H. J. Venvik and A. Holmen, Performance of a multi-slit packed bed microstructured reactor in the synthesis of methanol: Comparison with a laboratory fixed-bed reactor, *Chem. Eng. Sci.*, 2011, **66**, 24, 6350–6357.

377 B. Tidona, A. Urakawa and P. R. von Rohr, High pressure plant for heterogeneous catalytic CO$_2$ hydrogenation reactions in a continuous flow microreactor, *Chem. Eng. Process.*, 2013, **65**, 53–57.

378 B. Tidona, ~~Hydrogenation of carbon dioxide in a flow microreactor at pressures up to 1000 bar~~Hydrogenation of carbon dioxide in a flow microreactor at pressures up to 1000 bar, doctoral dissertation~~, doctoral dissertation, , ~~~~ETH Zurich~~ETH Zurich, Switzerand~~, Switzerand~~2013.

379 C. Chen and A. Yang, Power-to-methanol: The role of process flexibility in the integration of variable renewable energy into chemical production, *Energy Convers. Manage.*, 2021, **228**, 113673.

380 J. P. Lange, Methanol synthesis: a short review of technology improvements, *Catal. Today*, 2001, **64**, 1–2, 3–8.

381

A. Mirvakili, S. Chahibakhsh, M. Ebrahimzadehsarvestani, E. Soroush and M. R. Rahimpour, Modeling and assessment of novel configurations to enhance methanol production in industrial mega-methanol synthesis plant, *J. Taiwan Inst. Chem. Eng.*, 2019, **104**, 40–53.

382 Q. Zheng and S. Li, Process Optimization of Coke Oven Gas to Methanol Based on the Downgrade of By-Product Steam, *Trans. Tianjin Univ.*, 2019, **25**, 3, 214–225.

383 G. Leonzio and P. U. Foscolo, Analysis of a 2-D model of a packed bed reactor for methanol production by means of CO_2 hydrogenation, *Int. J. Hydrogen Energy*, 2020, **45**, 18, 10648–10663.

384 K. L. Fischer, M. R. Langer and H. Freund, Dynamic carbon dioxide methanation in a wall-cooled fixed bed reactor: comparative evaluation of reactor models, *Ind. Eng. Chem. Res.*, 2019, **58**, 42, 19406–19420.

385 A. Mirvakili, A. Bakhtyari and M. R. Rahimpour, A CFD modeling to investigate the impact of flow mal-distribution on the performance of industrial methanol synthesis reactor, *Appl. Therm. Eng.*, 2018, **128**, 64–78.

386 B. Rahmatmand, M. R. Rahimpour and P. Keshavarz, Introducing a novel process to enhance the syngas conversion to methanol over $Cu/ZnO/Al_2O_3$ catalyst, *Fuel Process. Technol.*, 2019, **193**, 159–179.

387 K. Hirotani, H. Nakamura and K. Shoji, Optimum catalytic reactor design for methanol synthesis with TEC MRF-Z® reactor, *Catal. Surv. Asia*, 1998, **2**, 1, 99–106.

388 B. Redondo, M. T. Shah, V. K. Pareek, R. P. Utikar, P. A. Webley, J. Patel, W. J. Lee and T. Bhatelia, Intensified isothermal reactor for methanol synthesis, *Chem. Eng. Process.*, 2019, **143**, 107606.

389 N. T. Do, S. Haag, V. Gronemann, T. Schuhmann, T. Oelmann, M. Gorny, H. Schwarz, S. Werner, S. J. Reitmeier, S. Gebert and A. Reitzmann, Layer Management for Methanol Process, *InDGMK Conference: Circular Economy-A Fresh View on Petrochemistry*, 2019.

390 S. Thirabunjongcharoen, P. Bumroongsakulsawat, P. Praserthdam, S. Charojrochkul, S. Assabumrungrat and P. Kim-Lohsoontorn, Thermally double coupled reactor coupling aqueous phase glycerol reforming and methanol synthesis, *Catal. Today*, 2020, **375**, 181–190.

391 V. Spallina, G. Motamedi, F. Gallucci and M. van Sint Annaland, Techno-economic assessment of an integrated high pressure chemical-looping process with packed-bed reactors in large scale hydrogen and methanol production, *Int. J. Greenhouse Gas Control*, 2019, **88**, 71–84.

392 H. Bakhtiary-Davijany, F. Hayer, X. K. Phan, R. Myrstad, H. J. Venvik, P. Pfeifer and A. Holmen, Modelling and simulation of a single slit micro packed bed reactor for methanol synthesis, *Catal. Today*, 2020, **343**, 226–233.

393 M. Son, Y. Woo, G. Kwak, Y. J. Lee and M. J. Park, CFD modeling of a compact reactor for methanol synthesis: Maximizing productivity with increased thermal controllability, *Int. J. Heat Mass Transfer*, 2019, **145**, 118776.

394 M. Yang and F. You, Modular methanol manufacturing from shale gas: Techno-economic and environmental analyses of conventional large-scale production versus small-scale distributed, modular processing, *AIChE J.*, 2018, **64**, 2, 495–510.

395 J. Bielenberg and M. Bryner, Realize the potential of process intensification, *Chem. Eng. Prog.*, 2018, **114**, 3, 41–45.

396 M. Baldea, T. F. Edgar, B. L. Stanley and A. A. Kiss, Modularization in Chemical Processing, *Chem. Eng. Prog.*, 2018, **114**, 3, 46–54.

397 M. Baldea, T. F. Edgar, B. L. Stanley and A. A. Kiss, Modular manufacturing processes: Status, challenges, and opportunities, *AIChE J.*, 2017, **63**, 10, 4262–4272.

398 S. Sadeghi, L. Vafajoo, M. Kazemeini and M. Fattahi, Modeling of the methanol synthesis catalyst deactivation in a spherical bed reactor: an environmental challenge, *APCBEE Proc.*, 2014, **10**, 84–90.

399 M. R. Rahimpour, A. Abbasloo and J. Sayyad Amin, A novel radial-flow, spherical-bed reactor concept for methanol synthesis in the presence of catalyst deactivation, *Chem. Eng. Technol.*, 2008, **31**, 11, 1615–1629.

400 M. R. Rahimpour, P. Parvasi and P. Setoodeh, Dynamic optimization of a novel radial-flow, spherical-bed methanol synthesis reactor in the presence of catalyst deactivation using Differential Evolution (DE) algorithm, *Int. J. Hydrogen Energy*, 2009, **34**, 15, 6221–6230.

401 G. A. Viecco and H. S. Caram, The spherical reverse flow reactor, *Chem. Eng. Sci.*, 2002, **57**, 18, 4005–4025.

402 M. Farsi, Mathematical Modeling and Optimization of a Radial Flow Tubular Reactor to Produce Methanol from Syngas, *Pet. Chem.*, 2018, **58**, 12, 1091–1098.

403 P. Parvasi and S. Mohammad Jokar, A novel reactor configuration for industrial methanol production from the synthesis gas, *J. Energy Resour. Technol.*, 2019, 4, 141.

404 L. Mencarelli, Q. Chen, A. Pagot and I. E. Grossmann, A review on superstructure optimization approaches in process system engineering, *Comput. Chem. Eng.*, 2020, 106808.

405 A. Huesman, Integration of operation and design of solar fuel plants: A carbon dioxide to methanol case study, *Comput. Chem. Eng.*, 2020, 106836.

406 C. Varela, M. Mostafa, E. Ahmetovic and E. Zondervan, Agile Operation of Renewable Methanol Synthesis under Fluctuating Power Inputs, in Computer Aided Chemical Engineering, Elsevier, 2020, vol. 48, 1381–1386

407 R. J. Dry, Possibilities for the development of large-capacity methanol synthesis reactors for synfuel production, *Ind. Eng. Chem. Res.*, 1988, **27**, 4, 616–624.

408 X. Chen and C. Li, Methanol synthesis under forced periodic operation with flow alternation, *Xiandai Huagong*, 2000, **20**, 7, 43–45.

409 E. Mancusi, P. Altimari, L. Russo and S. Crescitelli, Multiplicities of temperature wave trains in periodically forced networks of catalytic reactors for reversible exothermic reactions, *Chem. Eng. J.*, 2011, **171**, 2, 655–668.

410 S. A. Velardi and A. A. Barresi, Methanol synthesis in a forced unsteady-state reactor network, *Chem. Eng. Sci.*, 2002, **57**, 15, 2995–3004.

411 G. Leonzio and P. U. Foscolo, Analysis of a 2-D model of a packed bed reactor for methanol production by means of CO2 hydrogenation, *Int. J. Hydrogen Energy*, 2020, **45**, 18, 10648–10663.

412 J. J. Meyer, P. Tan, A. Apfelbacher, R. Daschner and A. Hornung, Modeling of a methanol synthesis reactor for storage of renewable energy and conversion of CO_2–comparison of two kinetic models, *Chem. Eng. Technol.*, 2016, **39**, 2, 233–245.

413 M. Kaiser and H. Freund, A multimodular pseudoheterogeneous model framework for optimal design of catalytic reactors exemplified by methanol synthesis, *Chem. Eng. Sci.*, 2019, **206**, 401–423.

414 F. Manenti, S. Cieri and M. Restelli, Considerations on the steady-state modeling of methanol synthesis fixed-bed reactor, *Chem. Eng. Sci.*, 2011, **66**, 2, 152–162.

415 J. Petera, L. Nowicki and S. Ledakowicz, New numerical algorithm for solving multidimensional heterogeneous model of the fixed bed reactor, *Chem. Eng. J.*, 2013, **214**, 237–246.

416 ~~I. Lovik~~I.Løvik, Modelling, estimation and optimization of the methanol synthesis with catalyst deactivation, PhD Thesis, The Norwegian University of Science and Technology (2001).

417 F. Manenti, S. Cieri, M. Restelli and G. Bozzano, Dynamic modeling of the methanol synthesis fixed-bed reactor, *Comput. Chem. Eng.*, 2013, **48**, 325–334.

418 A. Riaz, G. Zahedi and J. J. Klemeš, A review of cleaner production methods for the manufacture of methanol, *J. Cleaner Prod.*, 2013, **57**, 19–37.

419 N. Rezaie, A. Jahanmiri, B. Moghtaderi and M. R. Rahimpour, A comparison of homogeneous and heterogeneous dynamic models for industrial methanol reactors in the presence of catalyst deactivation, *Chem. Eng. Process.*, 2005, **44**, 8, 911–921.

420 D. Larrain, Solid oxide fuel cell stack simulation and optimization, including experimental validation and transient behavior, EPFL, 2005

421 F. Manenti, A. R. Leon-Garzona and G. Giulia Bozzano, Energy-process integration of the gas-cooled/water-cooled fixed-bed reactor network for methanol synthesis, *Chemical Engineering Transactions*, 2013, 35.

422 R. O. dos Santos, L. de Sousa Santos and D. M. Prata, Simulation and optimization of a methanol synthesis process from different biogas sources, *J. Cleaner Prod.*, 2018, **186**, 821–830.

423 P. Li, L. Chen, S. Xia and L. Zhang, Entropy generation rate minimization for methanol synthesis via a CO_2 hydrogenation reactor, *Entropy*, 2019, **21**, 2, 174.

424 W. L. Luyben, Design and control of a methanol reactor/column process, *Ind. Eng. Chem. Res.*, 2010, **49**, 13, 6150–6163.

425 P. Borisut and A. Nuchitprasittichai, Methanol Production via CO_2 Hydrogenation: Sensitivity analysis and simulation–based optimization, *Frontiers in Energy Research*, 2019, **7**, 81.

426 S. Hoseiny, Z. Zare, A. Mirvakili, P. Setoodeh and M. R. Rahimpour, Simulation–based optimization of operating parameters for methanol synthesis process: application of response surface methodology for statistical analysis, *J. Nat. Gas Sci. Eng.*, 2016, **34**, 439–448.

427 I. Stoica, I. Banu, I. Bobarnac and G. Bozga, Optimization of a methanol synthesis reactor, ~~UPB Sci. Bull. Ser. B Chem. Mater. Sci.~~ UPB Scientific Bulletin, Series B: Chemistry and Materials Science, 2015, **77**, 4, 134–146.

428 H. Zhang, L. Wang, F. Maréchal and U. Desideri, Techno-economic optimization of CO_2-to-methanol with solid-oxide electrolyzer, *Energies*, 2019, **12**, 19, 3742.

429 S. Szima and C. C. Cormos, Improving methanol synthesis from carbon-free H_2 and captured CO_2: a techno-economic and environmental evaluation, *J. CO2 Util.*, 2018, **24**, 555–563.

430 H. Zhang, L. Wang, F. Maréchal and U. Desideri, Techno-economic evaluation of biomass-to-fuels with solid-oxide electrolyzer, *Appl. Energy*, 2020, **270**, 115113.

431 D. Schack, G. Liesche and K. Sundmacher, The FluxMax approach: Simultaneous flux optimization and heat integration by discretization of thermodynamic state space illustrated on methanol synthesis process, *Chem. Eng. Sci.*, 2020, **215**, 115382.

432 P. Kenkel, T. Wassermann, C. Rose and E. Zondervan, A generic superstructure modeling and optimization framework on the example of bi-criteria Power-to-Methanol process design, *Comput. Chem. Eng.*, 2021, 107327.

433 L. Petrescu, S. C. Galusnyak, D. A. Chisalita and C. C. Cormos, Modelling and Simulation of Methanol Production and Conversion into Various Chemical Intermediates and Products, in Computer Aided Chemical Engineering, Elsevier, 2020, vol. 48, 553–558

434 M. A. Adnan and M. G. Kibria, Comparative techno-economic and life-cycle assessment of power-to-methanol synthesis pathways, *Appl. Energy*, 2020, **278**, 115614.

435 T. Wassermann, C. Schnuelle, P. Kenkel and E. Zondervan, Power-to-Methanol at Refineries as a Precursor to Green Jet Fuel Production: a Simulation and Assessment Study, in Computer Aided Chemical Engineering, Elsevier, 2020, vol. 48, 1453–1458

436 L. B. Rocha, M. L. Gimenes, S. H. Faria, L. Jiménez and T. Cavali, Design of a New Sustainable Methanol Plant Coupled to an Ethanol Distillery, in Computer Aided Chemical Engineering, Elsevier, 2017, vol. 40, 805–810

437 K. Afzali. The role of power-to-methanol technologies in the energy mix: Investigation of the impact of stimulating power-to-methanol technologies on reliability of the Dutch power grid and CO_2 reduction

438 N. Meunier, R. Chauvy, S. Mouhoubi, D. Thomas and G. De Wiereld, Alternative production of methanol from industrial CO_2, *Renewable Energy*, 2020, **146**, 1192–1203.

439 P. Kenkel, T. Wassermann and E. Zondervan, Design of a Sustainable Power-to-methanol Process: a Superstructure Approach Integrated with Heat Exchanger Network Optimization, in Computer Aided Chemical Engineering, Elsevier, 2020, vol. 48, 1411–1416

440 Y. D. Chaniago, M. A. Qyyum, R. Andika, W. Ali, K. Qadeer and M. Lee, Self-recuperative high temperature co-electrolysis-based methanol production with vortex search-based exergy efficiency enhancement, *J. Cleaner Prod.*, 2019, **239**, 118029.

441 K. Roh, R. Frauzem, R. Gani and J. H. Lee, Process systems engineering issues and applications towards reducing carbon dioxide emissions through conversion technologies, *Chem. Eng. Res. Des.*, 2016, **116**, 27–47.

442 T. Zhang, N. V. Sahinidis and J. J. Siirola, Pattern recognition in chemical process flowsheets, *AIChE J.*, 2019, **65**, 2, 592–603.

443 L. G. Hernandez-Perez, A. S. Alsuhaibani, N. Radwan, M. M. El-Halwagi and J. M. Ponce-Ortega, Structural and Operating Optimization of the Methanol Process Using a Metaheuristic Technique, *ACS Sustainable Chem. Eng.*, 2020, **8**, 8, 3135–3150.

444 P. L. Suryawanshi, S. P. Gumfekar, B. A. Bhanvase, S. H. Sonawane and M. S. Pimplapure, A review on microreactors: Reactor fabrication, design, and cutting-edge applications, *Chem. Eng. Sci.*, 2018, **189**, 431–448.

445 M. Martín, Methodology for solar and wind energy chemical storage facilities design under uncertainty: methanol production from CO_2 and hydrogen, *Comput. Chem. Eng.*, 2016, **92**, 43–54.

446 A. Sánchez, M. Martín and Q. Zhang, in Computer Aided Chemical Engineering, Elsevier, 2020, vol. 48, 1357–1362

447 L. Wang, Z. Yang, S. Sharma, A. Mian, T. E. Lin, G. Tsatsaronis, F. Maréchal and Y. Yang, A review of evaluation, optimization and synthesis of energy systems: methodology and application to thermal power plants, *Energies*, 2019, **12**, 1, 73.

448 H. Taghdisian, M. R. Pishvaie and F. Farhadi, Multi-objective optimization approach for green design of methanol plant based on CO_2-efficiency indicator, *J. Cleaner Prod.*, 2015, **103**, 640–650.

449 M. Martín and T. A. Adams II, Challenges and future directions for process and product synthesis and design, *Comput. Chem. Eng.*, 2019, **128**, 421–436.

450 T. Neveux, Ab-initio process synthesis using evolutionary programming, *Chem. Eng. Sci.*, 2018, **185**, 209–221.

451 S. E. Demirel, J. Li and M. F. Hasan, A general framework for process synthesis, integration, and intensification, *Ind. Eng. Chem. Res.*, 2019, **58**, 15, 5950–5967.

452 L. Wang, M. Lampe, P. Voll, Y. Yang and A. Bardow, Multi-objective superstructure-free synthesis and optimization of thermal power plants, *Energy*, 2016, **116**, 1104–1116.

453 X. Peng, T. W. Root and C. T. Maravelias, Process Synthesis under Seasonal and Daily Variability: Application on Concentrating Solar Power, in Computer Aided Chemical Engineering, Elsevier, 2018, vol. 44, 415–420

454 O. Onel, A. M. Niziolek, H. Butcher, B. A. Wilhite and C. A. Floudas, Multi-scale approaches for gas-to-liquids process intensification: CFD modeling, process synthesis, and global optimization, *Comput. Chem. Eng.*, 2017, **105**, 276–296.

455 H. Yu, C. Fu and T. Gundersen, Work and heat exchange networks–opportunities and challenges, in Computer Aided Chemical Engineering, Elsevier, 2018, vol. 44, 481–486

456 J. O. Odejobi and O. S. Ayorinde, Exergy and economic analyses of methanol production process, *Nigerian Journal of Technology*, 2018, **37**, 2, 365–373.

457 M. Colla, A. Ioannou and G. Falcone, Critical review of competitiveness indicators for energy projects, *Renewable Sustainable Energy Rev.*, 2020, **125**, 109794.

458 H. von Storch, M. Roeb, H. Stadler, C. Sattler, A. Bardow and B. Hoffschmidt, On the assessment of renewable industrial processes: Case study for solar co-production of methanol and power, *Appl. Energy*, 2016, **183**, 121–132.

459 R. Ruiz-Femenia, M. J. Fernández-Torres, R. Salcedo-Díaz, M. F. Gómez-Rico and J. A. Caballero, Systematic tools for the conceptual design of inherently safer chemical processes, *Ind. Eng. Chem. Res.*, 2017, **56**, 25, 7301–7313.

460 A. Bejan, Fundamentals of exergy analysis, entropy generation minimization, and the generation of flow architecture, *Int. J. Energy Res.*, 2002, **26**, 7, 545–565.

461 Z. Bai, Q. Liu, J. Lei, H. Li and H. Jin, A polygeneration system for the methanol production and the power generation with the solar–biomass thermal gasification, *Energy Convers. Manage.*, 2015, **102**, 190–201.

462 S. C. Nimkar, R. K. Mewada and M. A. Rosen, Exergy and exergoeconomic analyses of thermally coupled reactors for methanol synthesis, *Int. J. Hydrogen Energy*, 2017, **42**, 47, 28113–28127.

463 S. Kelly, G. Tsatsaronis and T. Morosuk, Advanced exergetic analysis: Approaches for splitting the exergy destruction into endogenous and exogenous parts, *Energy*, 2009, **34**, 3, 384–391.

464 G. Tsatsaronis and T. Morosuk, A general exergy-based method for combining a cost analysis with an environmental impact analysis: Part I – Theoretical Development, *Energy Convers. Resour., ASME Int. Mech. Eng. Congr. Expo.*, 2008, **48692**, 453–462.

465 S. Kjelstrup, E. Johannessen, A. Rosjorde, L. Nummedal and D. Bedeaux, Minimizing the entropy production of the methanol producing reaction in a methanol reactor, *Int. J. Thermodyn.*, 2000, **3**, 4, 147–153.

466 M. Ouda, C. Hank, F. Nestler, M. Hadrich, J. Full, A. Schaadt and C. Hebling, Power-to-Methanol: Techno-Economical and Ecological Insights, in Zukünftige Kraftstoffe, Springer Vieweg, Berlin, Heidelberg, 2019, 380–409

467 C. Hank, S. Gelpke, A. Schnabl, R. J. White, J. Full, N. Wiebe, T. Smolinka, A. Schaadt, H. M. Henning and C. Hebling, Economics & carbon dioxide avoidance cost of methanol production based on renewable hydrogen and recycled carbon dioxide–power-to-methanol, *Sustainable Energy Fuels*, 2018, **2**, 6, 1244–1261.

468

D. S. Kourkoumpas, E. Papadimou, K. Atsonios, S. Karellas, P. Grammelis and E. Kakaras, Implementation of the Power to Methanol concept by using CO_2 from lignite power plants: Techno-economic investigation, *Int. J. Hydrogen Energy*, 2016, **41**, 38, 16674–16687.

469 J. A. Baak, A. K. Pozarlik, M. J. Arentsen and G. Brem, Techno-economic study of a zero-emission methanol based energy storage system, *Energy Convers. Manage.*, 2019, **182**, 530–545.

470 A. González-Garay, M. S. Frei, A. Al-Qahtani, C. Mondelli, G. Guillén-Gosálbez and J. Pérez-Ramírez, Plant-to-planet analysis of CO_2-based methanol processes, *Energy Environ. Sci.*, 2019, **12**, 12, 3425–3436.

471 A. Darmani, N. Arvidsson, A. Hidalgo and J. Albors, What drives the development of renewable energy technologies? Toward a typology for the systemic drivers, *Renewable Sustainable Energy Rev.*, 2014, **38**, 834–847.

472 S. Michailos, S. McCord, V. Sick, G. Stokes and P. Styring, Dimethyl ether synthesis via captured CO_2 hydrogenation within the power to liquids concept: A techno-economic assessment, *Energy Convers. Manage.*, 2019, **184**, 262–276.

473 P. Charoensuppanimit, K. Kitsahawong, P. Kim-Lohsoontorn and S. Assabumrungrat, Incorporation of hydrogen by-product from NaOCH3 production for methanol synthesis via CO_2 hydrogenation: Process analysis and economic evaluation, *J. Cleaner Prod.*, 2019, **212**, 893–909.

474 Q. Chen, Y. Gu, Z. Tang and Y. Sun, Comparative environmental and economic performance of solar energy integrated methanol production systems in China, *Energy Convers. Manage.*, 2019, **187**, 63–75.

475 M. Asif, X. Gao, H. Lv, X. Xi and P. Dong, Catalytic hydrogenation of CO_2 from 600 MW supercritical coal power plant to produce methanol: a techno-economic analysis, *Int. J. Hydrogen Energy*, 2018, **43**, 5, 2726–2741.

476 M. Yu, K. Wang and H. Vredenburg, Insights into low-carbon hydrogen production methods: Green, blue and aqua hydrogen, *Int. J. Hydrogen Energy*, 2021, **46**, 41, 21261–21273.

477 S. Ghosh and S. Seethamraju, Feasibility of reactive distillation for methanol synthesis, *Chem. Eng. Process.*, 2019, **145**, 107673.

478 C. Heßelmann, T. Wolf, F. Galgon, C. Körner, J. Albert and P. Wasserscheid, Additively manufactured RANEY®-type copper catalyst for methanol synthesis, *Catal. Sci. Technol.*, 2020, **10**, 1, 164–168.

Queries and Answers

Q1

Query: Have all of the author names been spelled and formatted correctly? Names will be indexed and cited as shown on the proof, so these must be correct. No late corrections can be made.

Answer: Yes

Q2

Query: Text has been provided for footnote b in Table 3, but there does not appear to be a corresponding citation in the table. Please indicate suitable location for the footnote citation.

Answer: A superscript next on Nominal system efficiency(%)

Q3

Query: "Zurbel" is not cited as an author of ref. 326. Please indicate any changes that are required here.

Answer: It should be reference 336 only (i.e. Zurbel et al.)

Q4

Query: Please check that "Table 9" has been displayed correctly.

Answer: Yes, it is correctly displayed.

Q5

Query: "Zhang" is not cited as an author of ref. 406. Please indicate any changes that are required here.

Answer: Edited. It should be reference 430.

Q6

Query: The author's name is spelled "Martín" in ref. X, but in the text it is spelled "Martin". Please check and correct as necessary.

Answer: Corrected.

Q18

Query: Ref. 124: Please provide the page (or article) number(s).

Answer: The article was and is still listed as "In Press, Corrected Proof" and thus no page numbers are available.

Q19

Query: Ref. 127: Please provide the page (or article) number(s).

Answer: Added.

Q20

Query: Ref. 133: Please provide the page (or article) number(s).

Answer: Added.

Q21

Query: Ref. 161: Please give the name of this journal in full, including any other names by which this journal may be known (e.g. Chin. J. Struct. Chem. is also known as Jiegou Huaxue), so that its CASSI abbreviation can be checked for indexing purposes.

Answer: Edited.

Q22

Query: Ref. 168: Please provide the full list of author names (including initials), journal title, year of publication and page (or article) number(s).

Answer: Edited.

Q23

Query: Ref. 175: Please provide the page (or article) number(s).

Answer: Added.

Q24

Query: Ref. 183, 201 and 378: Please provide the year of publication.

Answer: Added.

Q25

Query: Ref. 184: Please provide the page (or article) number(s).

Answer: added.

Q26

Query: Ref. 192: Please provide the year of publication.

Answer: Added.

Q27

Query: Ref. 201: Please provide the year of publication.

Answer: Added.

Q28

Query: Ref. 209: Please provide the year of publication.

Answer: Added.

Q29

Query: Ref. 227: Please provide the year of publication.

Answer: Added.

Q30

Query: Ref. 233: Please provide the page (or article) number(s).

Answer: Added.

Q31

Query: Ref. 246: Please provide the page (or article) number(s).

Answer: Added.

Q32

Query: The page numbers provided for ref. 255, 262 and 309 appear to be incorrect. Please check and correct as necessary.

Answer: Edited.

Q33

Query: Please check that ref. 279 has been displayed correctly.

Answer:

Kindly edit to as below:

J. Sehested, Industrial and scientific directions of methanol catalyst development, J. Catal., 2019, 371, 368–375.

Remove the part " ; Matthey, Available......"

Q34

Query: Ref. 293: Please provide the year of publication.

Answer: Added.

Q35

Query: Ref. 343: Please provide the year of publication.

Answer: Added.

Q36

Query: Ref. 344: Please provide the page (or article) number(s).

Answer: Added.

Q37

Query: Ref. 357: Please provide the page (or article) number(s).

Answer: Added.

Q38

Query: Ref. 378: Please provide the year of publication.

Answer: Added.

Q39

Query: Ref. 383: Please provide the page (or article) number(s).

Answer: Added.

Q40

Query: Ref. 389: Please provide the year of publication.

Answer: Added.

Q41

Query: Ref. 390: Please provide the page (or article) number(s).

Answer: Added.

Q42

Query: Ref. 411: Please provide the page (or article) number(s).

Answer: Added.

Q43

Query: Ref. 416: Please provide the year of publication.

Answer: Added: 2001 "I.Løvik, Modelling, estimation and optimization of the methanol synthesis with catalyst deactivation, PhD Thesis, The Norwegian University of Science and Technology (2001)."

Q44

Query: Ref. 427: Please give the name of this journal in full, including any other names by which this journal may be known (e.g. Chin. J. Struct. Chem. is also known as Jiegou Huaxue), so that its CASSI abbreviation can be checked for indexing purposes.

Answer: Edited.

Q45

Query: Ref. 460: Please provide the page (or article) number(s).

Answer: Added: 545 - 565.

Q46

Query: Ref. 476: Please provide the page (or article) number(s).

Answer: Corrected: **46**, 41, 21261–21273.